Projecting Future Crop Yields under Impending Climate Change: A Study into the Importance of Soil Moisture and Soil Organic Carbon

A Thesis Presented for the
Master of Science
Degree
The University of Tennessee, Knoxville

Violeta Benvenuto Freudenberg
May 2018

ACKNOWLEDGEMENTS

Capturing nature's creativity, energy, and vibrancy prompts images of the people in my life. From friends and family of yesteryear to today, together they create my environment and assisted in forming who I am today, including my parents, in-laws, sister, grandparents, cousins, and friends. Through the process of obtaining this degree I would like to thank my loving husband Kevin and children Ashley and Eric for their patience and support. I would like to remember the late Dr. Chris Seiffert for his inspiration and friendship. This path wouldn't have been possible without the help of my advisor and committee chairman, Dr. Papanicolaou, whose vision and expertise guided me throughout the process. I am also grateful to him for giving me the opportunity to pursue a graduate degree. I would like to thank Dr. Wilson and Dr. Ghaneeizad for their assistance and direction, and the rest of our research group including the soon to be Dr. Abban and Christos Giannopoulos. I would also like to express my appreciation to my committee members, Dr. Hathaway and Dr. Schwartz, for their thesis review and guidance. Additionally I would like to thank the USDA for providing the means of pursuing environmental research.

ABSTRACT

This study presents a top-down, bottom-up modeling framework to investigate the effects of future climate on crop production in an intensively managed watershed of the Mississippi River Basin, a world leading crop producer. Specifically, this study will examine how climate modification will alter soil moisture, soil organic carbon, and ultimately crop yields in the Obion River, TN. Representative hydrologic response areas in the Obion River watershed are identified using the Variable Infiltration Capacity regional hydrologic model. This identification criterion considers both soil properties and changing hydrology, through the runoff coefficient and slope. Select hillslopes are further chosen in the representative areas and the physically based, hillslope-scale model, Water Erosion Prediction Project, is used to examine the cause-effect relations between management and climate. This includes changes in soil moisture, soil organic carbon loss, and soil erosion until 2050 under established climate scenarios to aid in the development of sustainable solutions. Results will indicate that effects from this changing climate are visible through a decrease in the utilization of available water and a decrease in soil organic carbon, with negative consequences to soil and water quality. Furthermore, these effects have a projected decrease to crop yields. Foreseeing potential impacts, through improvements to current management practices, could help improve future outcomes.

TABLE OF CONTENTS

Chapter One Introduction and General Information 1
Chapter Two Literature Review and Analysis BackGround 5
Evapotranspiration, Soil Moisture and Water Stress 5
Water Use Efficiency 10
Soil Organic Carbon 11
Chapter Three Hypotheses 17
Hypothesis 1 17
Hypothesis 2 17
Chapter Four Study Design 19
Geographic Location 19
Models 21
Top-Down Approach 22
Bottom-Up Approach 26
WEPP Soil Files 31
WEPP Management Files 32
WEPP Climate Files 37
Model Simulations 38
Chapter Five Results & Discussion 41
Hypothesis 1 41
Crop Yields 41
Evapotranspiration and Soil Moisture 41
Water Use Efficiency – Hamilton et al. (2015) 44
Water Use Efficiency – Dietzel et al. (2016) 50
Crop Stresses 53
System Water Use Efficiency – Dietzel et al. (2016) 58
Yield Potential 76
Hypothesis 2 82
Soil Organic Carbon 82
Respiration 82
Erosional Factor 84
Soil Organic Carbon 86
Chapter Six Conclusion and Recommendations 94
List of References 96
Appendix 103
A.1 Soil compositions 104
A.2 Calibrations 109
A.3 Modified sWUE = yields/((ET+runoff+drainage)/precipitation) 119
A.3.1 Corn 119
A.3.2 Soy 123
A.3.3 Cotton 127
A.4 sWUE Projected Climate Histograms 131
A.4.1 Corn 131
A.4.2 Soy 133
A.4.3 Cotton 135
Vita 137

LIST OF TABLES

Table 4-1: Values for the RC and Slope Classes....23
Table 4-2: Means and Extremes of each Class with associated county....24
Table 4-3: Class A Mean and Extreme Characteristics....28
Table 4-4: Class B Mean and Extreme Characteristics....28
Table 4-5: Class C Mean and Extreme Characteristics....29
Table 4-6: Class D Mean and Extreme Characteristics....29
Table 4-7: Class E Mean and Extreme Characteristics....30
Table 4-8: Composition of major soil types (Soil Survey 2016)....33
Table 4-9: Planting dates, harvest dates, and management rotation....34
Table 4-10: Climate Corn Growing Season Precipitations (mm) for A-Mean....40
Table 4-11: Climate Soy Growing Season Precipitations (mm) for A-Mean....40
Table 4-12: Climate Cotton Growing Season Precipitations (mm) for A-Mean....40
Table 5-1: Maximum Precipitation Point on Curve Corresponding to Optimal Utilization of Water....64
Table 5-2: Ordering of predicted sWUE of each location based on slope and shape....66
Table 5-3: Predicted and sWUE values based on shape and slope....70
Table 5-4: Climate projections of modified sWUE (kg ha-1) slopes for corn....72
Table 5-5: Climate Means of modified sWUE (kg ha-1) slopes for soy....73
Table 5-6: Climate slope of modified sWUE (kg ha-1) for cotton....74
Table 5-7: Distribution statistics for all locations and all climates for each crop, annual values....78
Table 5-8: Corn distribution statistics for all locations for each projected climate, annual values....79
Table 5-9: Soy distribution statistics for all locations for each projected climate, annual values....79
Table 5-10: Cotton distribution statistics for all locations for each projected climate, annual values....80
Table A.1-1: Soil composition location A-Mean....104
Table A.1-2: Soil composition location B-Mean....104
Table A.1-3: Soil composition location C-Mean....105
Table A.1-4: Soil composition location D-Mean....105
Table A.1-5: Soil composition location E-Mean....106
Table A.1-6: Soil composition location A-Extreme....106
Table A.1-7: Soil composition location B-Extreme....107
Table A.1-8: Soil composition location C-Extreme....107
Table A.1-9: Soil composition location D-Extreme....108
Table A.1-10: Soil composition location E-Extreme....108

LIST OF FIGURES

Figure 1-1: Effects of climate change and population increase....2
Figure 2-1: Water balance for a typical crop....5
Figure 2-2: Corn growth stages and water use per stage (Kranz 2008)....9
Figure 2-3: Impact on anaerobic conditions....14
Figure 2-4: Relationship of soil water leading to yields....15
Figure 4-1: Obion River Watershed, depicting the Kentucky and Tennessee portions (left), and Obion HUC-8 and South Fork HUC-8 (right)....20
Figure 4-2: Five Hydrologic Response Groups....23
Figure 4-3: Obion Watershed with Mean and Extreme VIC Identified Areas....25
Figure 4-4: Example of (a). GeoWEPP DEM input of the stream network area, (b). GeoWEPP output of the stream network and hillslopes, and (c). A-Mean VIC identified area with hillslopes....26
Figure 4-5: Example of a Hillslope in WEPP....27
Figure 4-6: Slope Profiles....27
Figure 4-7: Organic Matter Data....31
Figure 4-8: Typical land use distribution in the Obion Watershed, (USDA 2016)....32
Figure 4-9: Corn and Soy Calibration for A-Mean Location....36
Figure 4-10: Cotton Calibration for A-Mean Location....36
Figure 4-11: Annual average temperature for past and 4.5 climate projections....39
Figure 4-12: Annual average temperature for past and 8.5 climate projections....39
Figure 5-1: Corn crop yield projections for climate HadG 4.5....42
Figure 5-2: Soy crop yield projections for climate HadG 4.5....42
Figure 5-3: Cotton crop yield projections for climate HadG 4.5....43
Figure 5-4: Corn WEPP, VIC, and Modis ET Comparison for past 2007 data....45
Figure 5-5: Corn WEPP, VIC, and Modis ET Comparison for past 2008 data....45
Figure 5-6: Corn WEPP, VIC, and Modis ET Comparison for past 2009 data....46
Figure 5-7: Corn WEPP, VIC, and Modis ET Comparison for past 2010 data....46
Figure 5-8: Corn WEPP, VIC, and Modis ET Comparison for past 2011 data....47
Figure 5-9: Comparison of ET values from WEPP data and Sanford and Selnick (2013)....47
Figure 5-10: Fraction of ET and Precipitation for the Obion Watershed....48
Figure 5-11: Corn WUE for Past Climate based on Hamilton et al. (2015) WUE Method....49
Figure 5-12: Soy WUE for Past Climate based on Hamilton et al. (2015) WUE Method 49
Figure 5-13: Cotton WUE for Past Climate based on Hamilton et al. (2015)WUE Method....50
Figure 5-14: Differences in the ET measurement between two WUE calculation methods....51
Figure 5-15: Corn WUE for Past Climate based on (Dietzel et al. 2016) WUE method..51
Figure 5-16: Soy WUE for Past Climate based on (Dietzel et al. 2016) WUE method ...52
Figure 5-17: Cotton WUE for Past Climate based on (Dietzel et al. 2016) WUE method....52
Figure 5-18: A-Mean Corn and Soy WUE and harvest yield for GFDL RCP 4.5....53
Figure 5-19: A-Mean RCP 4.5 projected yearly cumulative precipitation....54
Figure 5-20: Water stresses on corn for a projected high precipitation year....55

Figure 5-21: Water stresses on corn for a projected low precipitation year 56
Figure 5-22: Harvested yield for corn, year 2043 is a low yield year 56
Figure 5-23: Water stresses on corn with the identification of the crop's critical stage ... 57
Figure 5-24: Corn Water and Temperature stresses with the identification of the critical stage 58
Figure 5-25: Corn sWUE for projected past climate scenario with added drainage 59
Figure 5-26: Soy sWUE for projected past climate scenario with added drainage 60
Figure 5-27: Cotton sWUE for projected past climate scenario with added drainage 60
Figure 5-28: Corn Water Stresses for 2007 61
Figure 5-29: sWUE/Corn Growing Season Precipitation for the entire Obion Watershed 62
Figure 5-30: sWUE/Soy Growing Season Precipitation for the entire Obion Watershed 63
Figure 5-31: sWUE/Cotton Growing Season Precipitation for the entire Obion Watershed 63
Figure 5-32: Yield / Corn Growing Season Precipitation for GFDL 4.5 projection 64
Figure 5-33: sWUE / Corn Growing Season Precipitation for GFDL 4.5 projection 65
Figure 5-34: Average corn sWUE values for past 2005-2011 67
Figure 5-35: Average corn sWUE values for all projected future climate 67
Figure 5-36: Average soy sWUE for past 2005-2011 68
Figure 5-37: Average soy sWUE values for all future projected climates 68
Figure 5-38: Average cotton sWUE for past 2005-2011 69
Figure 5-39: Average cotton sWUE Values for all future projected climates 69
Figure 5-40: Modified corn sWUE for past climate of 2005-2011 71
Figure 5-41: Modified soy sWUE for past climate of 2005-2011 71
Figure 5-42: Modified cotton sWUE for past climate of 2005-2011 72
Figure 5-43: Climate GFDL 4.5 modified sWUE (kg ha-1) for corn 73
Figure 5-44: Climate GFDL 4.5 of modified sWUE (kg ha-1) for soy 74
Figure 5-45: Climate GFDL 4.5 of modified sWUE (kg ha-1) for cotton 75
Figure 5-46: Modified corn sWUE values (kg ha-1) for all locations and climate projections 77
Figure 5-47: Modified soy sWUE values (kg ha-1) for all locations and climate projections 77
Figure 5-48: Modified cotton sWUE values (kg ha-1) for all locations and climate projections 78
Figure 5-49: Average yield potential 81
Figure 5-50: Parts of the SOC time-step including crop input, respiration, and erosional effects 82
Figure 5-51: R Term for the months of year 2043 in GFDL 4.5 Corn-Soy rotation 83
Figure 5-52: Monthly E Term values for GFDL 4.5 Corn-Soy rotation 84
Figure 5-53: Stages of plant cycle showing surface residue, submerged residue, and dead roots 85
Figure 5-54: Example of the three types of litter, submerged, dead roots, and surface .. 86
Figure 5-55: Monthly SOC for GFDL 4.5, Corn-Soy management for 2012-2050 88
Figure 5-56: Monthly % OM for GFDL 4.5, Corn-Soy management for 2012-2050 88
Figure 5-57: Monthly SOC for GFDL 4.5, Cotton-Soy management for 2012-2050 89
Figure 5-58: Monthly % OM for GFDL 4.5, Cotton-Soy management for 2012-2050 89
Figure 5-59: Evaluation of SOC terms 90
Figure 5-60: SOC results per decade for Corn-Soy, E-Mean, and 4.5 RCPs 90
Figure 5-61: SOC results per decade for Corn-Soy, E-Mean, and 8.5 RCPs 91

Figure 5-62: SOC results per decade for Cotton-Soy, E-Mean, and 4.5 RCPs 91
Figure 5-63: SOC results per decade for Cotton-Soy, E-Mean, and 8.5 RCPs 92
Figure 5-64: Percentage of water by volume (Hudson, 1994) 93
Figure A.2-1: A-Mean Corn and Soy Calibration 109
Figure A.2-2: A-Mean Cotton Calibration 109
Figure A.2-3: B-Mean Corn and Soy Calibration 110
Figure A.2-4: B-Mean Cotton Calibration 110
Figure A.2-5: C-Mean Corn and Soy Calibration 111
Figure A.2-6: C-Mean Cotton Calibration 111
Figure A.2-7: D-Mean Corn and Soy Calibration 112
Figure A.2-8: D-Mean Cotton Calibration 112
Figure A.2-9: E-Mean Corn and Soy Calibration 113
Figure A.2-10: E-Mean Cotton Calibration 113
Figure A.2-11: A-Extreme Corn and Soy Calibration 114
Figure A.2-12: A-Extreme Cotton Calibration 114
Figure A.2-13: B-Extreme Corn and Soy Calibration 115
Figure A.2-14: B-Extreme Cotton Calibration 115
Figure A.2-15: C-Extreme Corn and Soy Calibration 116
Figure A.2-16: C-Extreme Cotton Calibration 116
Figure A.2-17: D-Extreme Corn and Soy Calibration 117
Figure A.2-18: D-Extreme Cotton Calibration 117
Figure A.2-19: E-Extreme Corn and Soy Calibration 118
Figure A.2-20: E-Extreme Cotton Calibration 118
Figure A.3.1-1: Corn Modified sWUE for GFDL RCP 4.5 119
Figure A.3.1-2: Corn Modified sWUE for HadG RCP 4.5 119
Figure A.3.1-3: Corn Modified sWUE for IPSL RCP 4.5 120
Figure A.3.1-4: Corn Modified sWUE for MIRO RCP 4.5 120
Figure A.3.1-5: Corn Modified sWUE for GFDL RCP 8.5 121
Figure A.3.1-6: Corn Modified sWUE for HadG RCP 8.5 121
Figure A.3.1-7: Corn Modified sWUE for IPSL RCP 8.5 122
Figure A.3.1-8: Corn Modified sWUE for MIRO RCP 8.5 122
Figure A.3.2-1: Soy Modified sWUE for GFDL RCP 4.5 123
Figure A.3.2-2: Soy Modified sWUE for HadG RCP 4.5 123
Figure A.3.2-3: Soy Modified sWUE for IPSL RCP 4.5 124
Figure A.3.2-4: Soy Modified sWUE for MIRO RCP 4.5 124
Figure A.3.2-5: Soy Modified sWUE for GFDL RCP 8.5 125
Figure A.3.2-6: Soy Modified sWUE for HadG RCP 8.5 125
Figure A.3.2-7: Soy Modified sWUE for IPSL RCP 8.5 126
Figure A.3.2-8: Soy Modified sWUE for MIRO RCP 8.5 126
Figure A.3.3-1: Cotton Modified sWUE for GFDL RCP 4.5 127
Figure A.3.3-2: Cotton Modified sWUE for HadG RCP 4.5 127
Figure A.3.3-3: Cotton Modified sWUE for IPSL RCP 4.5 128
Figure A.3.3-4: Cotton Modified sWUE for MIRO RCP 4.5 128
Figure A.3.3-5: Cotton Modified sWUE for GFDL RCP 8.5 129
Figure A.3.3-6: Soy Modified sWUE for HadG RCP 8.5 129
Figure A.3.3-7: Cotton Modified sWUE for IPSL RCP 8.5 130
Figure A.3.3-8: Cotton Modified sWUE for MIRO RCP 8.5 130
Figure A.4.1-1: GFDL 4.5 and 8.5 Corn Modified sWUE histograms 131
Figure A.4.1-2: Had 4.5 and 8.5 Corn Modified sWUE histograms 131

Figure A.4.1-3: IPSL 4.5 and 8.5 Corn Modified sWUE histograms 132
Figure A.4.1-4: MIR 4.5 and 8.5 Corn Modified sWUE histograms 132
Figure A.4.2-1: GFDL 4.5 and 8.5 Soy Modified sWUE histograms 133
Figure A.4.2-2: Had 4.5 and 8.5 Soy Modified sWUE histograms 133
Figure A.4.2-3: IPSL 4.5 and 8.5 Soy Modified sWUE histograms 134
Figure A.4.2-4: MIR 4.5 and 8.5 Soy Modified sWUE histograms 134
Figure A.4.3-1: GFDL 4.5 and 8.5 Cotton Modified sWUE histograms 135
Figure A.4.3-2: Had 4.5 and 8.5 Cotton Modified sWUE histograms 135
Figure A.4.3-3: IPSL 4.5 and 8.5 Cotton Modified sWUE histograms 136
Figure A.4.3-4: MIR 4.5 and 8.5 Cotton Modified sWUE histograms 136

ABBREVIATIONS

A – impact factor
bd – bulk density ($\mathrm{kg\ m^3}$)
B_i- biomass
$B_{p,i}$ - potential increase in biomass
$°C - Celsius$
CEC - cation exchange capacity $(meq\ 100\ g^{-1})$
CENTURY – SOM computer model
$\mathrm{CO_2}$ – carbon dioxide
D – depth (m)
defac - adjustment for soil temperature and moisture
DEM - digital elevation model
E – amount of carbon loss due to erosion ($\mathrm{kg\ m^2}$)
$\mathrm{e_a}$ - actual vapour pressure (kPa)
$\mathrm{e_s}$ - saturation vapour pressure (kPa)
ER – enrichment ratio
$\mathrm{EROD_{Net}}$ - net erosion (mm)
ET – evapotranspiration (mm)
$\mathrm{ET_o}$ = $\mathrm{E_u}$ - potential evapotranspiration $(\mathrm{mm\ d^{-1}})$
$\mathrm{E_{sp}}$ - potential soil evaporation (mm)
$\mathrm{E_{tp}}$ - plant transpiration (mm)
F – crop input ($\mathrm{kg\ m^2}$)
°F – degree Fahrenheit
FC – field capacity
$fmaterial\ p$ – proportion of size fraction
fr – mass proportions in each fraction size
G - soil heat flux density (MJ $\mathrm{m^{-2}day^{-1}}$)
GDD – growing degree days °C
GEOWEPP – GIS version of WEPP
GFDL – GFDL-ESM2M Geophysical Fluid Dynamics Laboratory
GIS - Geographic Information System
h – depth (m)
ha - hectare
HadG – HADGEM2-CC – Hadley Global Environmental Model 2 – Carbon Cycle
HUC – Hydrologic Unit Code
IPSL – IPSL-CM5A-MR – Institute Pierre Simon Laplace – Climate Model
J - joule
$\mathrm{K_c}$ – crop coefficient
Kg - kilogram
$\mathrm{K_i}$ - first order decomposition constant 0.536
L - leaf area index
m – meter

MIRO – MIRCO-ESM-CHEM – Model for Interdisciplinary Research on Climate – Earth System Model
Modified sWUE – Modified system water use efficiency ($\mathrm{kg\ ha^{-1}}$)
OM – organic matter
P – precipitation (mm)
PET – potential evapotranspiration
R – respiration adjustment for soil temperature and moisture of SOC ($\mathrm{kg\ m^{2}}$)
RC – runoff coefficient
RCP - representative concentration pathways
$\mathrm{R_n}$- net raditation at the crop surface ($\mathrm{MJ\ m^{-2} day^{-1}}$)
RWC – relative water content
RZ - root zone depth (m)
SOC – soil organic carbon ($\mathrm{kg\ m^{2}}$)
SSA - specific surface area ($m^2 g^{-1}$)
Stemp – soil temperature (°C)
SWC - soil water content
sWUE – systems water use efficiency ($\mathrm{kg\ mm^{-1} ha^{-1}}$)
T - mean daily air temperature at 2 meters of height (°C)
T_a - average daily temperatures (°C)
TBCA - total below ground carbon allocation
T_b - base temperature of the crop (°C)
teff – soil temperature constants
tfunc – soil temperature correction factor
$T_{\max}$- maximum temperature of the crop (°C)
$T_{\min}$ – minimum temperature of the crop (°C)
TN - Tennessee
T_o - optimum temperature of the crop (°C)
TS – temperature stresses
U_i – actual water use in soil layer i
$\mathrm{UL_i}$ - upper limit of soil water content in each layer i
$\mathrm{U_{Pi}}$ - potential water use from layer i
$\mathrm{U_2} - \mathrm{mean\ daily\ wind\ speed\ at\ 2m\ height\ (m\ s^{-1})}$
V - rate-depth parameter
VIC - Variable Infiltration Capacity
WEPP - Water Erosion Prediction Project
wfunc – soil moisture correction factor
WP – wilting point
W_s - water stresses
WUE – water use efficiency ($\mathrm{kg\ mm^{-1} ha^{-1}}$)
γ - psychrometric constant ($\mathrm{kPa\ °C^{-1}}$)
Δ - slope vapor pressure curve ($\mathrm{kPa\ °C^{-1}}$)
Θ_i - soil water content in each layer i
Θ_c - critical soil water

CHAPTER ONE
INTRODUCTION AND GENERAL INFORMATION

Increasing food demands from an escalating world population call for an intensification of high-production agriculture. However, the accompanying increases in tillage and fertilizer use can threaten long-term soil health and local water quality due to the removal of soil, organic matter, and nutrients from the landscape through enhanced erosion and leaching to surface and ground water stores.

The effects of intensifying land management on soil and water quality are exasperated by a changing climate. The climate is predicted to become more variable as precipitation, temperature, and solar radiation will fluctuate much more frequently between extremes (e.g., droughts and floods). This increased variability will manifest itself in agriculture through changes in crop yields, i.e., yield gaps (Southworth et al. 2000). However, the climate modification does not automatically translate linearly to agriculture making it difficult to forecast.

The need to sustain adequate soil moisture throughout the growing season will become a primary challenge as expected temperature increases and rainfall pattern changes over the next 50 years will affect water availability. Yet, when analyzing the availability of water and the resulting yields, organic matter stocks must also be considered. Higher levels of organic matter produce a greater soil water holding capacity. When water is scarce, this enhanced ability to store water can help the plant survive (e.g., Papanicolaou et al. 2015a). Additionally, the organic matter limits erosion by holding the soil particles together (Papanicolaou et al. 2015b).

The intensification of industrial agriculture is predicted to deplete organic matter stocks through enhanced erosion. Understanding better the importance of a soil's ability to hold water effectively in times of ample and scarce water availability provides insight to better management for sustaining high yields in uncertain times.

The task of developing a sustainable management is difficult due to the connections between climate, the availability of water, soil moisture, erosion, and soil organic carbon (SOC) loss, as demonstrated through the connections of different processes in Figure 1-1. A combined top-down, bottom-up approach is needed to investigate the effects of future climate on crop production in intensively managed agroecosystems. The top-down component can identify areas of great concern, while the bottom-up approach can capture the cause and effect relations between these processes using more mechanistic tools.

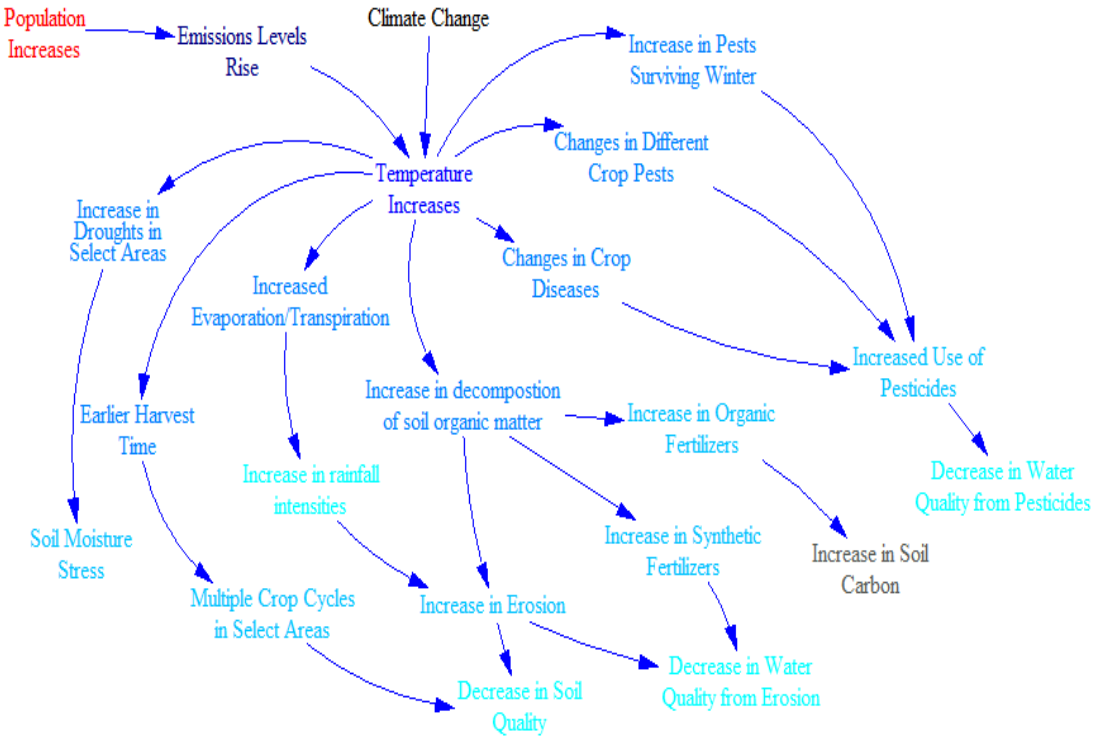


Figure 1-1: Effects of climate change and population Increase

The main objective of this study is to develop a top-down, bottom-up framework to investigate the effects of future climate on crop production in an intensively managed watershed of the Mississippi River Basin, a leading crop producer for the world. The top-down approach for this study uses outputs of a macro-scale hydrologic model, the Variable Infiltration Capacity model, or VIC (Liang et al. 1994), to identify representative

hydrologic response areas in the Obion River, TN watershed. These response areas help identify where soil moisture concerns can appear in the future, as seen through changes in infiltration. The changing infiltration is characterized by the product of the Runoff Coefficient (RC) and slope for each cell in the VIC model. This metric allows areas to be evaluated on its gradient and infiltration, both factors ultimately leading to potential impacts to crop yields.

Each response area is assessed further at a finer scale by selecting specific hillslopes for a bottom-up analysis. Specific hillslopes are chosen based on crop rotation and location. The primary commodity crops that are commonly found within the Obion watershed include corn, soybean, and cotton. The rotations of these crops are input into the Water Erosion Prediction Project model (WEPP) program (WEPP version 2012.8)(e.g., Flanagan and Nearing 1995, Savabi and Williams 1995, Alberts et al. 1995, Arnold et al. 1995, Stott et al. 1995, Foster et al. 1995, Nicks et al. 1995).

This study runs continuous simulations, which include past and projected climate periods. Projected future climate, until 2050, follows two representative concentration pathways (RCP). These climate projections, RCP 4.5 and RCP 8.5, represent average and extreme CO_2 emission scenarios (Stocker et al. 2013).

This study will use the RCPs from four Global Circulation Models: GFDL (GFDL-ESM2M), HadG (HadGEM2-CC), IPSL (IPSL-CM5A-MR), and MIRO (MIRCO-ESM-CHEM). Climate models were selected based on Gustafson et al. (2015) and datasets were downloaded from Multivariate Adaptive Constructed Analogs (MACA 2016).

The resulting outputs of evapotranspiration, erosion, and crop yields are used to quantify the changes in the Water Use Efficiency (WUE), which relates to the amount of biomass produced per unit of water, and organic matter (specifically SOC).

This thesis is organized into six chapters. Chapter 1 gives a background for the purpose of this study, its main objective and approach. Chapter 2 establishes a literary review and the analysis within three subsections; evapotranspiration, soil moisture, and water stress, water use efficiency, and soil organic carbon. Chapter 3 introduces the hypotheses that this study tests. Chapter 4 goes into detail regarding the study's design with subsections related to the location, models that were used, and the two approaches of this thesis, top-down and bottom-up. Chapter 5 discusses the findings for each hypothesis. Chapter 6 summarizes the results for the hypotheses of this study, potential impacts and solutions.

An overview of the analyze in this thesis is as follows:

1. This study explores the role of climate modification on soil moisture and soil quality through the use of 8 different climate projection models.
2. The study design has a two-way approach, top-down and bottom-up.
    a. The top-down approach uses the output of a VIC model to identify areas of interest with critical low soil water holding capacity within the Obion Watershed.
    b. These areas of interests are then analyzed with a bottom-up approach, with the aid of WEPP software, in order to quantify soil moisture and crop yields at the hillslope scale.
3. Hypothesis 1 is addressed by using various water use efficiency definitions:
    a. Hamilton et al (2015) definition of WUE relating biomass to evapotranspiration (ET).
    b. Dietzel et al. (2016) definition of WUE relating yields to ET.
    c. Dietzel et al (2016) definition of a system water use efficiency (sWUE) relating yields to ET, runoff, and drainage.
    d. Modifying the sWUE definition by normalizing ET, runoff, and drainage with precipitation.
4. Hypothesis 2 is addressed by using equations derived from CENTURY software (Metherell et al. 1993).

CHAPTER TWO

LITERATURE REVIEW AND ANALYSIS BACKGROUND

This section contains an outline and review of the significant variables and equations used in this study. In addition, each hypothesis is addressed in subsequent subsections, water use efficiency and soil organic carbon, along with the framework and literary review of the calculations.

Evapotranspiration, Soil Moisture and Water Stress

The water balance, as seen in Figure 2-1, encompasses many parameters that affect crop growth. In this study, all aspects of the water balance are important with the goal to target the water content in the soil and its relation to crop yields.

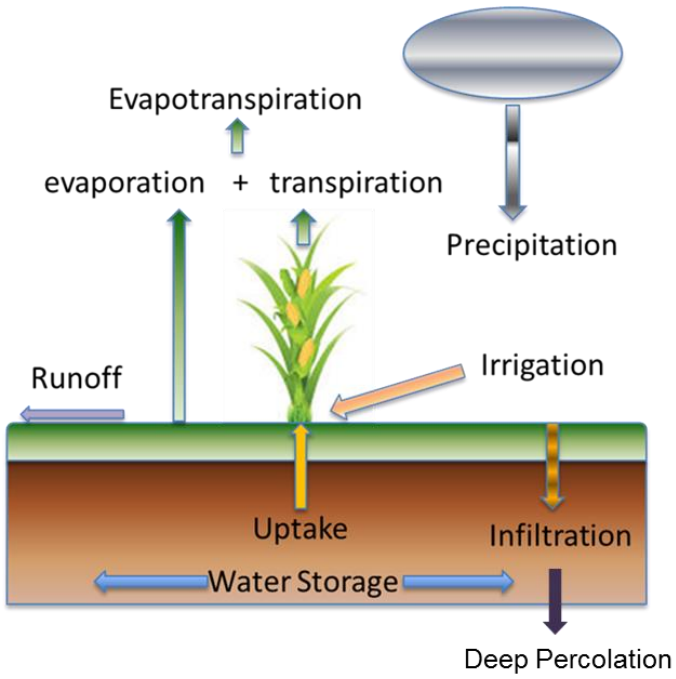


Figure 2-1: Water balance for a typical crop

The amount of moisture that resides in the upper portion of the soil column is most relevant to crop yields (Zipper et al. 2015). ET, which is the combination of soil

evaporation from the bare ground and the transpiration from vegetative cover, strongly influences the moisture of this upper soil layer. It is the layer from which evaporation can occur and in which plant roots grow (Verstraeten et al. 2008). ET in the United States varies significantly both spatially and temporally; however, the mean annual ET is highest in the Southeast, where it averages over 762 mm/yr and it can even exceed precipitation inputs during the summer months leading to soil water deficits (Sanford and Selnick 2013).

Models such as WEPP and VIC can estimate ET using the Penman-Monteith equation (Allen et al. 1998) which calculates the daily potential evapotranspiration, ET_0 (mm d^{-1}).

$$\mathrm{ET_o} = \mathrm{E_u} = \frac{0.408\Delta(\mathrm{R_n}-\mathrm{G})+\gamma\frac{900}{\mathrm{T}+273}\mathrm{U_2}(\mathrm{e_s}-\mathrm{e_a})}{[\Delta+\gamma(1+0.34\mathrm{U_2})]} \quad (2\text{-}1)$$

Where Δ = slope vapor pressure curve (kPa $^{o}C^{-1}$); Rn = net radiation at the crop surface (MJ m^{-2} d^{-1}); U_2 = mean daily wind speed at 2m height (m s^{-1}); T = mean daily air temperature at 2 meters of height (°C); G = soil heat flux density (MJ m^{-2} d^{-1}); e_s = saturation vapor pressure (kPa); e_a = actual vapor pressure (kPa); and γ = psychrometric constant (kPa $^{o}C^{-1}$). The Penman-Monteith method is recommended for calculating ET since it is applicable to multiple locations and climates. It also includes surface resistance and aerodynamic transfer allowing ET peaks to be captured (Allen et al. 1998). Other methods, such as the modified Penman equation can overestimate ET by as much as 20%.

ET_0 is then multiplied with a crop coefficient, K_c. The crop coefficients for a multitude of crops and plants can be found in the Food and Agriculture Organization (FAO) Irrigation And Drainage Paper No. 56 (Allen et al. 1998). The K_c term relating to the mid-season of the crop is the value used in WEPP. For this study the calculated K_c coefficient for corn is 1.20, soy is 1.15, and cotton is 1.18.

A soil depletion term is also needed and is obtained from the FAO Irrigation and Drainage Paper No. 56. For this study, 0.55 is used for corn, 0.50 for soy, and 0.65 for cotton. This value considers the fraction of water that can be depleted before moisture stress occurs for each particular crop.

ET_o can be used to determine the amount of water needed for optimal growth. By comparing this value to the amount of water available in the water column, it can be determined if the plant is under water stress. U_{Pi} is the potential water use from layer *i*, which is determined using the following equation:

$$\mathrm{U_{Pi}} = \frac{\mathrm{E_{tp}}}{1-\mathrm{e^{(-V)}}}\left(1-\ \mathrm{e^{\left(-\mathrm{V}\frac{\mathrm{h_i}}{\mathrm{RZ}}\right)}}\right) - \sum_{\mathrm{j=1}}^{\mathrm{i-1}} \mathrm{U_j} \qquad (2\text{-}2)$$

Where E_{tp} is the potential plant transpiration; V is a rate-depth parameter based on use with a default value of 3.065; h is depth; RZ is the root zone depth; and U is the actual water use. E_{tp} is calculated through the following equation:

$$\mathrm{E_{tp}} = (1 - \mathrm{e^{(-0.4\ L)}})\mathrm{ET_0} \qquad (2\text{-}3)$$

The actual water use must be adjusted for water stress and is obtained based on the following parameters:

$$\mathrm{U_i} = \mathrm{U_{Pi}},\ \Theta_\mathrm{i} > \Theta_\mathrm{c}\,\mathrm{UL_i} \qquad (2\text{-}4)$$

$$\mathrm{U_i} = \mathrm{U_{Pi}}\frac{\Theta_\mathrm{i}}{\Theta_\mathrm{c}\,\mathrm{UL_i}},\ \Theta_\mathrm{i} < \Theta_\mathrm{c}\,\mathrm{UL_i} \qquad (2\text{-}5)$$

Where θ_i is each layer's soil water content; and θ_c is the minimum amount of soil water needed before the plant experiences water stress. It is a crop dependent value. U_{Li} is each layer's upper limit of soil water content. Once the U_{Pi} value is adjusted, it becomes the actual water use, U_i. This value is used in the water stress equation:

$$W_s = \frac{\sum_{i=1}^{n} U_i}{E_{tp}} \quad (2\text{-}6)$$

If W_s equals 1, then no stress is experienced. Values less than 1 indicate a water stress. This value shows not only the amount that doesn't affect crop yields, through crop stress, but if it necessitates irrigation.

In addition to the water stress, temperature stresses can profoundly affect crop growth (Hatfield and Prueger 2015). WEPP calculates the temperature stresses (*TS*) by accounting for the average daily temperatures (T_a), the base temperature of the crop (T_b), and crop's optimum temperature (T_o).

$$TS = sin\left(\frac{\pi}{2} * \frac{T_a - T_b}{T_o - T_b}\right) \quad (2\text{-}7)$$

Similarly, a value of 1 indicates no temperature stress whereas a value less than 1 indicates stress. If either a water or temperature stress is determined, then the smaller of these two values is used as the regulator (*REG*) for determining biomass, $Bi_,$ in WEPP.

$$\Delta B_i = \Delta B_{p,i} * REG \quad (2\text{-}8)$$

Where $B_{p,i}$ is the potential increase in biomass. If a crop is under stress than the generated biomass is less than its potential.

Stresses during critical crop stages have a profound effect on biomass and yield. There are varying levels of importance of stages that are affected by stresses for each crop. Figure 2-2 lists the stages of corn and the approximate water use requirements for each stage (Kranz 2008). These stages vary from year to year and differ for crops planted at the same date but are located in different regions. A means of determining a crop's stage is estimated from growing degree days (*GDD*).

$$GDD = \frac{(T_{max}+T_{\min})}{2} - T_{\mathrm{b}} \quad (2\text{-}9)$$

The maximum (T_{max}) and minimum (T_{min}) temperatures of the crop are calculated along with its base (T_b) temperature, below which growth does not occur. *GDD* values accumulate during the crop growing season. The R1 stage of corn occurs at 1400 *GDD* °F or 660 GDD °C (Neild and Newman 1987).

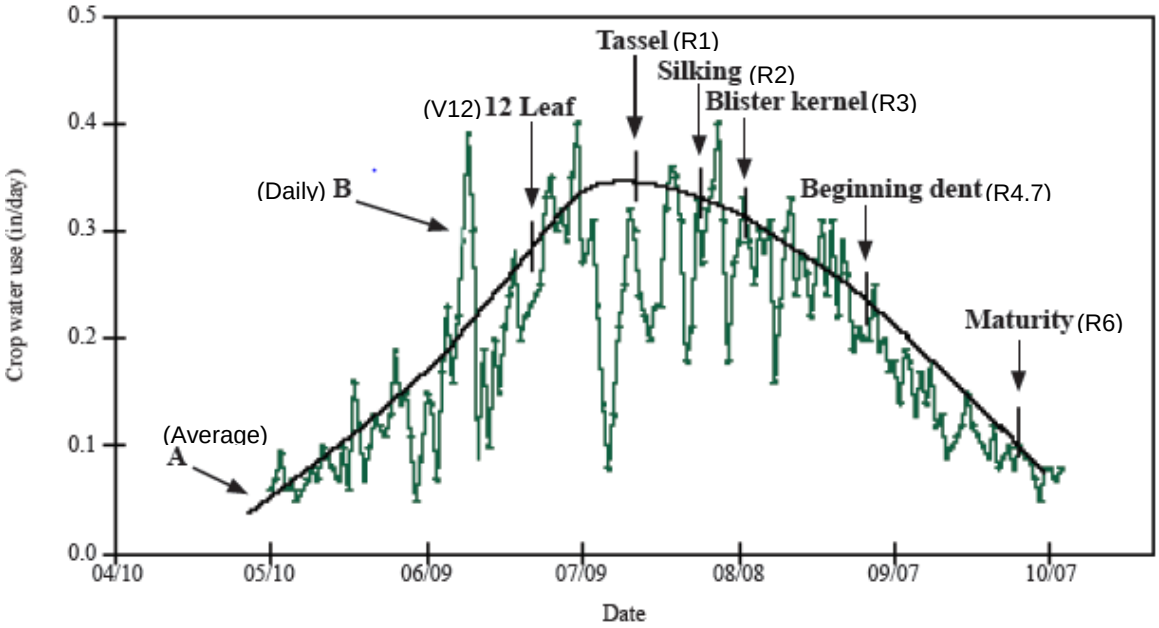


Figure 2-2: Corn growth stages and water use per stage (Kranz 2008)

Angel et al. (2017) defines two significant corn stages that are susceptible to stress as the silk and black layer stages. The silks are part of the corn plant's flowers and a future kernel for the season. The R1 stage of corn, where corn silks emerge, has significant harvest yield reductions if water stress occurs during this time. Other corn stages such as R2 and R3, where stress contributes to kernel loss, also have yield reduction characteristics, but certain stages are more significant than others (Abendroth et al. 2009).

Soybean's critical stage occurs after flowering completes and during seed growth, between stages R4.5 and 5.5 (Casteel, 2010). Stress experienced during this timeframe results in a reduction of the number of pods and is reflected in the yield. The end of soybean's key critical stage is marked by the plant's full seed capacity (Lee et al.2007). The cotton plant's critical time for water stress occurs between first square when the fruit bud begins to form and first flower (Bauer et al. 2012).

Programs, such as the U2U Corn Growing Degree Day Tool (Angel et al. 2017), provide site specific estimates for critical stages such as the silking and black layer dates. Targeting irrigation during these identified projected high stress years lead to an increase in crop yields. This contributes towards more efficient precision farming practices.

Water Use Efficiency

As shown above, ET and soil moisture are related. Additionally, ET can provide a sense of how much water a plant needs. Taking it one step further, the relationship between ET and crop yields can be seen through the WUE. Again, a broad definition of WUE is the relationship of a crop's water use to its biomass.

Multiple variations to this broad definition have been developed (Sadras et al. 2011), including the following: the maximum above ground live biomass value for the crop season divided by the cumulative ET for the growing season until the maximum biomass measurement (Hamilton et al. 2015).

$$water\ use\ efficiency\left(\frac{kg}{mm*ha}\right) = \frac{maximum\ above\ ground\ live\ biomass\left(\frac{kg}{m^2}\right)*\frac{10{,}000\ m^2}{1\ ha}}{evapotranspiration\ (mm) of\ growing\ season\ up\ until\ biomass\ measurement} \quad (2\text{-}10)$$

The maximum biomass occurs prior to harvest since deterioration of the plant occurs after the crop reaches senescence, and thus biomass decreases.

Another definition of WUE is the relation of the crop yield to the ET of the growing season (Dietzel et al. 2016). This places the timeframe as the growing season and relates it to the resulting crop yields.

$$water\ use\ efficiency\ (WUE)\left(\frac{kg}{mm*ha}\right) = \frac{yield\left(\frac{kg}{m^2}\right)*\frac{10{,}000\ m^2}{1\ ha}}{evapotranspiration\ (mm) of\ growing\ season} \quad (2\text{-}11)$$

Besides water stress occurring from a lack of water, excessive water also has unwanted consequences. More water than is needed for optimal crop yields leads to runoff and potential water quality concerns from excessive fertilizer use.

Dietzel et al. (2016) presents a systems level approach to water use efficiency that considers drainage and runoff along with ET portion. This takes into account efficiency due to the underutilization of water, which previous studies fail to consider.

$$systems-level\ water\ use\ efficiency\ (sWUE)\left(\frac{kg}{mm*ha}\right) = \frac{yield\left(\frac{kg}{m^2}\right)*\frac{10{,}000\ m^2}{1\ ha}}{evapotranspiration\ (mm)+runoff\ (mm)+drainage\ (mm) of\ growing\ season} \quad (2\text{-}12)$$

Soil Organic Carbon

The amount of organic matter, and specifically SOC, in the soil dictates its water holding capacity. The total soil organic carbon (SOC_T) along a hillslope can be determined using a mass balance and equations derived from CENTURY (Metherell et al. 1993).

$$SOC_T\left(\frac{kg}{m^2}\right) = \mathrm{SOC}_{T-1}\left(\frac{kg}{m^2}\right) + \Delta F_T\left(\frac{kg}{m^2}\right) - R_T\left(\frac{kg}{m^2}\right) - E_T\left(\frac{kg}{m^2}\right) \quad (2\text{-}13)$$

Where ΔF_T is the change in crop input; R_T is SOC adjusted for respiration; E_T is the SOC loss from erosion; and T is time.

The initial value of soil organic carbon, SOC_0, is calculated from the initial percentage of organic in the soil layer (Eq. 2-14). It is then multiplied by the volume and bulk density of the hillslope which is then divided by the width and length of the hillslope (Eq. 2-15). The addition of the litter currently on the surface, subsurface, and in the form of dead roots is added to these conditions, after it is converted to SOC (Eq. 2-17).

$$\%\ Organic\ Matter\ (each\ location) * \frac{SOC}{1.73\ OM} = \%\ SOC \quad (2\text{-}14)$$

$$\mathrm{SOC}_0\left(\frac{kg}{m^2}\right) = \frac{\left(\frac{\%\ OC}{100}\right) * length(m) * depth(m) * width(m) * bd\left(\frac{kg}{m^3}\right)}{width\ (m) * length\ (m)} + \left(\mathrm{crop\ residue}_0\left(\frac{kg}{m^2}\right) * \frac{0.43\ kg\ SOC}{1\ kg\ crop\ residue}\right) \quad (2\text{-}15)$$

$$\mathrm{SOC}_0\left(\frac{kg}{m^2}\right) = \left(\frac{\%\ OC}{100}\right) * depth(m) * bd\left(\frac{kg}{m^3}\right) + \left(\mathrm{crop\ residue}_0\left(\frac{kg}{m^2}\right) * \frac{0.43\ kg\ SOC}{1\ kg\ crop\ residue}\right)$$

The crop residue that resides on the surface, subsurface, and from the dead roots is considered as ΔF_T. WEPP calculates the effects of decomposition on the crop residue, including those from water and temperature, in the output.

$$Crop\ residue\left(\frac{kg}{m^2}\right)_T = \left(subsurface\ litter\left(\frac{kg}{m^2}\right) + dead\ roots\left(\frac{kg}{m^2}\right) + surface\ litter\left(\frac{kg}{m^2}\right)\right) \quad (2\text{-}16)$$

$$\Delta F_T\left(\frac{kg}{m^2}\right) = \left(crop\ residue\left(\frac{kg}{m^2}\right)_T - crop\ residue\left(\frac{kg}{m^2}\right)_{T-1}\right) * \frac{0.43\ kg\ SOC}{1\ kg\ crop\ residue} \quad (2\text{-}17)$$

R_T is determined using monthly first order decomposition constant, K_i, which is a weighted average of carbon pools (0.044667):

$$R_T = \mathrm{SOC}_{T-1}\left(\frac{kg}{m^2}\right) * (\mathrm{K_i} * defac * A) \quad (2\text{-}18)$$

It is adjusted due to soil temperature and moisture with a multiplier, *Defac*.

$$Defac = tfunc * wfunc \quad (2\text{-}19)$$

Defac is broken into two parts accounting for soil temperature effects ($tfunc$) and soil moisture effects ($wfunc$) and results in a value between 0-1 (Parton et al. 1998). Where teff1 = 0 (intercept), teff2 = 0.125 (slope), and teff3 = 0.07 (exponent (Q10 value), which is the temperature coefficient that demonstrates temperature sensitivity due to increasing by $10\ ℃$).

$$tfunc = teff1 + e^{teff3 * soil\ temperature} * teff2 \quad (2\text{-}20)$$

The soil temperature is the average of the maximum and minimum air temperature since this is approximately equivalent to the soil temperature in the top layer.

$$soil\ temperature(℃) = \left(\frac{air\ temperature_{\mathrm{maximum}}(℃) + air\ temperature_{minimum}(℃)}{2}\right) \quad (2\text{-}21)$$

Soil moisture effects are considered through the *wfunc* term:

$$wfunc = \frac{1}{1+10*e^{-6*RWC}} \quad (2\text{-}22)$$

Where the relative water content (*RWC*) is the weighted average of each of the soil water layers calculated to a depth of 0.2 m with a value between 0-1.

$$RWC = \frac{\left(\frac{soil\ water\ content\ (m) * area\ (m^2)}{volume\ (m^3)}\right) - WP}{FC - WP} \quad (2\text{-}23)$$

If *RWC* > 1, an impact factor (*A*) is also applied to R_T to account for the dormancy of the microbes due to anaerobic conditions. One of the major contributors to the decomposition of SOC is moisture, but this influence subsides after a certain point. An excess of water in the soil can create anaerobic conditions and reduces the decomposition effects.

The impact factor is derived from CENTURY (Parton et al. 1998) by calculating $\frac{Precipitation + \sum soil\ water\ content}{PET}$. If this value is >1.5 then an impact factor is used, which decreases linearly until it is $\geq$ 3.0. At 3.0, the minimum impact is set at 0.3. If the value is <1.5, then the factor is set at 1 (Figure 2-3).

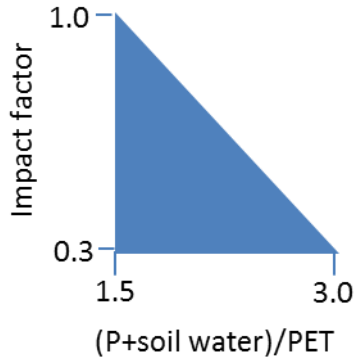


Figure 2-3: Impact on anaerobic conditions

Finally, the amount of SOC loss for each precipitation event is estimated by using net erosion, the bulk density, and enrichment ratio (ER) values. The ER ratio is defined as the amount of SOC contained in the eroded material compared to the amount of SOC in the uneroded soil (Wilson et al. 2016). Soil erosion leads to a decrease in SOC stocks, which decrease in the soil's ability to retain water, and ultimately crop yields (Figure 2-4).

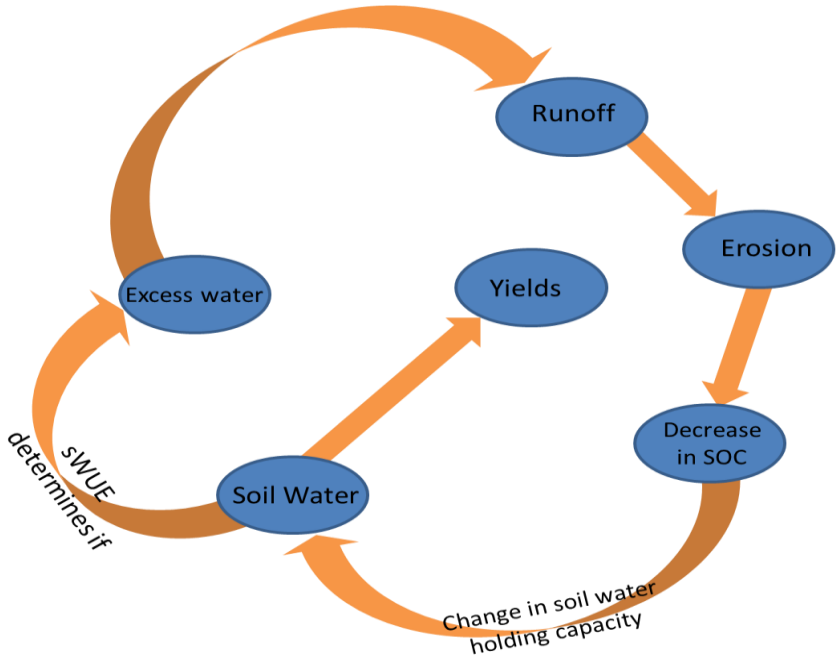


Figure 2-4: Relationship of soil water leading to yields

Determining the amount of SOC loss from erosional effects (*E*) uses the following relationship:

$$\mathrm{E}_T\left(\frac{kg}{m^2}\right) = \mathrm{SOC}_{T-1}\left(\frac{kg}{m^2}\right) * \left(\frac{\mathrm{ER\ (ratio)} * \frac{(\mathrm{EROD_{Net}}\left(\frac{kg}{m}\right))}{length\ (m)}}{\mathrm{bd}\left(\frac{kg}{m^3}\right) * \mathrm{depth(m)}}\right) = \frac{kg}{m^2} \qquad (2\text{-}24)$$

Where SOC is the initial input, WEPP provides the net erosion ($EROD_{Net}$); *bd* is the soil bulk density; *w* is the width of the hillslope, and d is the depth. The depth is evaluated on the top 20 cm, which is considered the active layer (Papanicolaou et al. 2010).

Papanicolaou et al.(2015b) differentiate between the ER values between upslope and downslope zones. Depending on the profile, certain hillslopes will have higher ER values in their upslope region. Profiles with this inclination tend to have a concave shape, this leads to a potential deposition of eroded SOC and higher ER leaving the upslope regions. Whereas ER values in the downslope region ranged from 0.99-1.17

with the higher part of the range correlating with a lower RC value. ER calculations start with the calculation of the specific surface areas (SSA).

$$SSA\left(\frac{m^2}{g}\right) = \sum_{\rho} f_{materialp}\left(\frac{(fr_{sand\,p} * SSA_{sand} + (fr_{silt\,p} * SSA_{silt}) + (fr_{clay\,p} * SSA_{clay})}{1 + fr_{organic\,p}} + \frac{(fr_{organic\,matter\,p} * SSA_{organic})}{1.73}\right) \quad (2\text{-}25)$$

Where $f_{material\,p}$ is the proportional fraction size; *fr* are the mass proportions; and *SSA* are the specific surface areas, using the values of 0.05, 4.0, 20.0, and 1000 $m^2\ g^{-1}$ for sand, silt, clay and SOC respectively). The ER values are determined by taking the ratio of the SSA of the eroded material and SSA of the soil, values greater than 1 indicate that the eroded material has more OM then the soil and less if values are less than 1 (Wilson et al. 2016).

$$ER = \left(\frac{SSA_{Eroded}}{SSA_{Soil}}\right) \quad (2\text{-}26)$$

The resulting value of SOC from equation 2-18 is then converted to organic matter (Papanicolaou et al. 2010) and converted back into a percent organic matter by weight.

$$OM\left(\frac{kg}{m^2}\right) = SOC\left(\frac{kg}{m^2}\right) * 1.73 \quad (2\text{-}27)$$

$$\frac{OM\left(\frac{kg}{m^2}\right)}{density\ of\ soil} = \frac{\frac{OM\left(\frac{kg}{m^2}\right)}{depth\ (m)}}{ending\ month\ of\ average\ bd\ \left(\frac{kg}{m^3}\right)} * 100 = \% \quad (2\text{-}28)$$

This percent organic matter by weight can be used to determine the available water capacity, field capacity, and permanent wilting (Hudson 1994) to determine changes to the system for each climate projection.

CHAPTER THREE
HYPOTHESES

Hypothesis 1

The amount of soil moisture can have a significant effect on resulting crop yields. Differing soil textures and SOC amounts, in turn, can affect the amount of soil moisture retained in the upper layers above the root zone (Papanicolaou et al. 2015a). When the amount of water that is available to particular crops is less than the amount needed, crop yield gaps develop. In addition, if the amount of water that is available is more than the crop needs this also leads to a system underutilization of the available water (i.e., a lower water use efficiency). Underutilization from excess precipitation can present as runoff, runoff leads to erosion, resulting in a degradation of soil and water quality.

A hypothesis is made that amid the impending climate change; there will be a projected decreased response in the utilization of available water due to a decrease in crop yield and /or increase in runoff. This leads to a need for irrigation in drought years to obtain "optimal yields" and preserving water and soil quality during years of abundant precipitation. This study investigates how crops in the Obion River watershed will utilize water with specifically chosen locations within the watershed that represent mean and extreme values forecasted under several climate projections. These climate projections anticipate increases in temperatures and recurrent extreme fluctuations in precipitation. Since crops utilize water differently, corn, soybean, and cotton are examined in this study.

Hypothesis 2

The amount of water that a crop requires to result in optimal crop yields is generally a concern in times of water stress or droughts. Years of ample precipitation, might not correlate with a decline in crop yields, but does depict an inefficient system. This

inefficiency is demonstrated through runoff, a principal cause of soil erosion. Erosion affects SOC and the ability of soil to store water, which in turn influences crop yields.

Erosion is an important factor to consider since excessive erosion leads to a loss in SOC, leading to a reduction in the water storage capacity of the soil, and ultimately reduced crop yields. In addition, the impending climate change is projected to produce an overall temperature increase. This temperature increase leads to accelerated degradation of the SOC. It is hypothesized that the responding change in SOC, due to runoff and erosion, with the addition of anticipated temperature increases, will lead to a decrease in SOC and the soil water holding capacity. This change would demonstrate a potential impact to crop yields.

CHAPTER FOUR
STUDY DESIGN

This chapter describes the design of the study in detail. It commences with a location section explaining the geographic location, area soils, terrain, and land use of the Obion River watershed. The next section explains the use of this study's models, VIC and WEPP, and their contributions. Concluding this chapter is a description of the top-down and bottom-up approaches where the VIC model is used to identify study areas and WEPP is used to analyze these areas at the hillslope scale. Subsections include those related to WEPP inputs of management, climate, and soils.

Geographic Location

This study focuses in two Hydrologic Unit Code (HUC) 8 watersheds, namely the Obion (08010202) and South Fork Obion (08010203). Figure 4-1 illustrates the Obion and South Fork Obion HUC-8s, which are referred herein collectively as the Obion River watershed. The 6400-km^2 Obion River watershed is located primarily in northwestern Tennessee, with a portion in southwestern Kentucky. This part of Tennessee has the highest percentage of row crop production in the state.

The Obion watershed transitions east to west, towards the Mississippi River. In the eastern headwaters, the rolling topography contains north-south bands of sand and clay formations. The local streams have a moderately high gradient over generally sandy substrates. The loess plains in the middle of the watershed also have a gently rolling topography. The hilly areas contain sand, clay, silt, and lignite overlaid by loess that can be 50-60 feet thick, and even deeper in the bluff regions towards the west. Streams in this part of the watershed have silty sand bottoms with low slopes. Many of the stream corridors have been deforested for agricultural purposes. Channel sand plugs have formed where aggradation and driftwood accumulate to form blockages and alter

flow patterns. Along the Mississippi alluvial plain, there are predominantly poor draining clayey soils, sometimes including oxbow lakes and swamps.



Figure 4-1: Obion River Watershed, depicting the Kentucky and Tennessee portions (left), and Obion HUC-8 and South Fork HUC-8 (right)

Land use for the Obion is mostly agriculture (68%), namely croplands and pastured grasslands. Most of the very large farms in the Obion exist along the Mississippi River, with smaller family farms comprising the rest of the watershed. In general, there are two major rotations. Grain rotations consist of corn and soybeans with winter wheat planted as a cover crop or as a double crop. Alternatively, cotton is planted with soybean. The watershed is 80-90% continuous no-till. The remainder of the Obion is covered with forests (28%) with only a small percentage of residential areas.

The annual average precipitation in the watershed over the last 40 years is approximately 1310 mm. The largest portion of rain occurs in the spring and winter, although heavy convective thunderstorms occur in the summer. Additionally, the annual

average temperature is 14.5°C. During the summer, high temperatures and low rainfall often causes ET to become the dominant parameter in the hydrologic cycle.

Models

The Variable Infiltration Capacity model (Liang et al. 1994) was used in this study to identify representative hydrologic response units where soil moisture concerns may develop in the future. The VIC model has been extensively utilized for water resources management, land-atmosphere interactions, and climate change in many large and small basins worldwide (e.g., Sivapalan and Woods 1995; Lohmann et al. 1998; Wu et al. 2007; Houborg et al. 2012).

Using precipitation (and other climate parameters) as input, VIC calculates water balance components including ET, soil moisture, base flow, and runoff for each grid cell at specific time steps. In this study, the cell size was 1 km x 1 km, and the time step was daily but aggregated monthly. The soil characteristics are defined for each cell and held constant over time. One or more vegetation types can describe the surface of each grid cell, and the vegetation characteristics such as LAI, albedo, resistance, roughness root depth and its relative fraction in each soil layer, were assigned for each type.

WEPP is a process-based model that can perform analysis at small watershed scales and hillslopes. (Dermisis et al. 2010 and Papanicolaou and Abaci 2008). Additionally, the Water Erosion Prediction Project (e.g., Abaci and Papanicolaou 2009) is used to capture the cause and effect relations between key processes in Figure 1-1. Ascough et al. (1997) and Flanagan and Livingston (1995) provide additional information regarding WEPP.

For different agricultural fields WEPP calculates erosion and surface runoff under various managements and lands uses for continuous and single storm events (e.g.,

Nearing et al. 1996). WEPP uses Hortonian flow, with infiltration computed from the Green-Ampt, Mein-Larson model (Flanagan et al. 2012). WEPP simulates water-driven, interrill and rill erosion. The 1-D steady-state sediment continuity equation is used to compute the transport, detachment, and deposition of sediment contained in the rills. WEPP contains a robust management section; with inputs that include tillage procedures and various crops.

Two different approaches are used for this study. The top-down approach uses the outputs from a VIC model (Papanicolaou Group, 2017) in order to identify areas of interest with critical low soil water holding capacity within the Obion Watershed. These areas are then assessed with WEPP software from a bottom-up approach. A bottom-up approach estimates soil moisture and crop yields at the hillslope scale.

Top-Down Approach

Recognizing areas where there will be insufficient moisture for crop growth and areas of enhanced erosion and SOC loss is important for establishing the most optimal locations where best management practices should be targeted especially. A combined top-down, bottom-up approach is considered in this study to identify different hydrologic response areas where these soil moisture and SOC concerns may develop.

The initial top-down approach was conducted using VIC and considered the interrelated nature of adequate soil moisture, erosion, SOC loss, and crop productivity. Five different hydrologic response groups are identified (Figure 4-2) based on the RC and slope (Table 4-1) to capture water fluxes and soil moisture retention. In each of the five groups, two 1-km x 1-km grid cells are identified that capture the mean and extreme ranges of the RC and slope product (Table 4-2), one for each group (Papanicolaou et al. 2017).

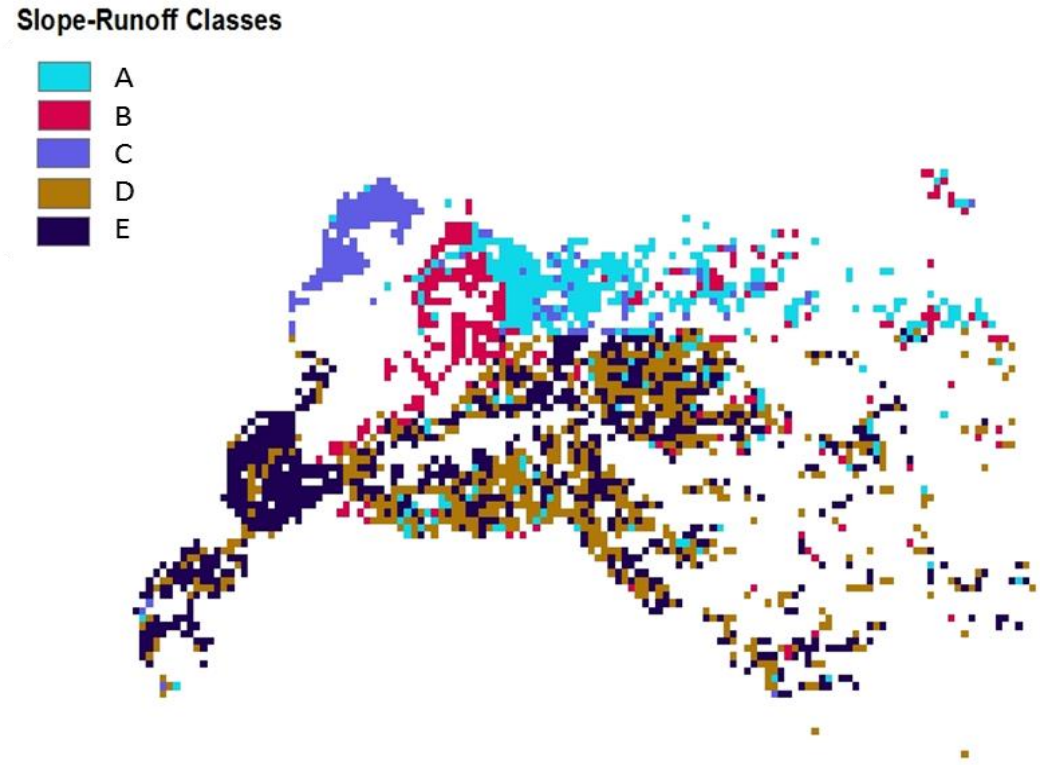


Figure 4-2: Five Hydrologic Response Groups

Table 4-1: Values for the RC and Slope Classes

	Runoff Coefficient				
Slope	0.0-0.5	0.05-0.11	0.11-0.18	0.18-0.23	0.23-0.44
0-1	Class E				Class C
1-5	Class D	Class E	Class D	Class A	Class C
5-10				Class B	
10-17.53				Class B	

Table 4-2: Means and Extremes of each Class with associated county

Location	Class	RC * Slope	County in TN
A-Mean	9	0.67	Obion
A-Extreme	9	1.08	Obion
B-Mean	103	1.74	Obion
B-Extreme	103	2.77	Obion
C-Mean	101	0.26	Lake
C-Extreme	101	1.40	Dyer
D-Mean	104	0.35	Weakley
D-Extreme	104	0.84	Carroll
E-Mean	102	0.12	Dyer
E-Extreme	102	0.43	Gibson

The RC correlates runoff to precipitation, which allows for estimating infiltration. Higher RC values mean there is less infiltration and less soil moisture. Less accessible soil moisture decreases the amount of water available to crops, which can increase crop stresses and lead to a decrease in crop yields. A higher amount of runoff leads to higher erosion values, with impacts to soil quality and potential crop yields. The combination of RC with slope allows for the addition of the area's gradient to be included, which increases the effects from runoff.

By investigating the means and extremes of each group alternating perspectives and therefore conclusions can be derived from the results. This methodology of looking at both the mean and extreme cases will help develop best management practices. Examining the mean cases will help determine if suggested practices can handle the majority of storm event, examining the extreme cases will help determine the limits of the practices. Figure 4-3 shows the resulting five mean and five extreme grid cells areas, and Figure 4-4 shows an example of these regions at a smaller scale (with the 1-kilometer by 1-kilometer area highlighted).

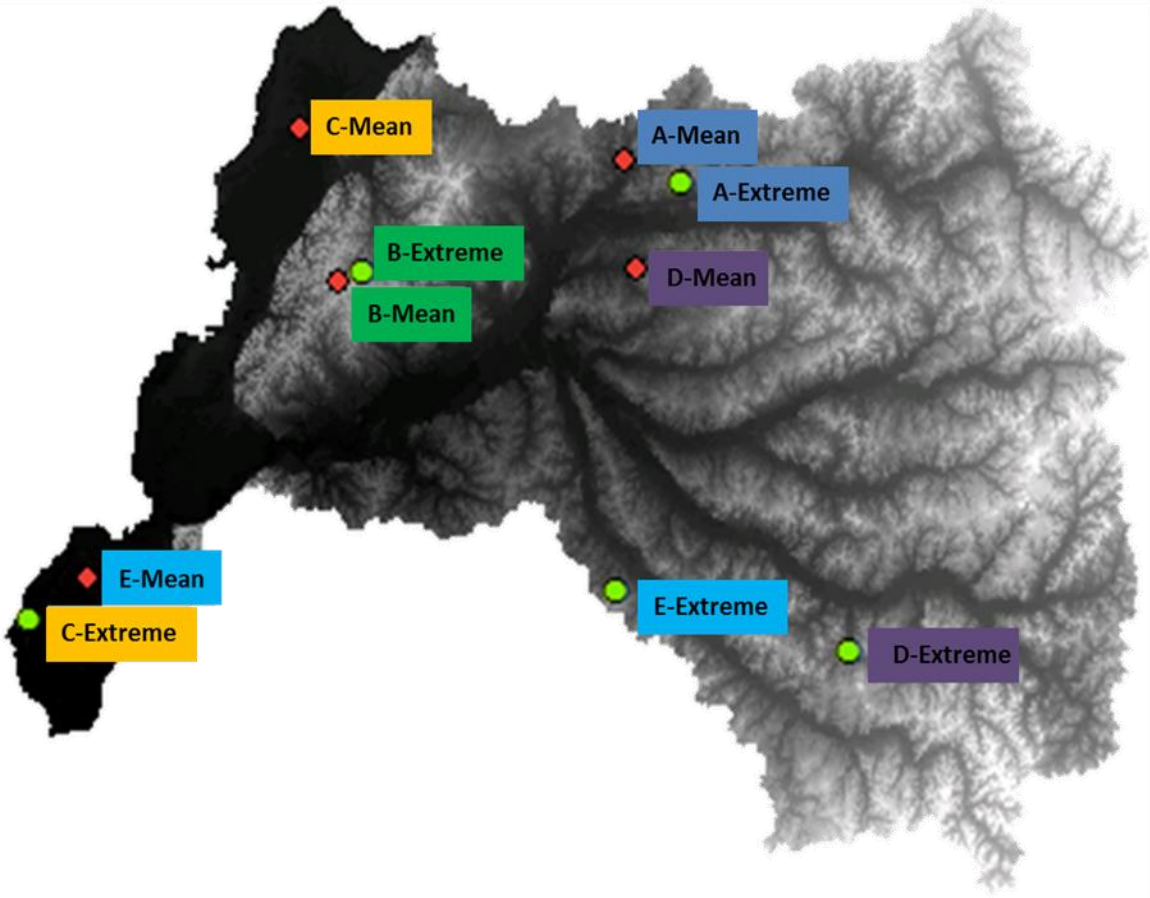


Figure 4-3: Obion Watershed with Mean and Extreme VIC Identified Areas

Bottom-Up Approach

Within each of the selected hydrologic response areas, smaller hillslopes are selected for the simulations with WEPP. To identify the hillslopes that are examined within each 1-km x 1-km region of each hydrologic response group, several steps are required. The DEM for each stream network is input into GEOWEPP (the geospatial version of WEPP) to delineate the watershed into smaller sub-watersheds/ hillslopes within each grid cell (Figure 4-4). This delineation is verified using ArcHydro, a set of tools available within ArcGIS produced by Environmental Systems Research Institute (2017).

Each smaller hillslope (Figure 4-4) are further examined through certain criteria. Criteria include the existence of current crops at the hillslope scale and verification that each chosen hillslope only contains fields with the same rotations. GEOWEPP then creates hillslope files that can be utilized in WEPP (Figure 4-5) (Laflen and Flanagan 2013).

Figure 4-6 illustrates all of the slope profiles together in order to illustrate the variations between them. Table 4-3 - Table 4-7 provide additional insight of each hillslope's RC, average slope, class, length, and dominate shape.

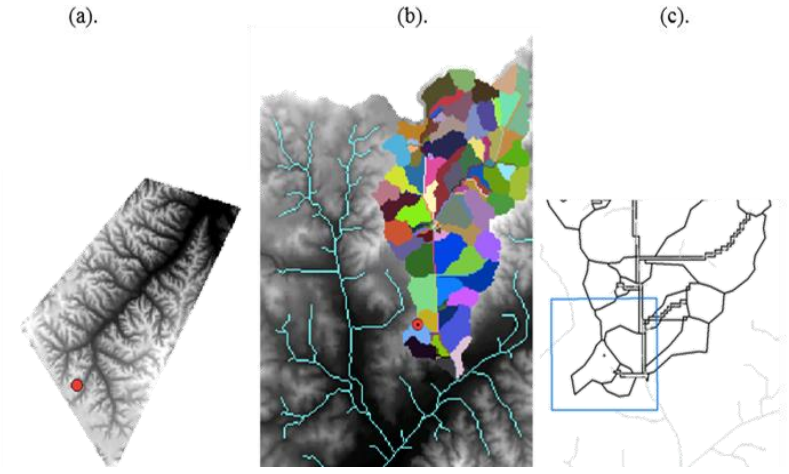


Figure 4-4: Example of (a). GeoWEPP DEM input of the stream network area, (b). GeoWEPP output of the stream network and hillslopes, and (c). A-Mean VIC identified area with hillslopes

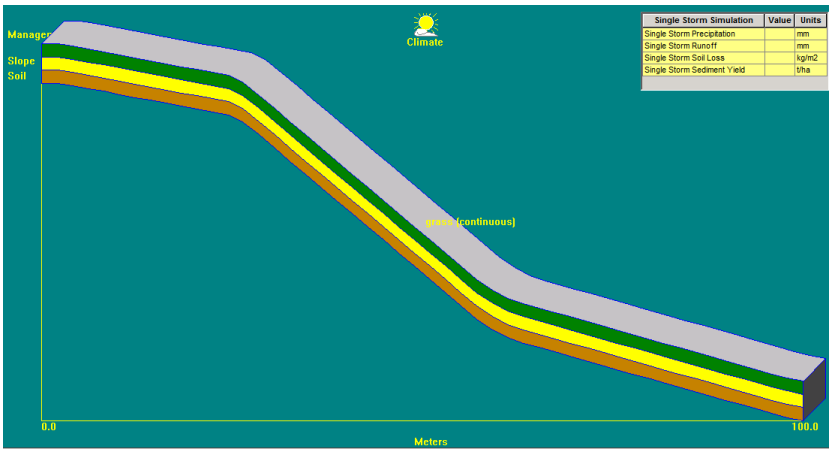


Figure 4-5: Example of a Hillslope in WEPP

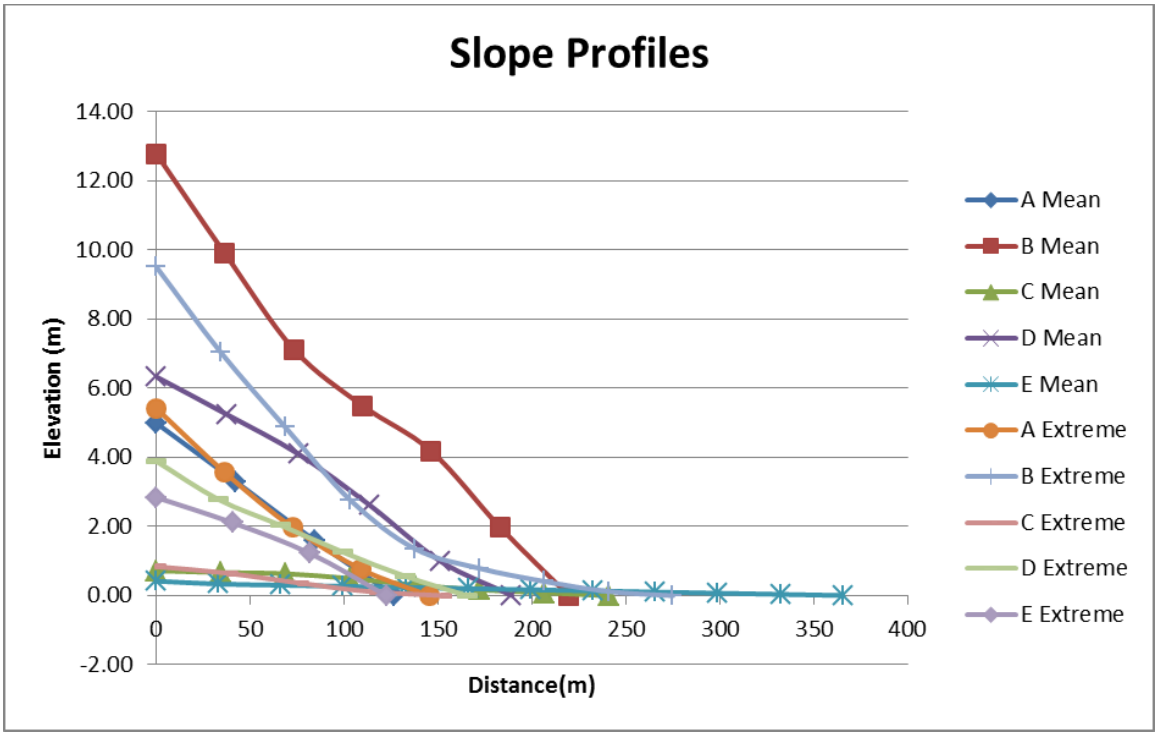


Figure 4-6: Slope Profiles

Table 4-3: Class A Mean and Extreme Characteristics

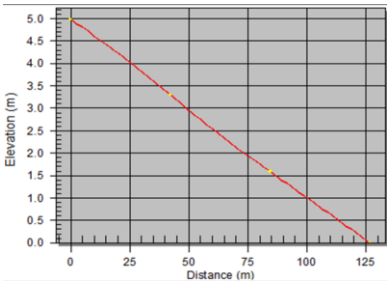
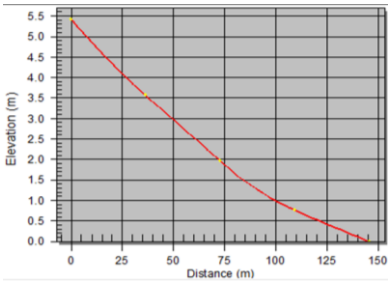
Class	Class A	
Location	Mean	Extreme
RC	0.212	0.216
Profile		
Hillslope Average Slope	3.9%	3.8 %
Length (m)	126.75	145.62
Dominant Shape	Linear	Linear/mild concave

Table 4-4: Class B Mean and Extreme Characteristics

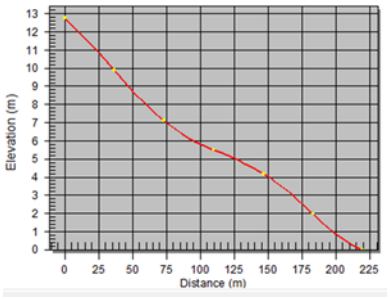
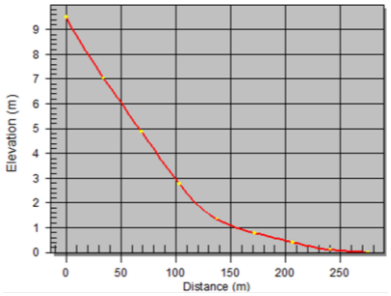
Class	Class B	
Location	Mean	Extreme
RC	0.208	0.224
Profile		
Hillslope Average Slope	5.7 %	6.7% / 1.2 %
Length (m)	219.67	275.16
Dominant Shape	Mild S shape	Linear / Concave

Table 4-5: Class C Mean and Extreme Characteristics

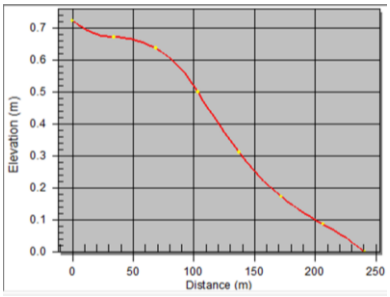
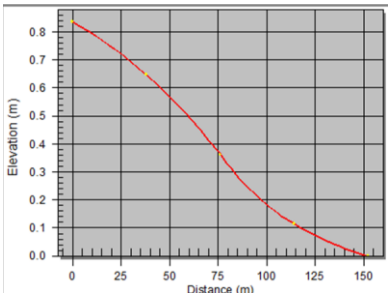
Class	Class C	
Location	Mean	Extreme
RC	0.276	0.435
Profile		
Hillslope Average Slope	0.3 %	0.5 %
Length (m)	240.85	152.22
Dominant Shape	Mild S shape	Linear

Table 4-6: Class D Mean and Extreme Characteristics

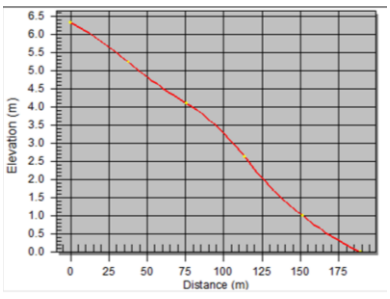
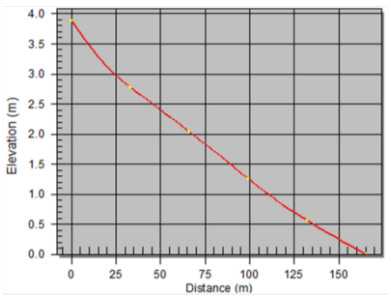
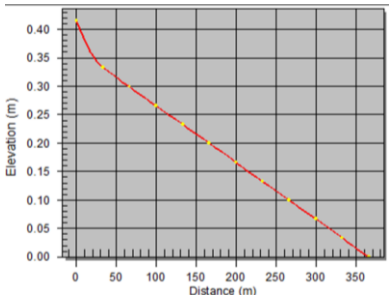
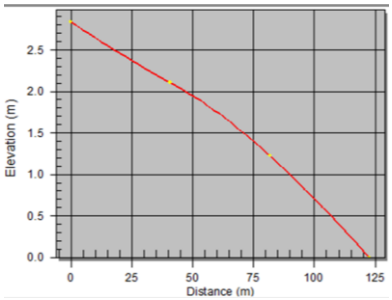
Class	Class D	
Location	Mean	Extreme
RC	0.122	0.173
Profile		
Hillslope Average Slope	3.1 %	2.5 %
Length (m)	189.37	165.46
Dominant Shape	Linear	Linear

Table 4-7: Class E Mean and Extreme Characteristics

Class	Class E	
Location	Mean	Extreme
RC	0.088	0.101
Profile		
Hillslope Average Slope	0.1 %	2.4 %
Length (m)	365.62	122.63
Dominant Shape	Linear	Convex

WEPP Soil Files

WEPP requires a comprehensive set of soil parameters for each hillslope. These include cation-exchange capacity, critical shear, albedo, initial saturation, rill erodibility, interrill erodibility, soil texture, SOC, and effective hydraulic conductivity, obtained from STATSGO2 (Soil Survey 2016) soil information and literary publications (Appendix A.1). Each layer of the soil data is modified for each hillslope including the percent sand, silt, clay, and OM .

The soil pattern that is illustrated in Figure 4-7, demonstrates how the percent organic matter increases from the upland regions towards the Mississippi basin region.

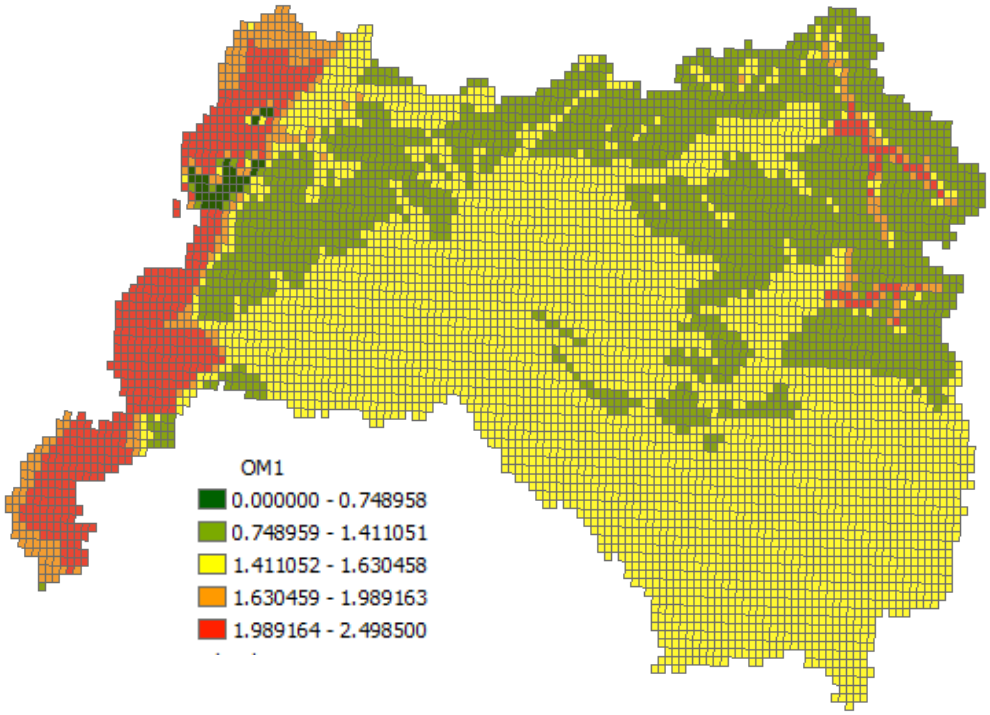


Figure 4-7: Organic Matter Data

The soil type for each location is portrayed in Table 4-8 along with estimated soil characteristics of the site that include the SOM, drainage, permeability, typical crops, and texture.

WEPP Management Files

The management files in WEPP reflect the typical management and crop rotations in the selected areas, and include the dominant no-till practices of this watershed. Cropscape (USDA 2016) data are assessed for the years 2008-2015. The configurations of the hillslopes were intersected with the crop layers to extract the dominant land-use of each hillslope. Figure 4-8 shows the distribution of land-use in the Obion watershed, including crops such as corn, soy, cotton, and winter wheat, open and developed areas, and undeveloped areas such as forests, wetlands, grasslands and water. By assessing the eight years of data, a rotation schedule with the dominant crops of corn-soy and cotton-soy is established for further analysis.

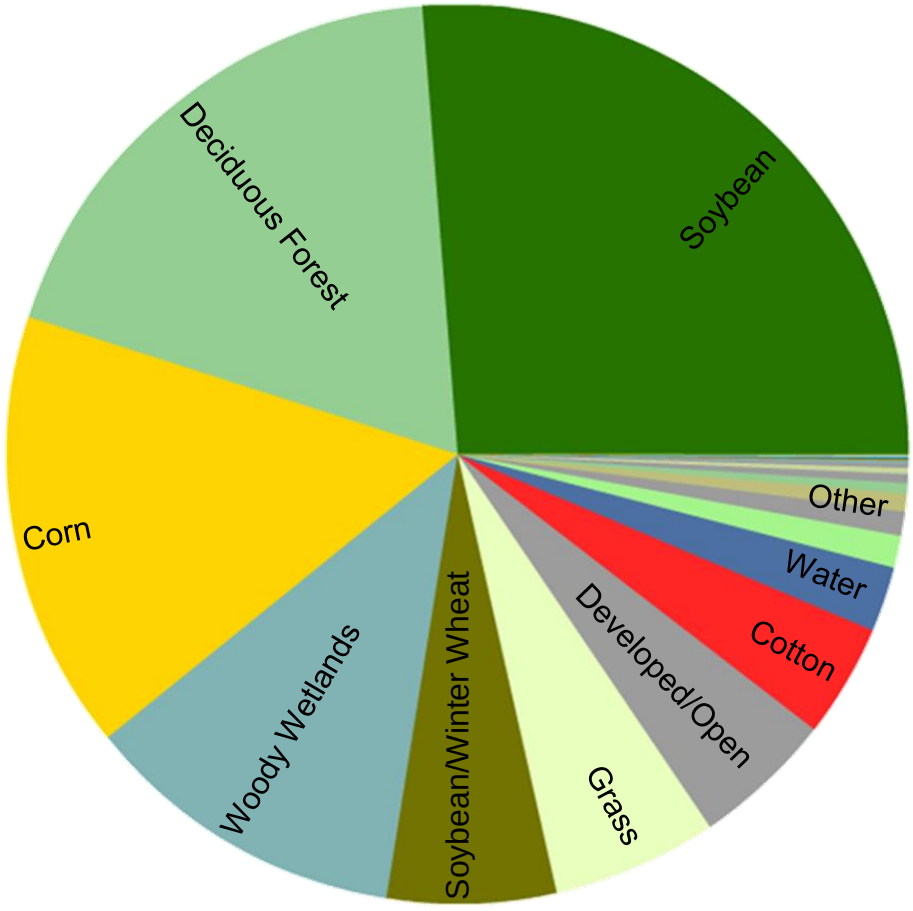


Figure 4-8: Typical land use distribution in the Obion Watershed, (USDA 2016)

Table 4-8: Composition of major soil types (Soil Survey 2016)

Soil Type (-)	AOI (-)	SOM (high-low)	Drainage (excessively-poorly)	Permeability (rapid-slow)	Principal Crops (-)	Texture (A horizon) (-)
Alligator	E-Mean	Medium	Poorly drained	Very slow	Soybean, rice, cotton, wheat	Clay, silty clay, or silty clay loam
Collins	A-Extreme, D-Extreme	Medium	Moderately well drained	Moderate	Cotton, corn, soybean, small grains	Silt loam
Commerce	C-Extreme	Low-medium	Somewhat poorly drained	Moderately slow	Cotton, soybean, corn, wheat	Very fine sandy loam, loam, silt loam, or silty clay loam
Grenada	A-Mean, E-Extreme	Medium	Moderately well drained	Moderate above fragipan and slow in fragipan	Cotton, corn, soybean	Silt loam
Loring	D-Mean	Medium	Well drained-Moderately well drained	Moderate above fragipan, moderately slow in fragipan	Cotton, small grains, soybean	Silt loam
Memphis	B-Mean, B-Extreme	Medium	Well drained	Moderate	Cotton, soybean, small grains	Silt loam or silt
Reelfoot	C-Mean	High	Somewhat poorly drained	Moderate	Soybean, corn, cotton	Silt loam or loam

Planting and harvesting dates for western Tennessee differ from other states and within the state. Literature was used to determine the planting and harvesting dates for the Obion River watershed (Table 4-9).

Table 4-9: Planting dates, harvest dates, and management rotation

Crop	Planting Date	Harvest Date	Rotation
Corn	April 1st	September 10th	Corn-Soybean
Soy	April 25th	October 5th	Corn-Soybean
Cotton	April 5th	October 1st	Cotton-Soybean
Soy	April 25th	October 5th	Cotton-Soybean

For this study, April 1st was used for corn planting and September 10th for corn harvesting. Flinchum (2001) recommends an April 1st to May 1st planting window for the western part of the state, which corresponds to the National Agricultural Statistic Service, NASS (2010) most active planting period of April 5th to May 10th for the state of Tennessee. McClure and Cannon (2016) recommend an early April planting based on studies in Milan, TN, located in the Obion Watershed. Harvest dates in the state of Tennessee are most active between September 1st and October 10th (NASS 2010).

There is a correlation between the planting windows and yields. County Standard Corn Tests were conducted in numerous counties throughout Tennessee, including those in Milan, TN. The hybrid corn tests (Sykes 2016) showed decreasing yields starting with late April plantings.

The soybean planting and harvesting dates chosen for this study are April 25th and October 5th without a corresponding cover/double crop. If soy has a winter wheat double crop in its rotation the planting and harvest dates of May 20th and October 20th

are more suitable. This later planting date allows the winter wheat to mature into the spring for a successful wheat harvest, but minimizes the impact on soy yields.

The most active soybean planting period for all of Tennessee is between May 15th – June 25th (NASS 2010). Harvest dates range between September 20th – November 25th. Flinchum et al. (2013) advises planting dates between April 25th – June 15th for Tennessee. Thompson et al. (2006) suggests planting between mid-May and early July with harvests beginning in late September, which could go as late as December depending on weather conditions. A decrease in yields occurred with all studied cultivars commencing with May 15th plantings in Milan, TN (McClure et al. 2016).

Cotton rotations in this model have a planting date of April 5th and harvest date of October 1st. Usual planting dates in the state range from April 25th to June 5th and harvest dates from September 30th to November 10th (NASS 2010). Earlier cotton planting dates correspond to higher yields with yield decreasing starting every day after May 15th (Robinson 2004). This correlates with Raper (2014) and Main (2012) which recommend planting in a range between April 20th and May 10th.

This study follows the methods described in Abaci and Papanicolaou (2009) for calibrating and validating the WEPP model. Crop calibration (Figure 4-9 and Figure 4-10) included adjusting the dates and crop parameters from the database within WEPP to account for crops grown in the western TN area.

Characteristics include a GDD for the growing season of 1700 °C days, 1150 °C days, and 2200 °C days for corn, soybean, and cotton respectively (Arnold et al. 1995). Base daily temperatures were also adjusted with inputs of 12°C for corn (McClure 2009), 9°C for soybean (Casteel 2010), and 12°C for cotton (Arnold et al. 1995). Optimal plant growth temperature includes 25°C for corn (Arnold et al. 1995), 25°C for soybean (Arnold et al. 1995), and 32°C for cotton (Wright et al. 2005).

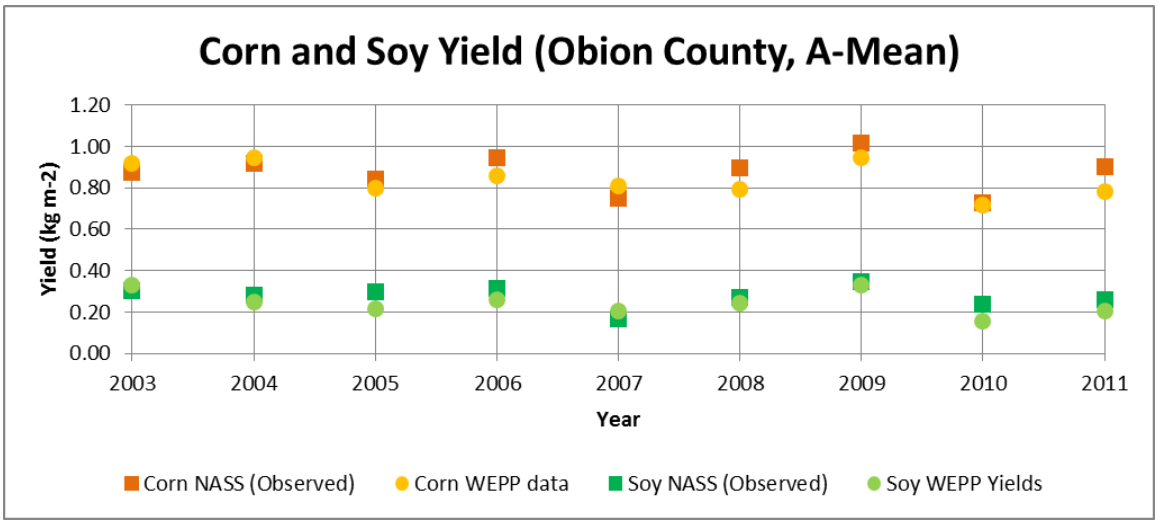


Figure 4-9: Corn and Soy Calibration for A-Mean Location

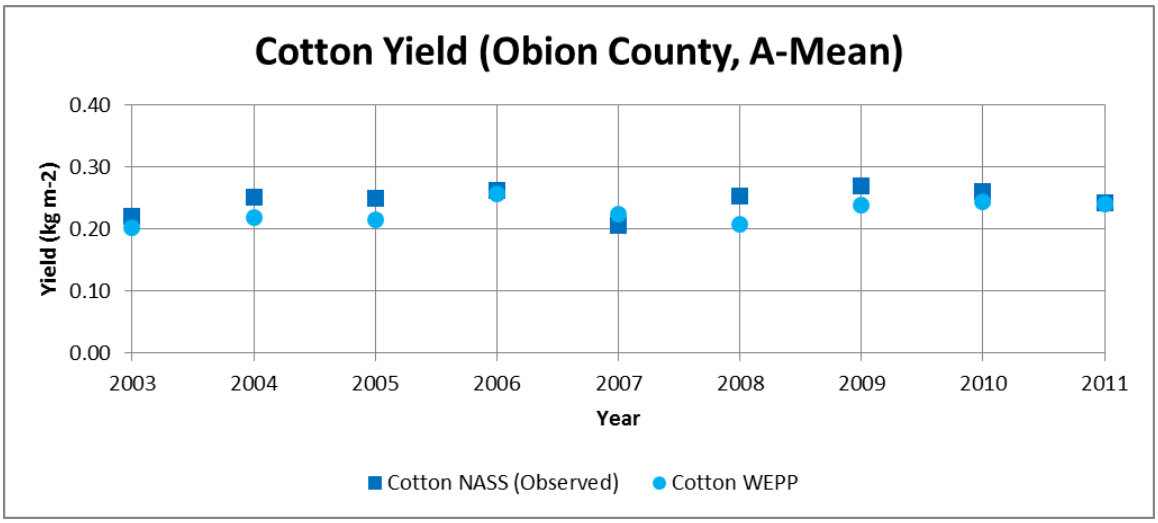


Figure 4-10: Cotton Calibration for A-Mean Location

Calibrations utilized yearly countywide NASS yield data (NASS 2010) for each crop (Appendix A.2). Since WEPP is unable to account for changes in management practice such as those related to diseases and pest control, adjustments were based on the more recent years of 2003-2011.

WEPP Climate Files

This study runs continuous simulations, which include past and projected climate periods. The future climate until 2050 follows two representative concentration pathways (RCP). These climate projections, RCP 4.5 and RCP 8.5, represent average and extreme CO_2 emission scenarios (Stocker et al. 2013). CO_2 emissions for RCPs of 4.5 have an expected peak around 2040 whereas RCPs of 8.5 continue to increase to 2100.

This study will use the RCPs from four Global Circulation Models: GFDL (GFDL-ESM2M), HadG (HadGEM2-CC), IPSL (IPSL-CM5A-MR), and MIRO (MIRCO-ESM-CHEM). Climate models were selected based on Gustafson et al. (2015) and datasets were downloaded from Multivariate Adaptive Constructed Analogs (MACA 2016).

Readily available statistically downscaled climate data is used, since only negligible feedbacks is expected between the landscape and the climate due to the scope of the study. Extreme forecasted climate projections aid in the development of successful best management practices in the long-term as more frequent extreme events are expected to occur in the future.
Increased CO_2 concentrations have a projected influence on temperature. Temperature shows a significant increase, which Figure 4-11 and Figure 4-12 illustrate for all 4.5 and 8.5 scenarios.

Since precipitation across the Obion watershed does not vary greatly between locations an example location of A-Mean is provided (Table 4-10 - Table 4-12). Information in the

tables includes not only ranges but the slope of the mean values; showing that most climates have a projected decrease in the mean precipitation per growing season.

WEPP requires additional climate parameters aside from those available; obtaining them is accomplished by utilizing CLIGEN (Nicks et al. 1995) weather station data. Available in WEPP, CLIGEN utilizes existing information of each location's precipitation, maximum temperature, minimum temperature, and wind velocity along with each location's coordinates in order to output a complete climate file.

Model Simulations

Once all the input information is completed for each hillslope WEPP is run to determine various outputs such as runoff, soil loss, ET, sediment yield, and crop yields. The resulting evaluation for varying crops and past and projected climate scenarios is displayed with the aid of Matlab software (MATLAB 2017).

This study will forecast until 2050 using the current rotations to quantify variances over time. The primary tool will be continuous simulations; this is in order to enhance our information regarding different long-term best management practices that preserve and build OM.

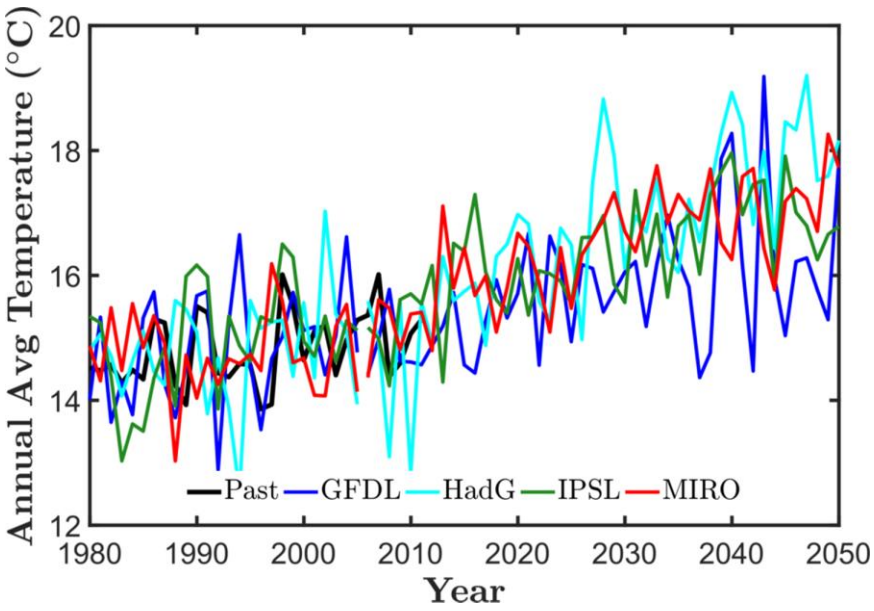


Figure 4-11: Annual average temperature for past and 4.5 climate projections

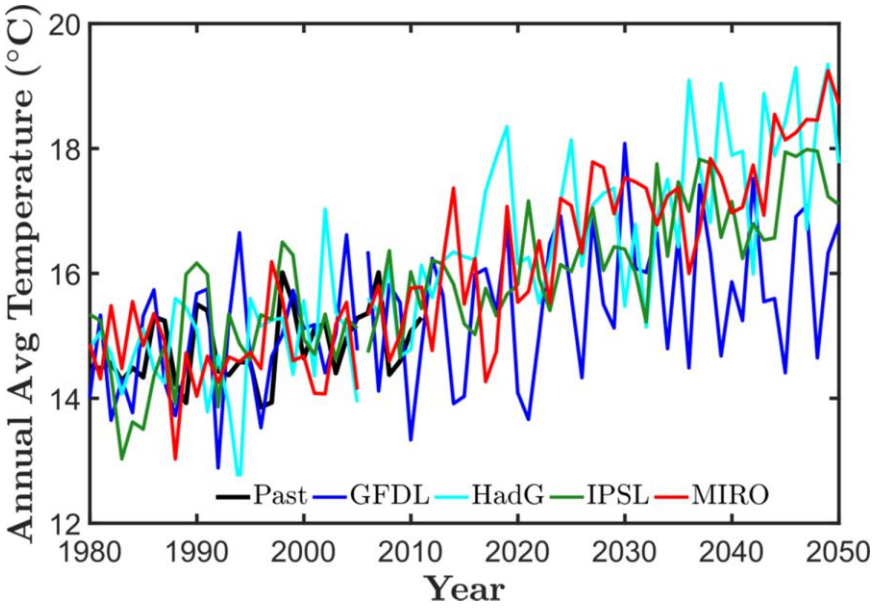


Figure 4-12: Annual average temperature for past and 8.5 climate projections

Table 4-10: Climate Corn Growing Season Precipitations (mm) for A-Mean

	GFDL 4.5	GFDL 8.5	HadG 4.5	HadG 8.5	IPSL 4.5	IPSL 8.5	MIRO 4.5	MIRO 8.5
Mean	584	610.3	566.2	556.5	603.1	578.5	571.4	586.8
Maximum	970.7	1177	859	900.5	990	1047	921.8	917.6
Minimum	104.2	292.7	262.5	201.5	230.3	199.6	320.1	308.5
Slope	-22	7.4	-37	-34	-7.6	-22	-21	-14

Table 4-11: Climate Soy Growing Season Precipitations (mm) for A-Mean

	GFDL 4.5	GFDL 8.5	HadG 4.5	HadG 8.5	IPSL 4.5	IPSL 8.5	MIRO 4.5	MIRO 8.5
Mean	587	616.2	559	545.7	618.5	588.1	568.9	595.1
Maximum	966.3	1074	908.7	891.9	1231	1096	972.2	965.8
Minimum	163.6	241.7	222.3	129.8	279.5	265.7	308.5	238.8
Slope	-22	2.5	-53	-58	-12	-20	-33	-20

Table 4-12: Climate Cotton Growing Season Precipitations (mm) for A-Mean

	GFDL 4.5	GFDL 8.5	HadG 4.5	HadG 8.5	IPSL 4.5	IPSL 8.5	MIRO 4.5	MIRO 8.5
Mean	647.4	669.6	620	611.8	678.5	645	635.9	663.3
Maximum	1041	1136	978	978	1263	1165	1033	1030
Minimum	163.6	304.8	240.8	186.6	321.4	306.7	391.8	369
Slope	-23	1.5	-52	-53	-9.9	-21	-30	-13

CHAPTER FIVE
RESULTS & DISCUSSION

This chapter contains the results of the study's hypotheses. Commencing with the first hypothesis, the key variables of crop yields, evapotranspiration, and soil moisture are analyzed. The water use efficiency is outlined next using several methods. These include WUE results using methods from Hamilton et al. (2015) and Dietzel et al. (2016) where the ratio of biomass/yields and ET are investigated. A section on crop stresses explain the water dependency for critical stages of development. Followed by a sWUE section explaining the importance of analyzing the efficiency of the entire system. This takes into account the variables from WUE calculations and adds runoff and drainage to the equation. This chapter concludes with yield potential estimates for the Obion River watershed.

Hypothesis 1

Crop Yields

Simulations are performed through WEPP in order to project crops yields under two future climate scenarios. Figure 5-1 - Figure 5-3 show, as an example, the crop yields for the mean hillslopes under the 4.5 climate projection from 2012-2050. Decreases in the corn, soybean, and cotton yields were seen for all hillslopes under both climate scenarios using all four global circulation models.

Evapotranspiration and Soil Moisture

ET is calculated in VIC and WEPP using the Penman-Monteith equation. These daily ET values are averaged monthly and compared with Moderate Resolution Imaging Spectroradiometer (MODIS) derived ET from 2007-2011 in Figure 5-4 - Figure 5-8 (Senay et al. 2013; Velpuri et al. 2013). The MODIS data are reported every 8 days but are averaged monthly, as well.

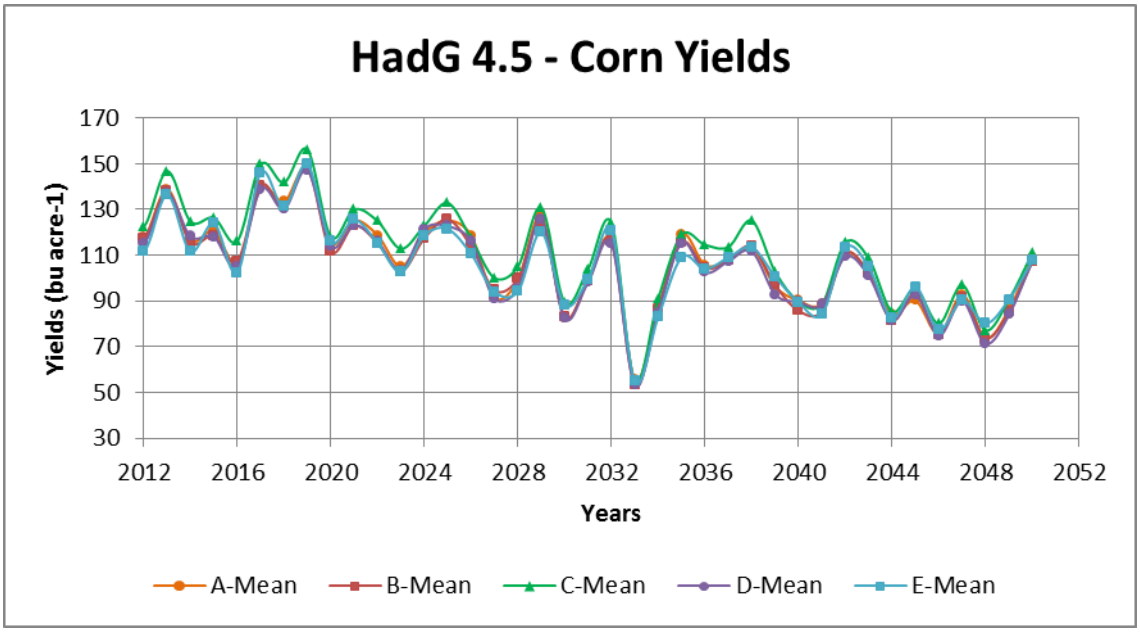


Figure 5-1: Corn crop yield projections for climate HadG 4.5

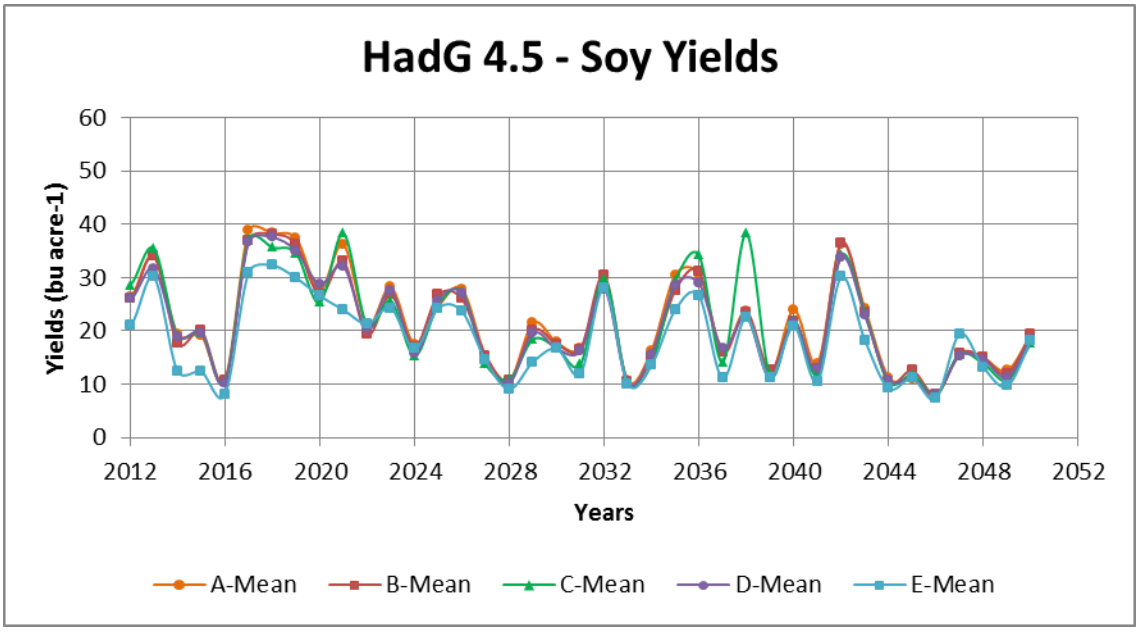


Figure 5-2: Soy crop yield projections for climate HadG 4.5

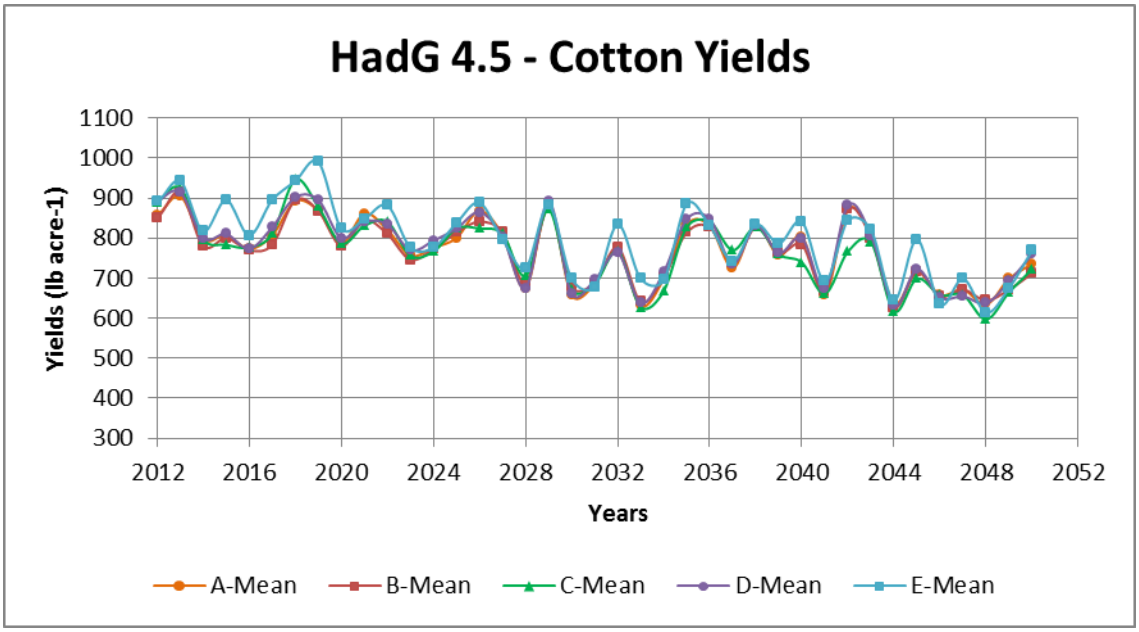


Figure 5-3: Cotton crop yield projections for climate HadG 4.5

The WEPP values in Figure 5-4 - Figure 5-8 are for the A-Mean hillslope, while the corresponding VIC values are for the 1-km x 1-km grid in which this hillslope resides. The corresponding MODIS data are averaged for the whole Obion watershed. The WEPP and VIC data correspond only to corn, while MODIS data is for a variety of vegetation throughout the watershed (e.g., crops, pasture grass, deciduous trees).

For the most part, the VIC and MODIS ET data correspond in timing and magnitudes, peaking in June-July between 140 and 160 mm/month. However, the WEPP ET data tend to peak in May around 100 mm/month. The difference may be attributed to the vegetation varieties represented by each model with differences ranging from 0% to 48% between WEPP and VIC and 0% to 62% between WEPP and MODIS. Regarding the WEPP values, corn, which covers less than 20% of the watershed, is planted in early April. Thus, it will peak earlier than the more abundant soybean. MODIS includes all the vegetation in the area. Soybeans, which cover over a third of the watershed are planted later than corn causing the peak to shift and magnitudes to increase.

Sanford and Selnick (2013) calculated the fraction of precipitation that is lost through ET for the years 1971 to 2000 and developed the map seen in Figure 5-9. For the Obion River watershed this loss ranges between 0.5-0.59 (Figure 5-10). This correlates well with the reported 62% ET/precipitation fraction in the Hamilton et al. (2015) study for the Michigan area. Projected ET values for the climates portrayed in this study have an overall mild decrease.

A sensitivity analysis was performed on each hillslope, which were partitioned into upslope and downslope regions. WEPP runs were performed on each portion and the soil water levels compared. This study saw a negligible change in soil water between the regions. Example differences in soil water layers, to a depth of 0.2 m for projection GFDL 4.5, are 0.2%, 0.5%, and 0.7% difference for locations B-Extreme, C-Extreme, and C-Mean respectively.

Water Use Efficiency – Hamilton et al. (2015)

WEPP's daily outputs are used to calculate the WUE for the hydrologic response areas in the Obion River watershed using the definition in Hamilton et al. (2015) which is the maximum above ground live biomass value for the crop season divided by the cumulative ET during the growing season until the maximum biomass measurement is reached.

Figure 5-11 - Figure 5-13 show the approximate ranges are 35-65 $\frac{kg}{ha*mm}$ for corn, 15-30 $\frac{kg}{ha*mm}$ for soy, and 15-20 $\frac{kg}{ha*mm}$ for cotton. Hamilton et al. (2015) found that these differences in WUE values between crops are more likely associated with the biomass measurement rather than the ET values. Corn produces more biomass than soybean and cotton and hence the highest estimated WUE measurements.

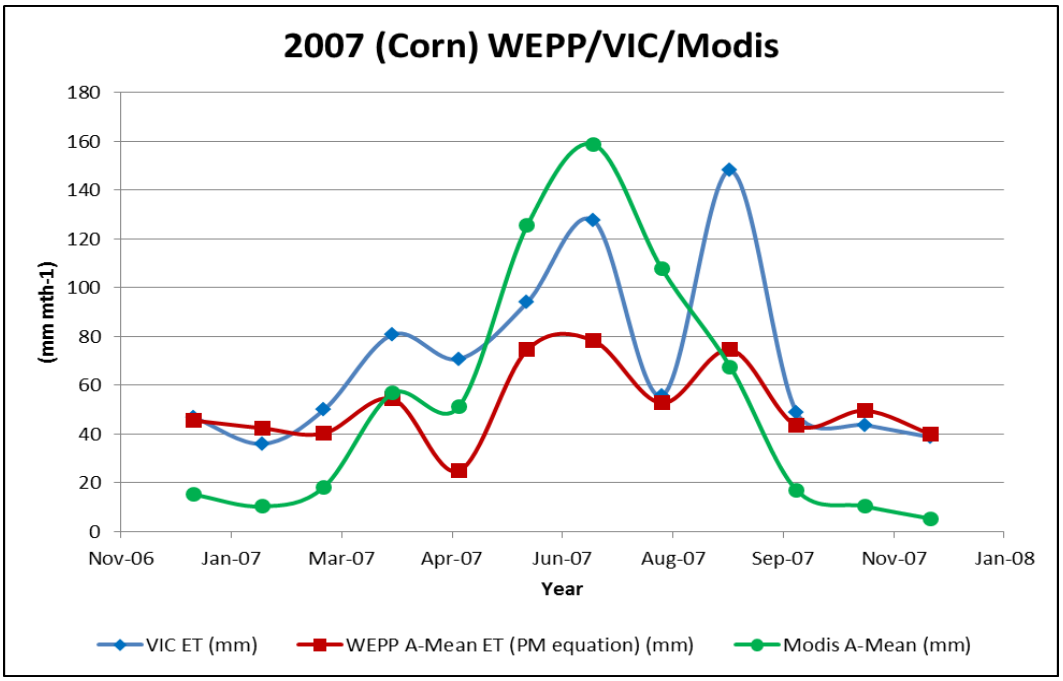


Figure 5-4: Corn WEPP, VIC, and Modis ET Comparison for past 2007 data

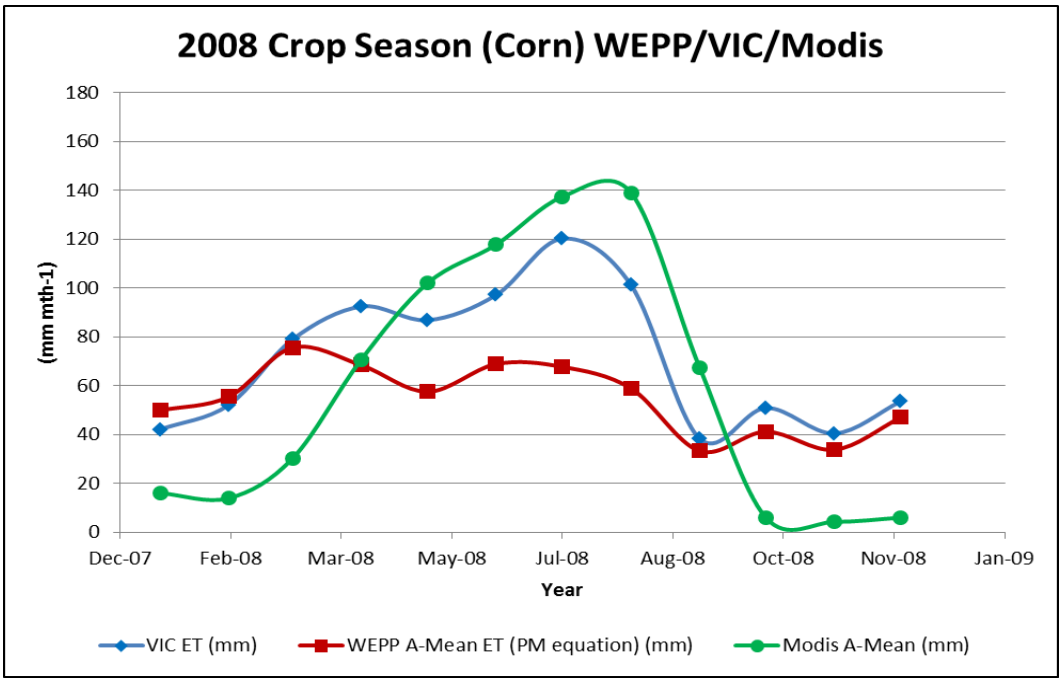


Figure 5-5: Corn WEPP, VIC, and Modis ET Comparison for past 2008 data

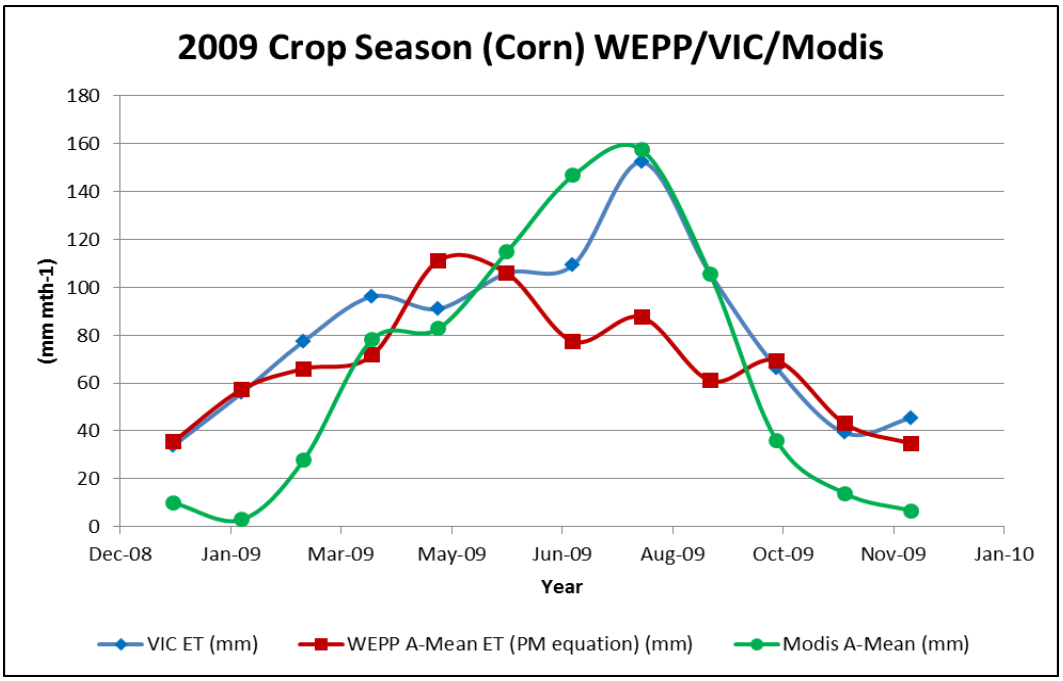


Figure 5-6: Corn WEPP, VIC, and Modis ET Comparison for past 2009 data

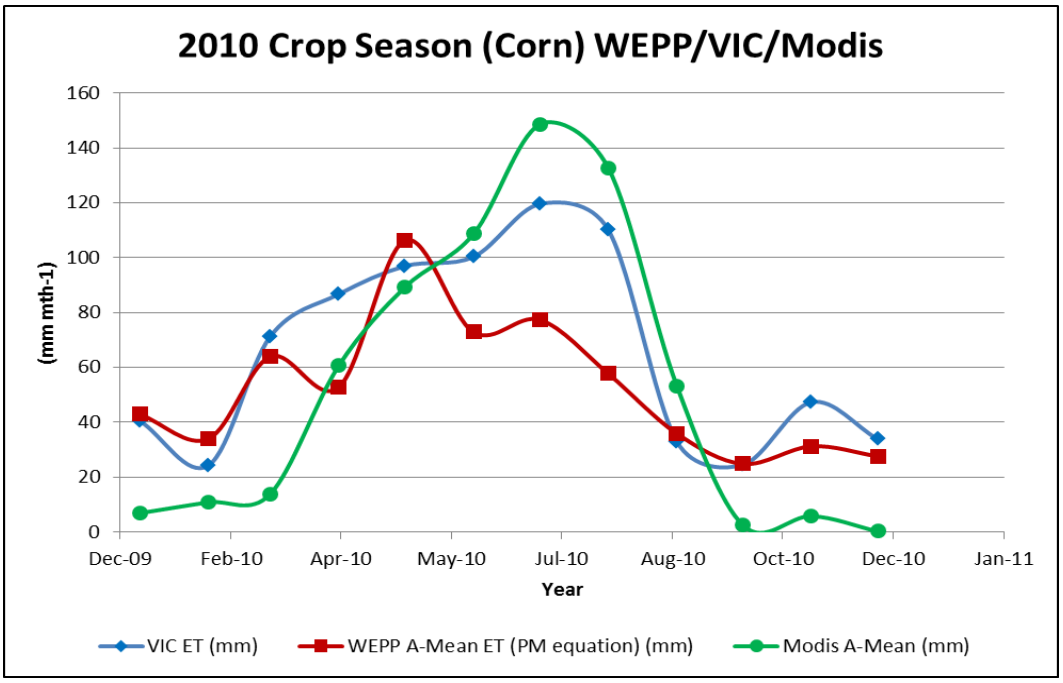


Figure 5-7: Corn WEPP, VIC, and Modis ET Comparison for past 2010 data

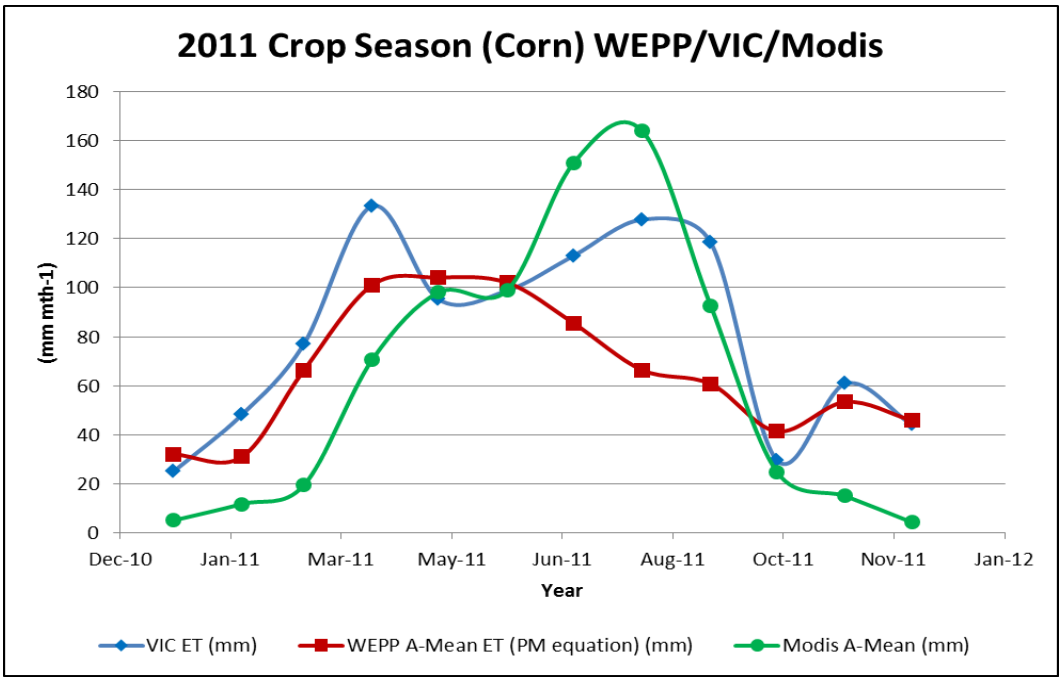


Figure 5-8: Corn WEPP, VIC, and Modis ET Comparison for past 2011 data

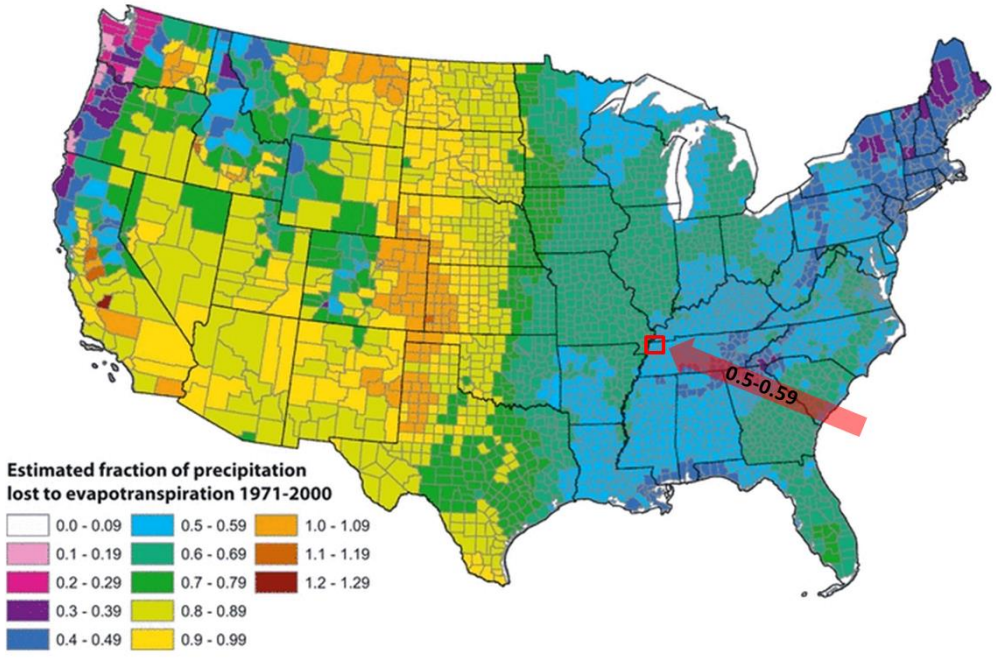


Figure 5-9: Comparison of ET values from WEPP data and Sanford and Selnick (2013)

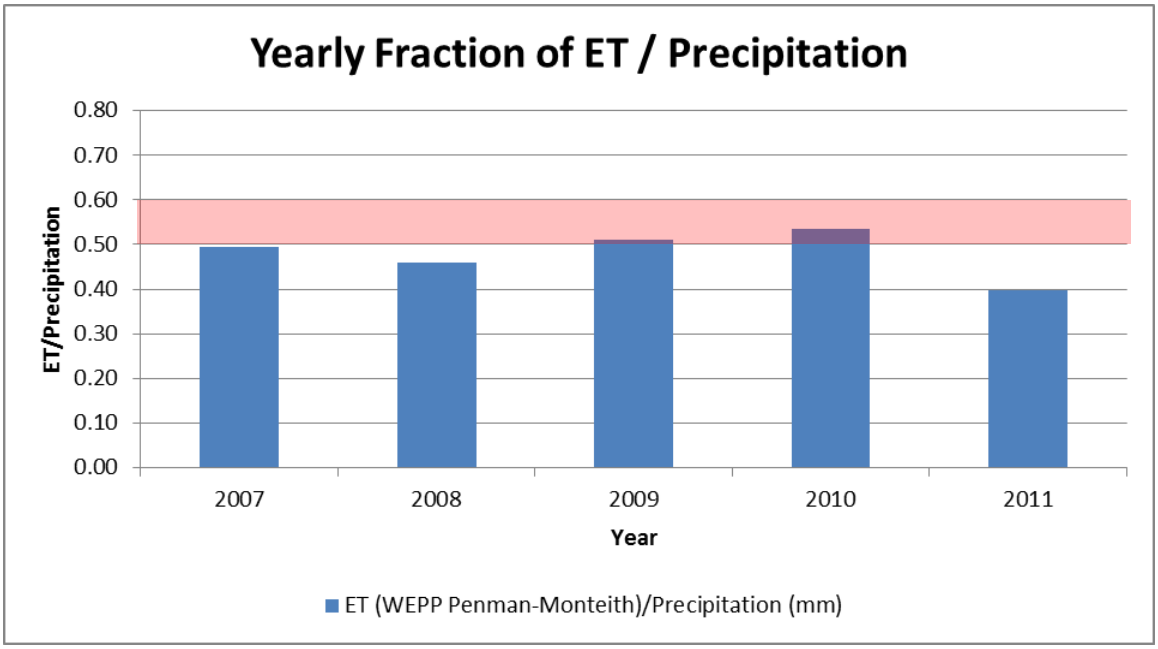


Figure 5-10: Fraction of ET and Precipitation for the Obion Watershed

WUE values are expected to be lower during years with low precipitation, although Figure 5-11 demonstrates that 2007, a low precipitation year, has a higher WUE value. Figure 4-9 shows that the crop yields for this year are lower but not substantially lower compared to other years. This in combination with a lower ET value in the denominator results in a higher WUE. This is also seen to a lesser extent in Figure 5-12 and Figure 5-13 for soy and cotton.

Overall all mean locations have higher WUE values compared to the extreme locations for the past and future climate scenarios. This is expected since location selection criteria was based on the RC and slope (Table 4-2), which takes into account the infiltration and gradient. Although this distinction is seen mainly in corn and to a lesser extent in soy and cotton.

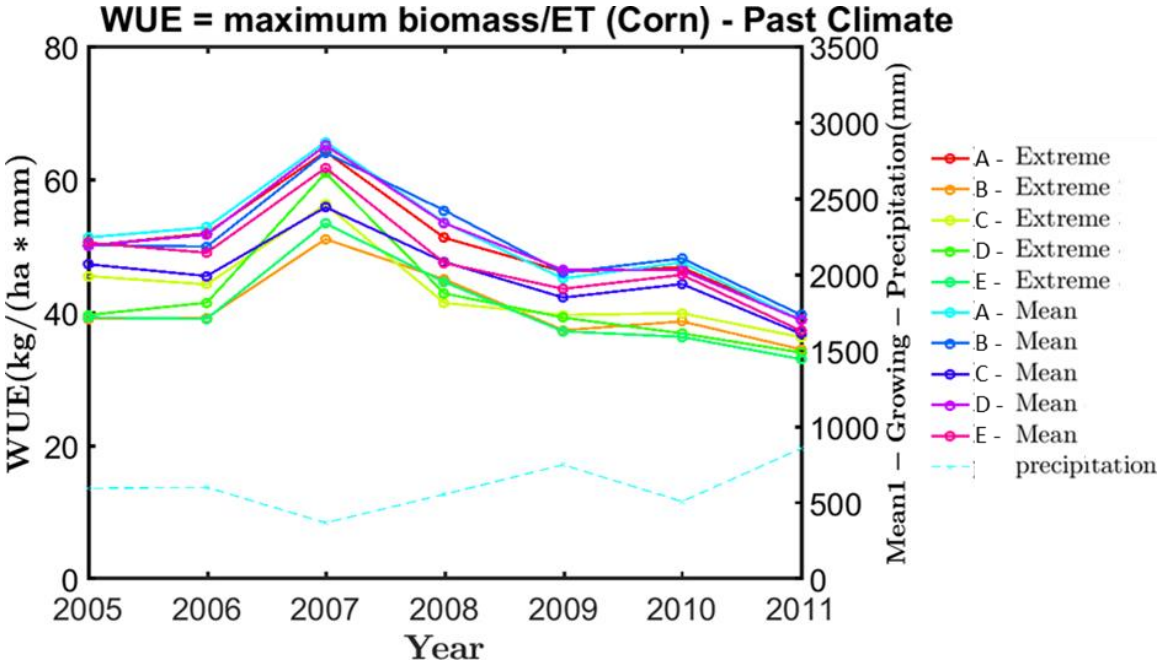


Figure 5-11: Corn WUE for Past Climate based on Hamilton et al. (2015) WUE Method

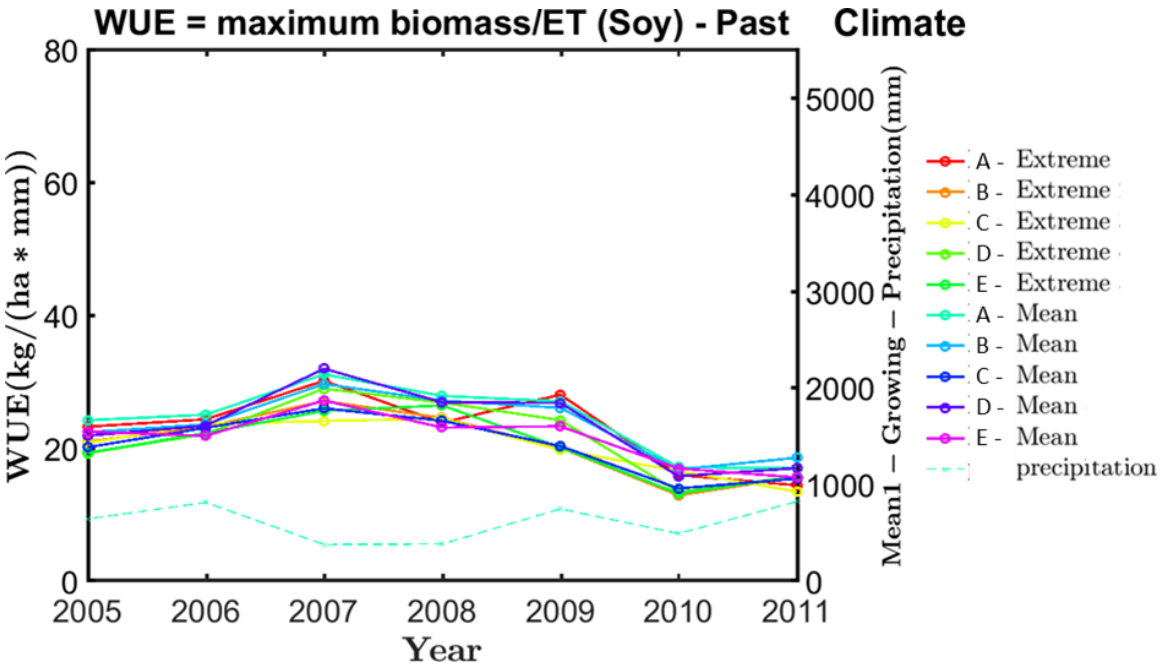


Figure 5-12: Soy WUE for Past Climate based on Hamilton et al. (2015) WUE Method

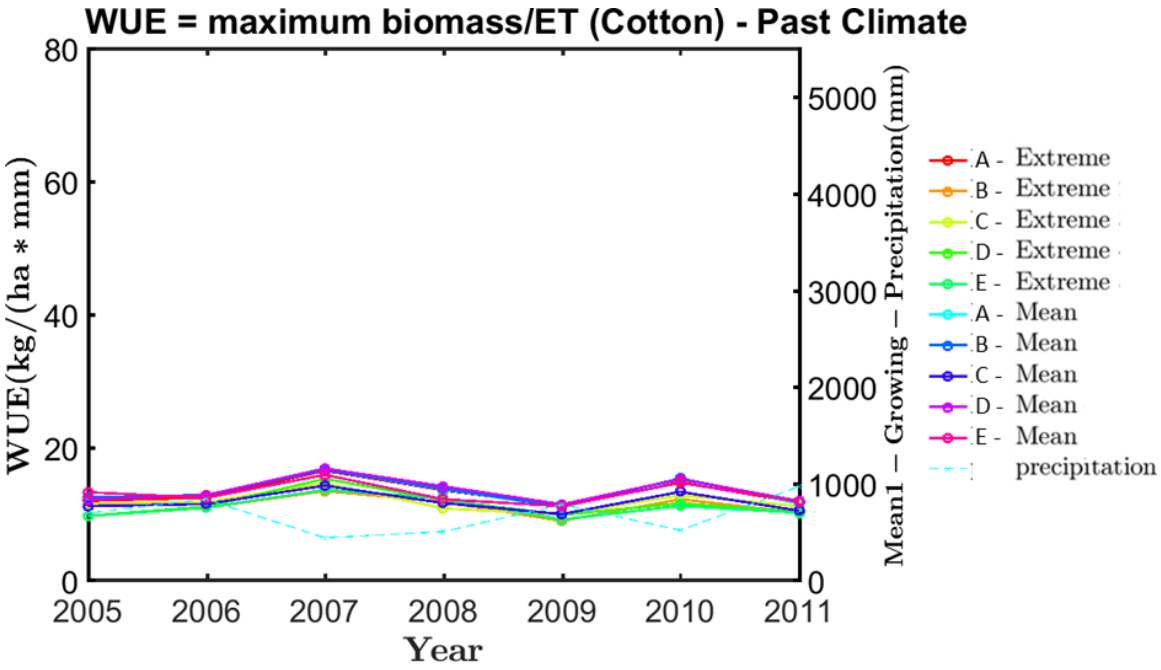


Figure 5-13: Cotton WUE for Past Climate based on Hamilton et al. (2015)WUE Method

Water Use Efficiency – Dietzel et al. (2016)

Using the definition in Dietzel et al. (2016), WUE is the ratio of the crop yield to the ET of the growing season (Figure 5-14). A similar trend is expected since the maximum biomass measurement is a close estimate to the biomass at harvest, but the crop yield is a lower measurement since it is only a portion of the total biomass. Also, ET is expected to be higher since there is a continuation of this value after the maximum biomass measurement is reached until harvest (Figure 5-14). These results show a slightly lower magnitude, as seen in the past comparison graphs of Figure 5-15, Figure 5-16, and Figure 5-17 for corn, soy, and cotton.

Comparing the WUE outputs to the harvested yield (Figure 5-18) of corn and soy at the A-Mean hillslope and a projected GFDL 4.5 climate as an example, there is an overall relationship between the results. This verifies Hamilton et al. (2015)'s findings that differences were more likely related to biomass rather than ET.

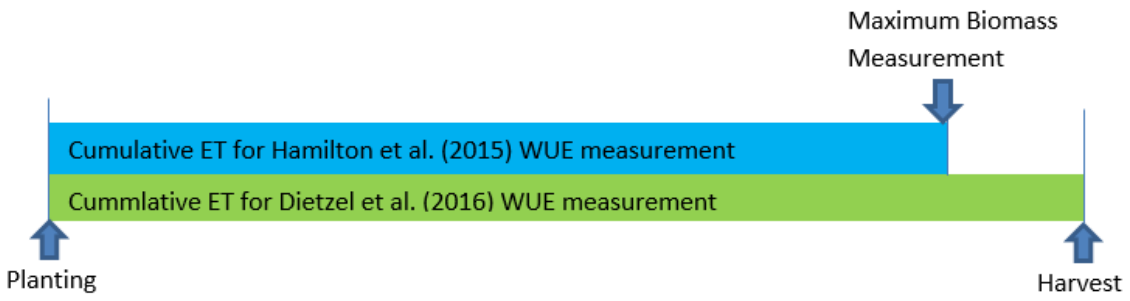


Figure 5-14: Differences in the ET measurement between two WUE calculation methods

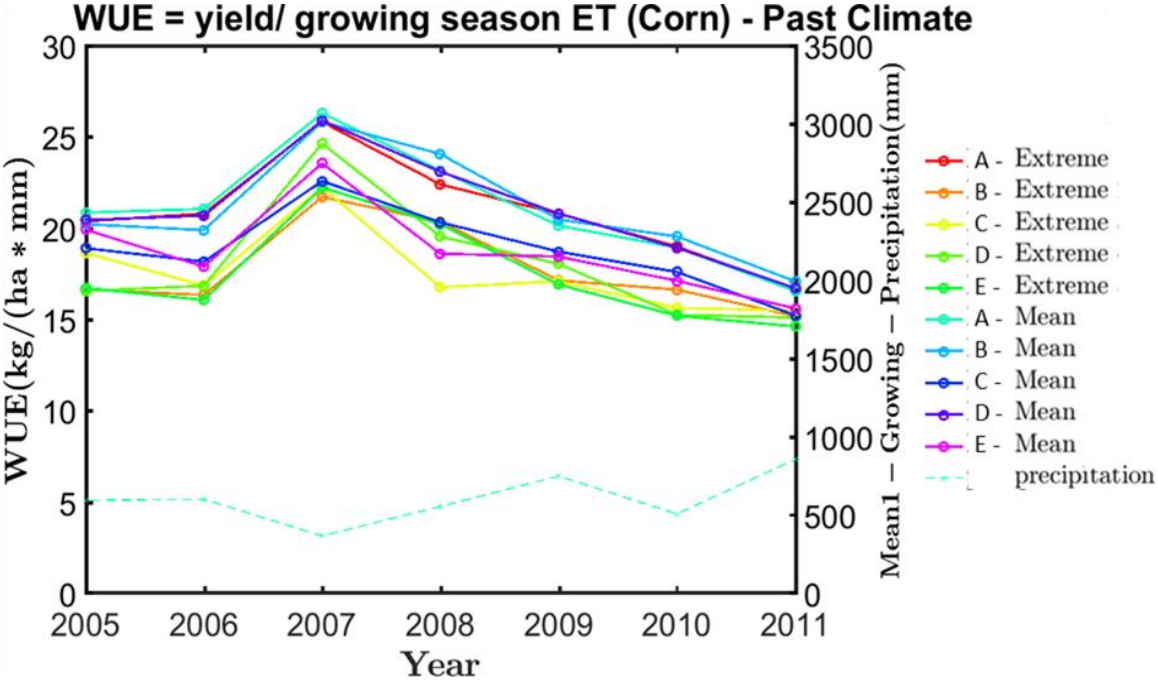


Figure 5-15: Corn WUE for Past Climate based on (Dietzel et al. 2016) WUE method

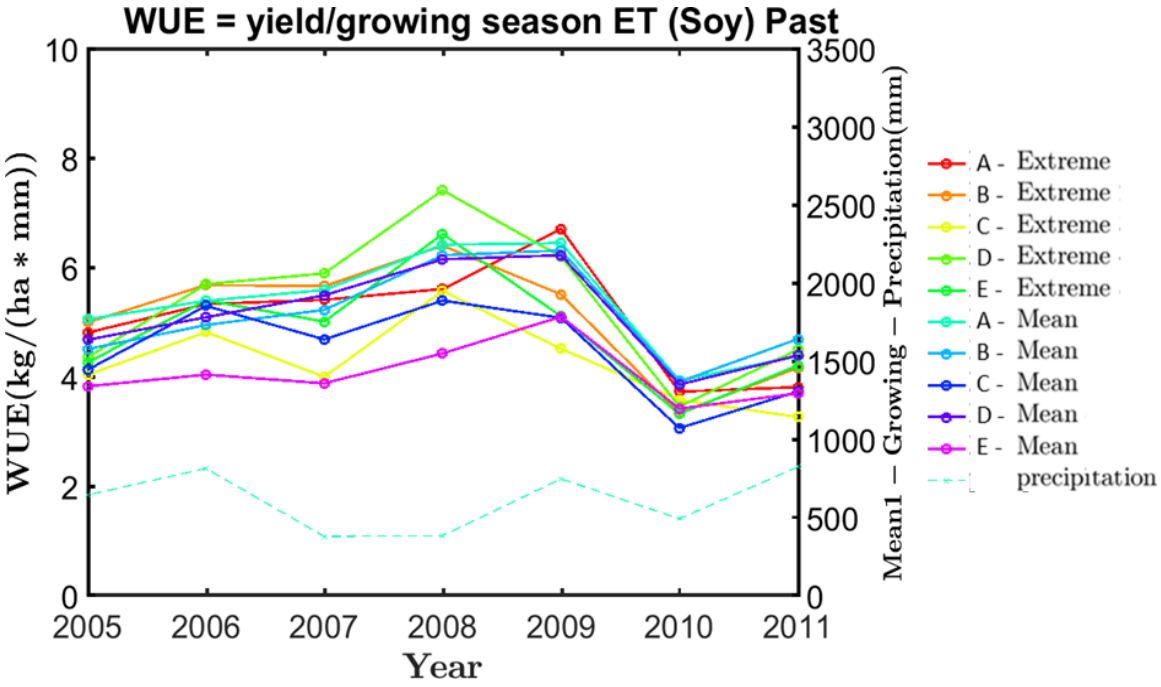


Figure 5-16: Soy WUE for Past Climate based on (Dietzel et al. 2016) WUE method

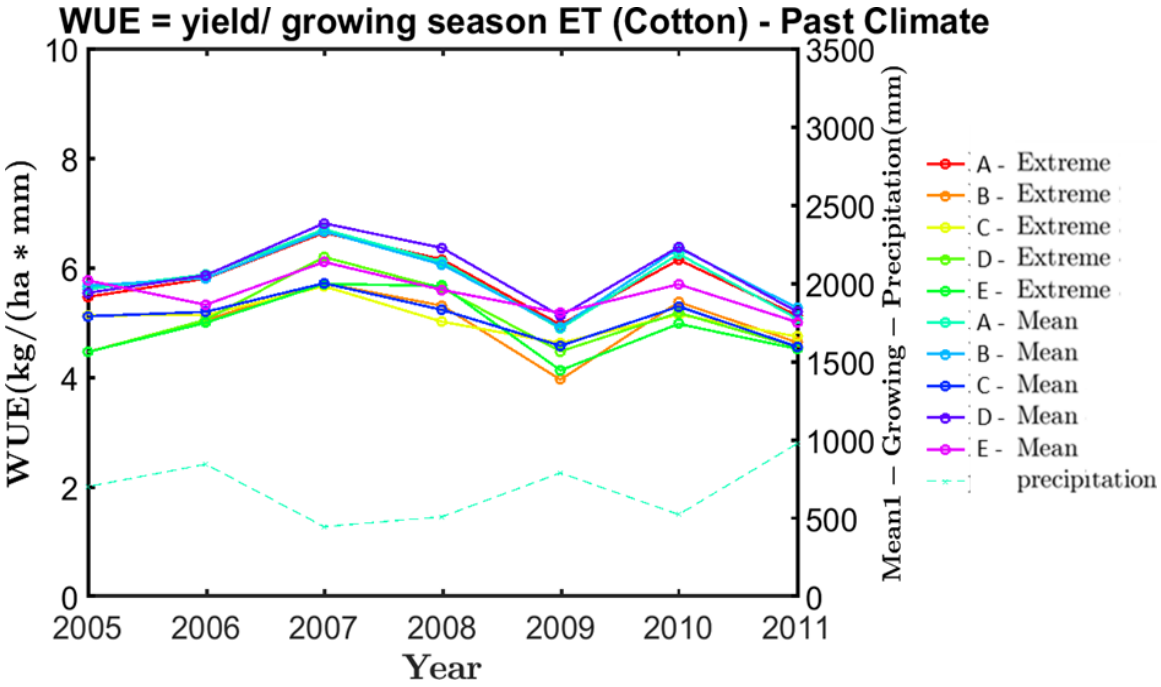


Figure 5-17: Cotton WUE for Past Climate based on (Dietzel et al. 2016) WUE method

The future analysis also shows a connection between years of low/high growing season precipitation and low/high yields by comparing the harvest yields and precipitation years in Figure 5-22 and Figure 5-19 respectively. The years 2037 and 2048, which are high yield and high precipitation years, and the years 2040 and 2043, which are low yield and precipitation years for GFDL 4.5 are bookends and show this connection most vividly.

Crop Stresses

Looking into the water stresses for a high precipitation year, such as the year 2048 GFDL 4.5, (Figure 5-20) WEPP does not display a water stress (values =1) during the growing season. The opposite is seen in a low precipitation year (Figure 5-21), with water stresses occurring continuously during approximately day 190 to day 250. These water stresses have an expected negative impact on crop yields as they occur during the growing season.

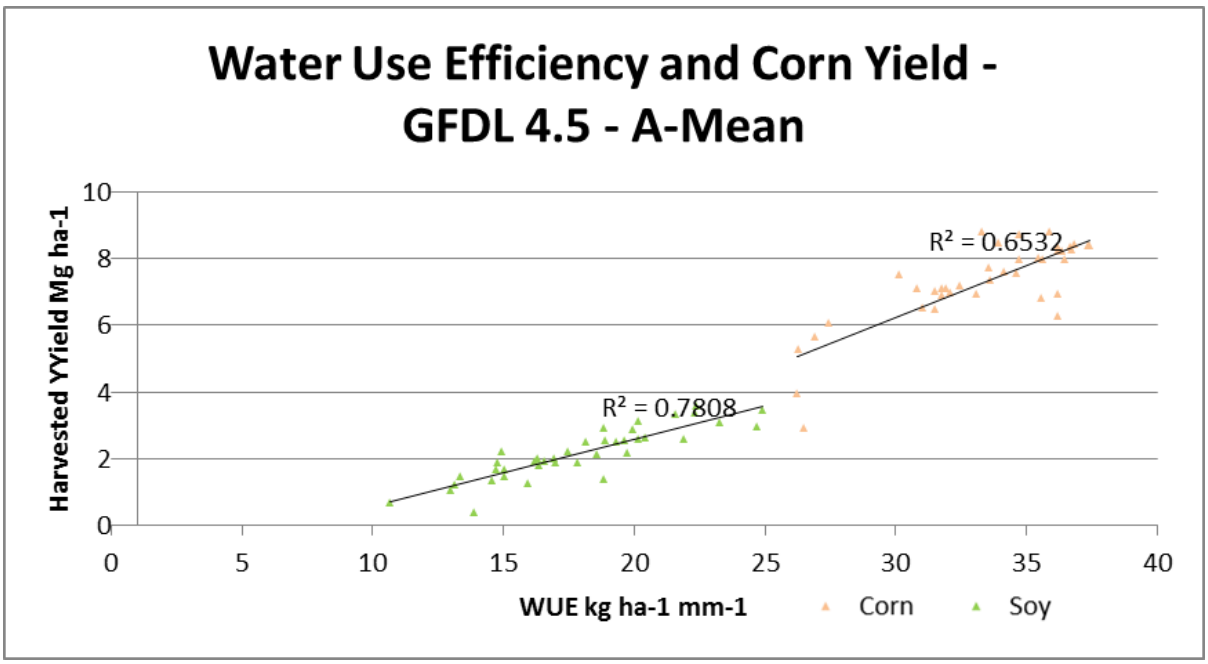


Figure 5-18: A-Mean Corn and Soy WUE and harvest yield for GFDL RCP 4.5

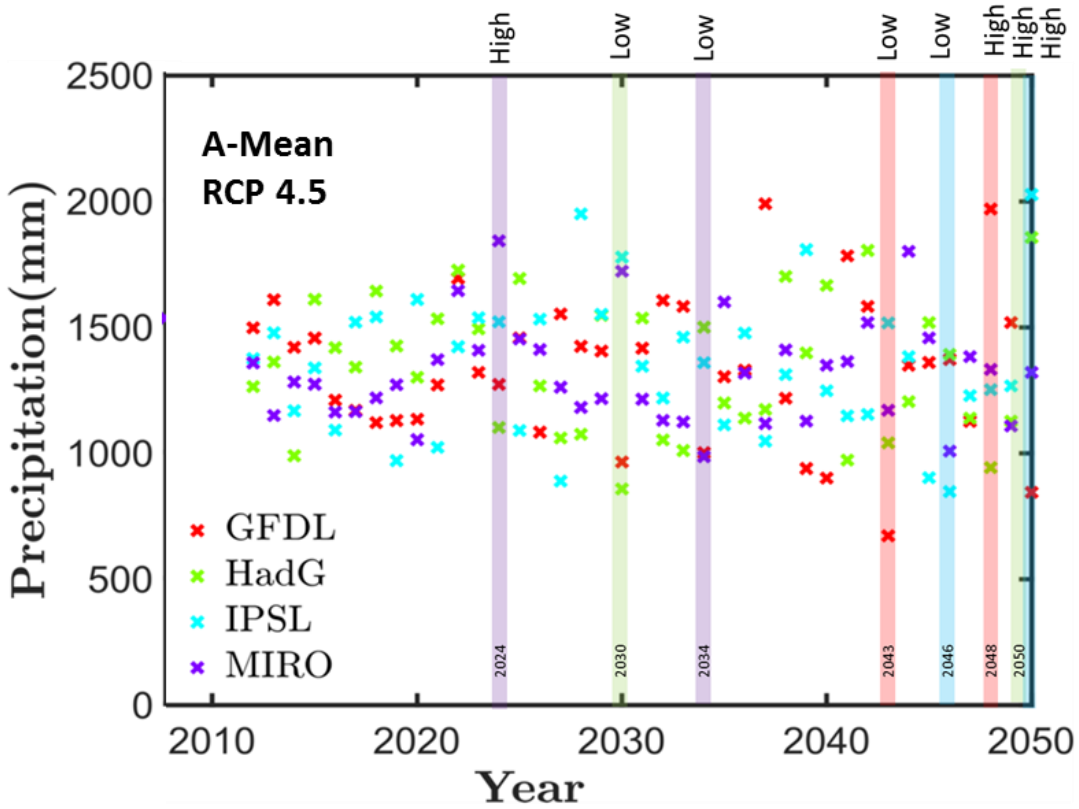


Figure 5-19: A-Mean RCP 4.5 projected yearly cumulative precipitation

Factors limiting the identification of water stresses are determining how much precipitation is actually needed and when an insufficient amount would affect growth or critical crop stages. Corn needs an estimated 500-800 mm during its growing season and has a medium to high drought sensitivity, soybean needs 450-700 mm and has a low to medium sensitivity, and cotton needs 700-1300 mm and has a low sensitivity (Brouwer and Heibloem 1986).

Figure 2-1 demonstrates that one of the elements of the water balance is water storage, which includes water stored before planting. Factors affecting water storage include the type of soil texture and if there is a fragipan or impermeable layer located within the soil column. Hamilton et al. (2015) calculates precipitation for the year as time of harvest

from the year before to harvest time of the current year in order to take water storage into account.

Another reason for years that deviate from the average harvest yields (i.e., yield gaps) are timing considerations such as the planting and harvesting dates. Occurrence of pests, diseases, droughts, and floods all contribute to this variability. For example, if right after planting a large precipitation event occurs and the fields require reseeding a deviation from the typical planting date would occur. Although temperature and water stresses are the dominate yield limiting factors, the timing of these factors are also a critical component.

How water and temperature stresses affect yield is demonstrated by evaluating the crop yield with the added insight of the crop's critical stage. The year 2043 represents a low precipitation (Figure 5-19) and a historical and projected low yield year (Figure 5-22).

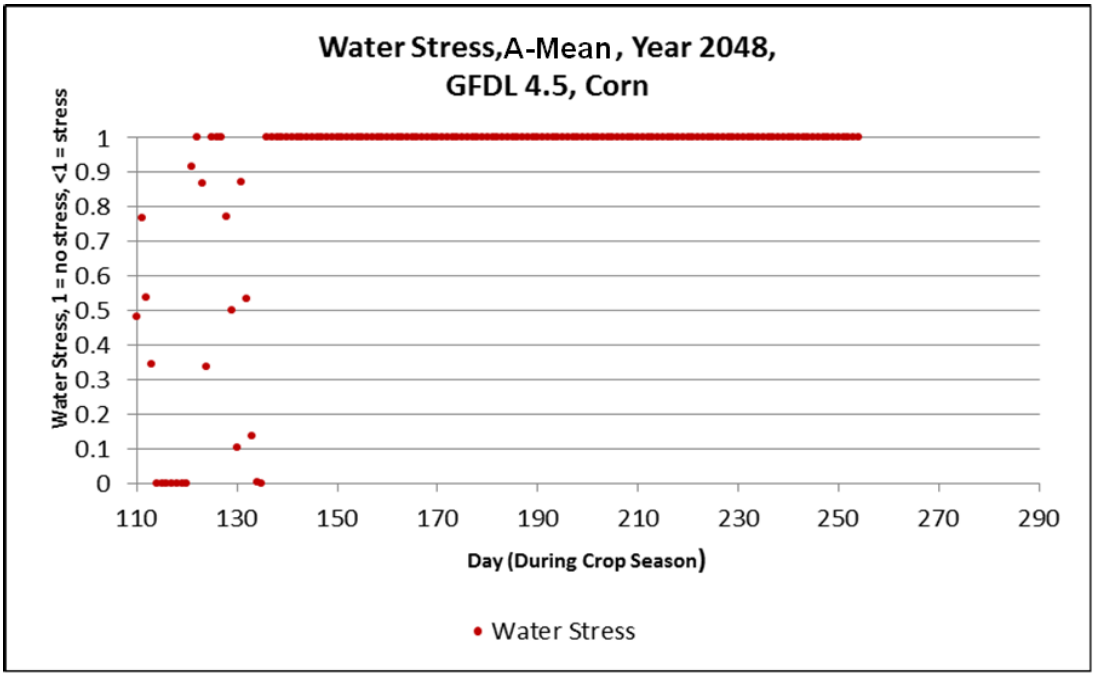


Figure 5-20: Water stresses on corn for a projected high precipitation year

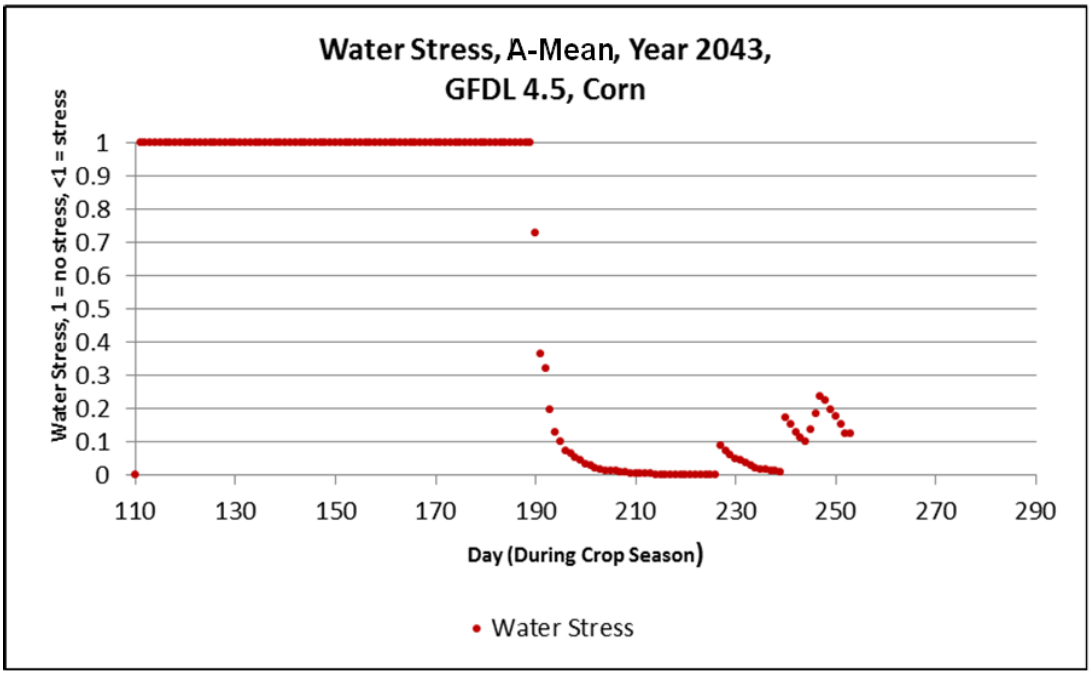


Figure 5-21: Water stresses on corn for a projected low precipitation year

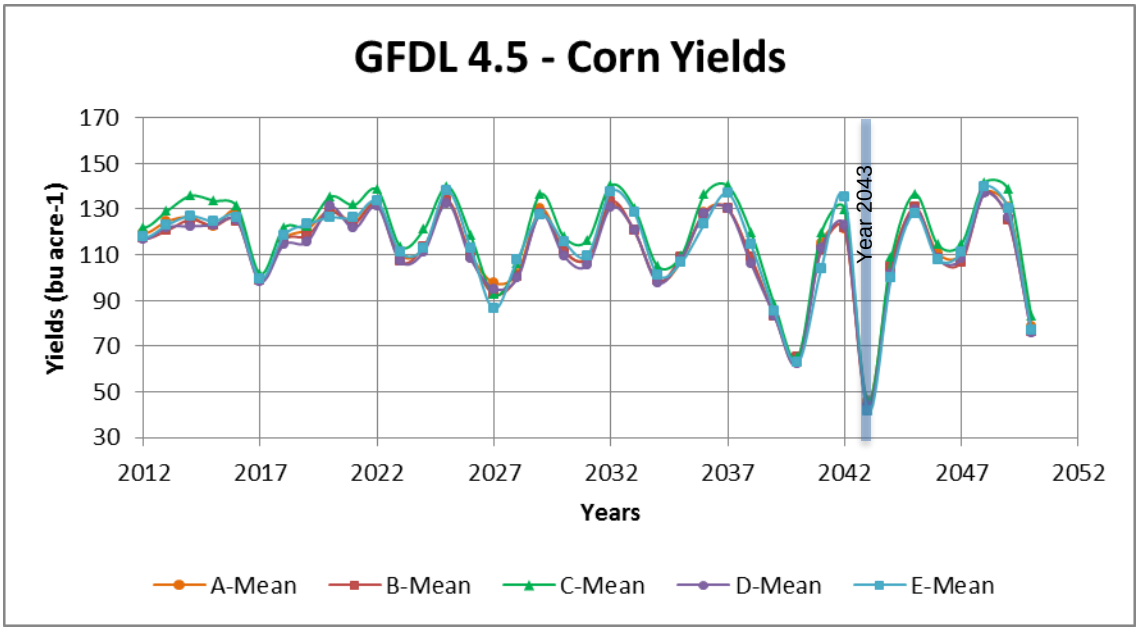


Figure 5-22: Harvested yield for corn, year 2043 is a low yield year

Figure 5-23 highlights one of corn's critical stages, R1, along with the water stresses for the growing season. It shows that this year is not a water stress period for the targeted stage as defined by WEPP. Whereas Figure 5-24 has the added insight of the addition of the temperature stresses, which does show values less than one during this critical time. A reexamination of the biomass equation, where the variable REG is the lesser value due to either temperature or water stress, demonstrations that there are many occurrences during the growing season that the water stress value is 0 and therefore no increase in biomass. Although this is not occurring during the targeted critical period, other stages of a crop's growing season can also have profound effects on harvest yield.

This example shows that variable climate conditions present challenges in the identification of these critical times. Influences include planting and harvest dates, the existing water storage or precipitation before planting, water and temperature stresses and at what time during the crop's cycle that they occur.

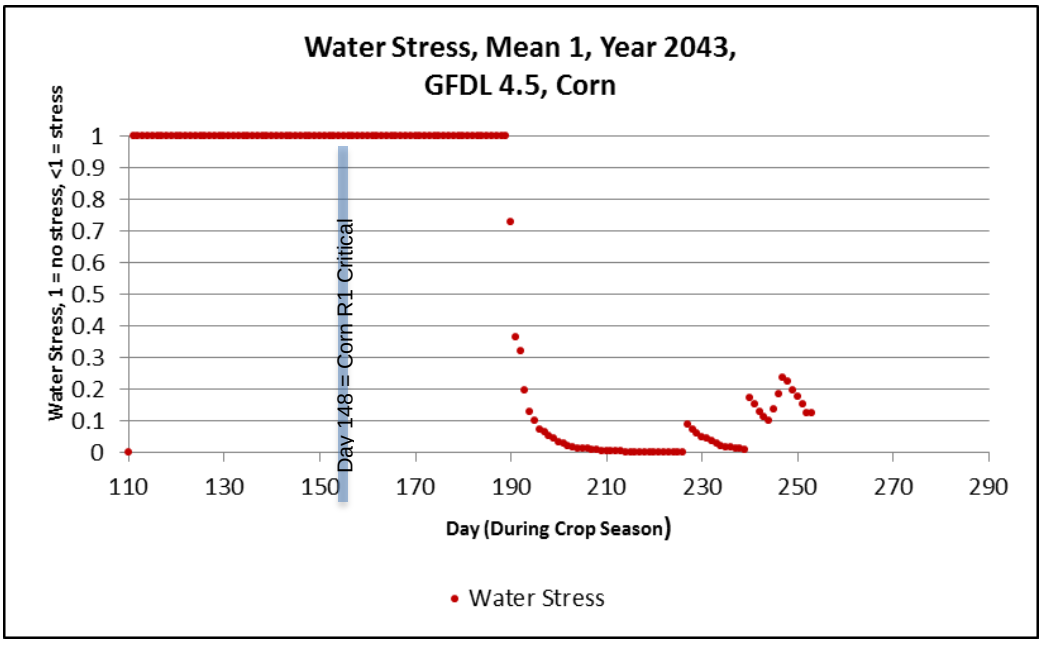


Figure 5-23: Water stresses on corn with the identification of the crop's critical stage

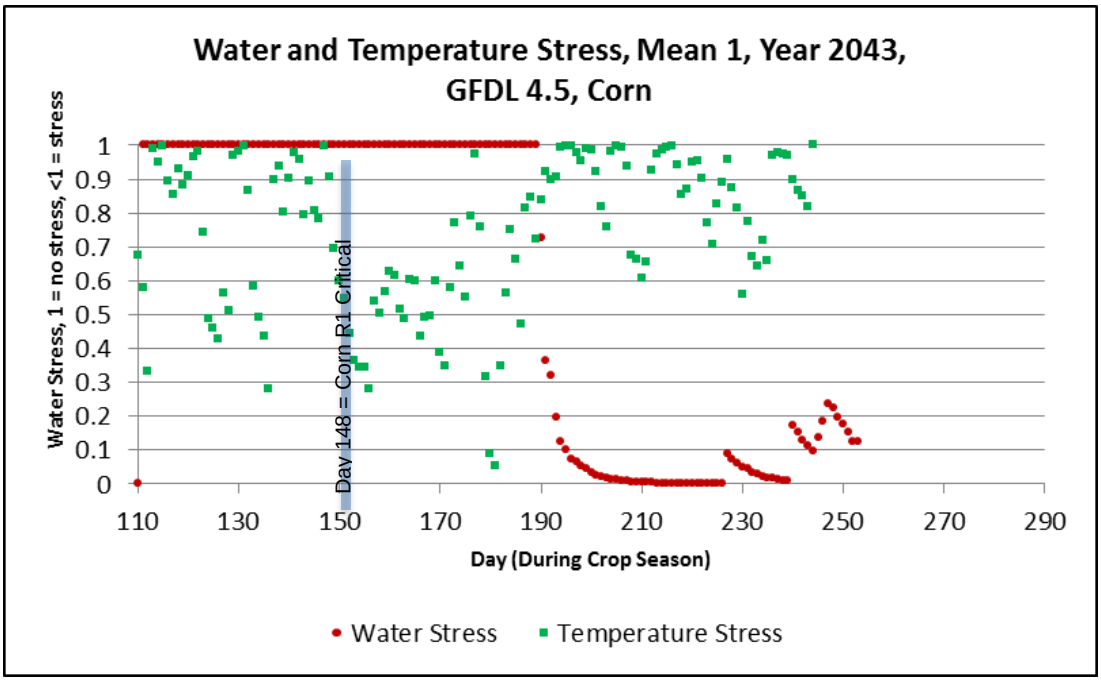


Figure 5-24: Corn Water and Temperature stresses with the identification of the critical stage

System Water Use Efficiency – Dietzel et al. (2016)

A systems level approach to water use efficiency, by incorporating the addition of drainage and runoff to the ET portion of the equation (Dietzel et al. 2016), provides additional insight into the underutilization of water, which previous studies fail to address. An underutilization can occur in two ways. A lack of available water can lead to an underutilization by placing water stresses that effect growth and result in decreased crop yields.

An underutilization can also occur through an excess of available water, where an increase in runoff can also lead to soil erosion. SOC relates to the soil's ability to retain water (Wilson et al. 2016), of which erosion and temperature increases are contributing factors leading to its decrease in stocks. This can lead to reduced crop yields.

The sWUE calculation aids in determining if the amount of water available is sufficient for optimal crop growth with minimal runoff. The greatest sWUE values are not necessarily correlated with the largest yields, since high yields usually occur in years with greater quantities of precipitation, but relates more to how efficient is the entire system. This demonstrates that the amount of water produces the largest amount of yield, while contributing the least amount of runoff and drainage.

Figure 5-25, Figure 5-26, and Figure 5-27 graph the past sWUE values for each of the crops, corn, soy, and cotton. Observing that while 2007 is a low precipitation year it is also a high sWUE year. Further investigation into water stress (Figure 5-28) show that although the precipitation levels are low there are only water stresses in the beginning of the crop season. Also looking at the crop yields in Figure 4-9, the crop yields are lower but not significantly lower if compared to other low years.

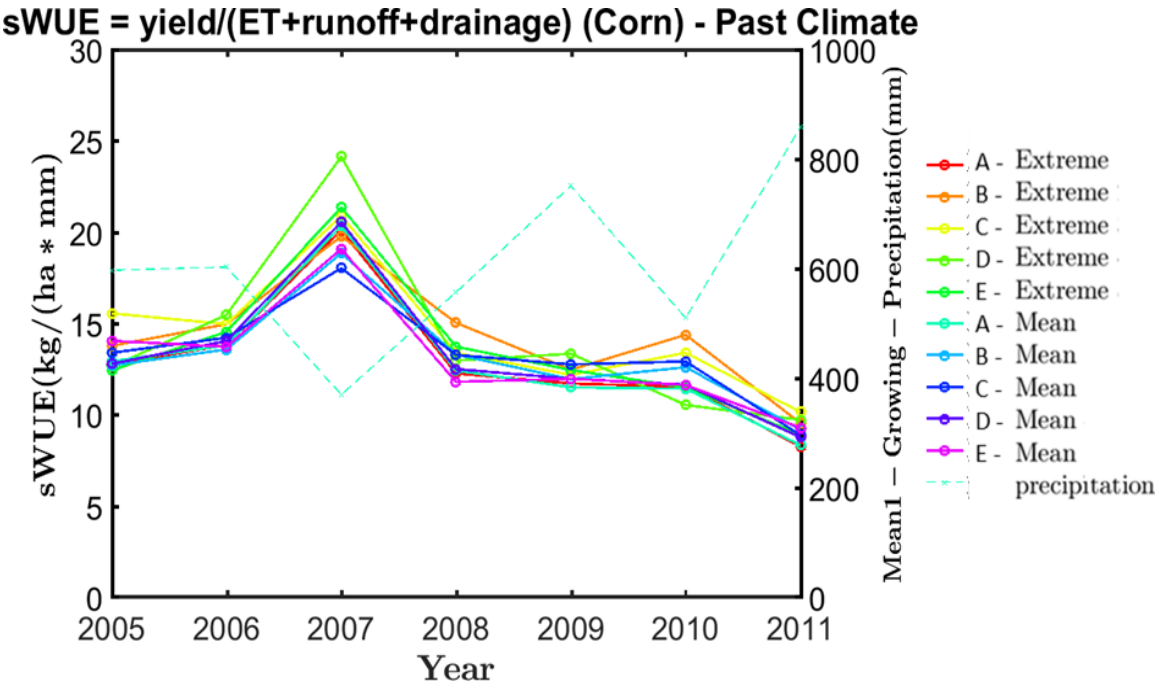


Figure 5-25: Corn sWUE for projected past climate scenario with added drainage

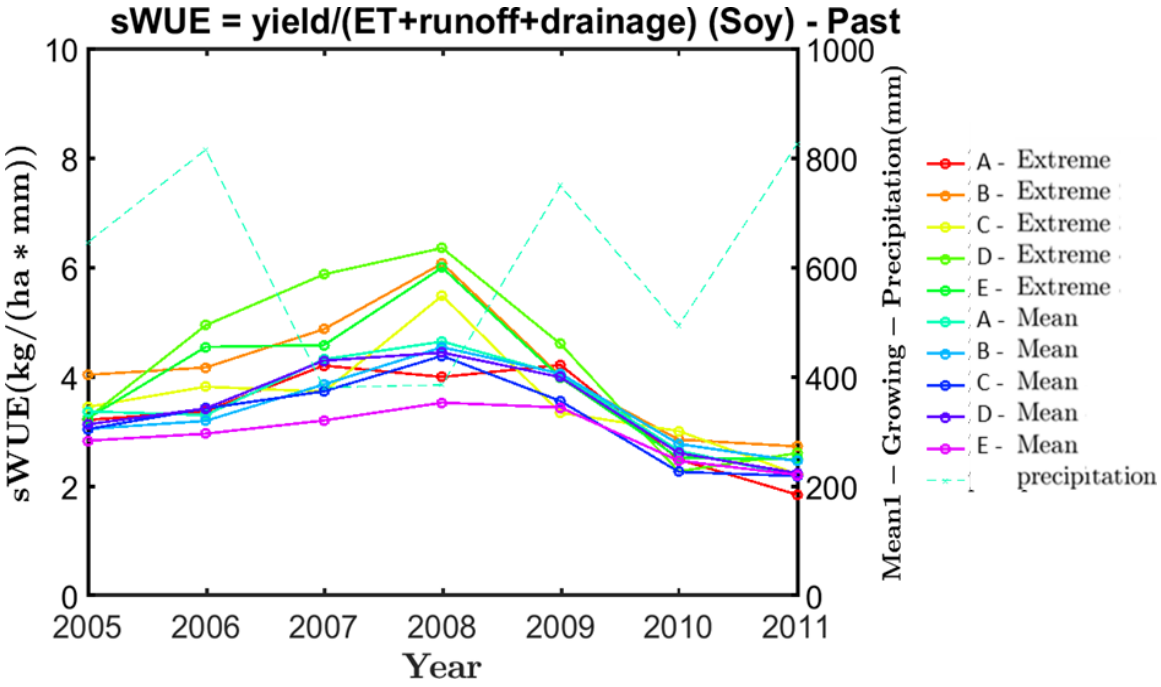


Figure 5-26: Soy sWUE for projected past climate scenario with added drainage

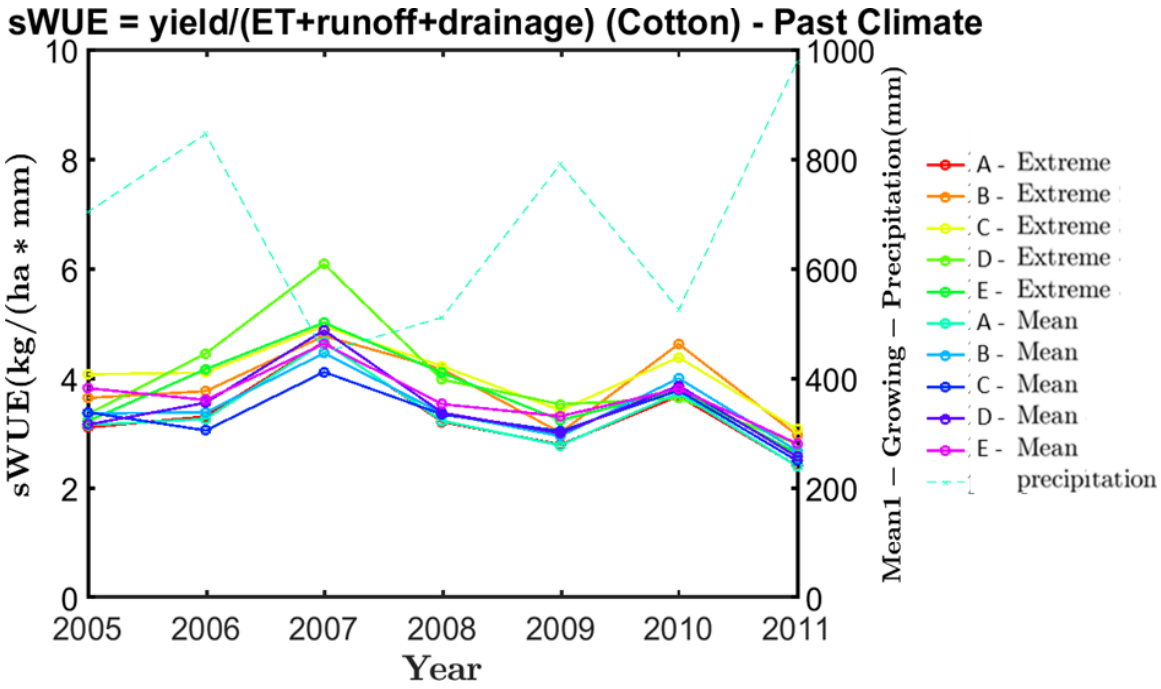


Figure 5-27: Cotton sWUE for projected past climate scenario with added drainage

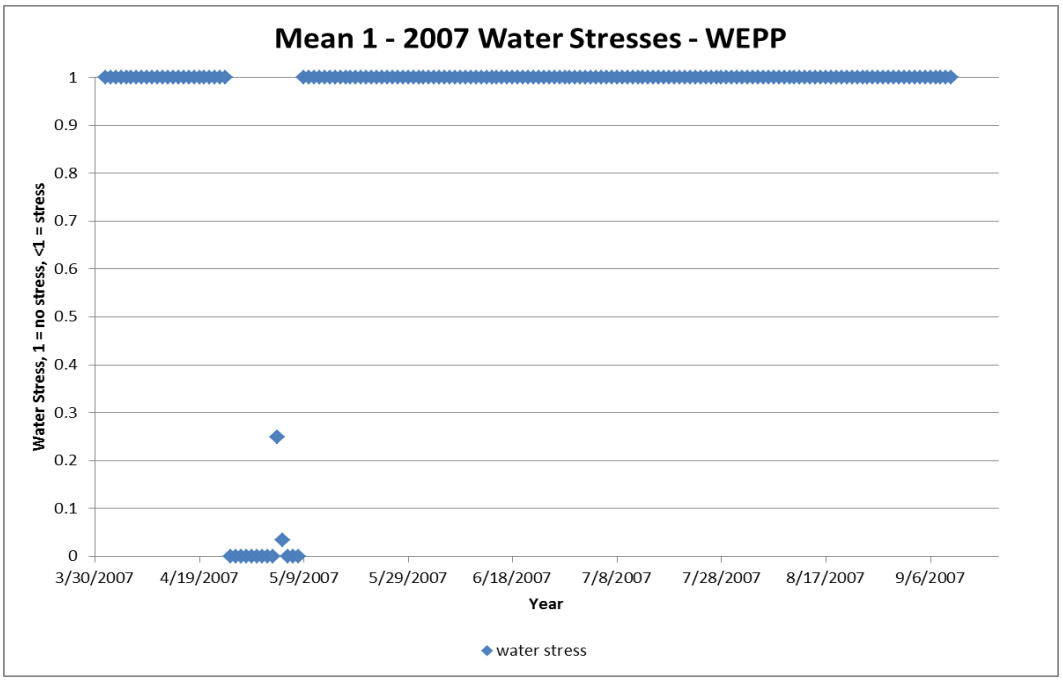


Figure 5-28: Corn Water Stresses for 2007

High precipitation years, 2006, 2009, and 2011 have decreased sWUE values, but determining the ideal amount of precipitation for a system and when this transition of optimal sWUE occurs differs for each crop. Using the methods of Dietzel et al. (2016) and the Ricker's curve equation (5-1), the maximum precipitation for each crop that leads to the most optimal sWUE is calculated using the data points for all 8 projected climates.

The Ricker's curve (Archontoulis and Miguez 2015) is fitted through the sWUE and growing precipitation data points using SPSS (SPSS Statistics for Windows 2013) software (Figure 5-29, Figure 5-30, and Figure 5-31).

$$Y = A_1 * X * e^{-A_2 * X} \quad (5\text{-}1)$$

The maximum point of the curve for each crop (Table 5-1) estimates where additional increases in precipitation causes sWUE to decrease, runoff to increase, and yields not to increase (Dietzel et al. 2016). This approximate growing season precipitation point

highlights an important distinction compared to other methods, which after a certain amount, precipitation contributions to underutilization and a lower sWUE.

By graphing the yields per precipitation amount, it is apparent that the rate of increase decelerates after the maximum precipitation point, as seen in the representative subset of Figure 5-32. Variations of this deceleration are apparent in corn, soy, and cotton; although after 800 mm there is an apparent trend of no additional increases for all crops. Figure 5-33 demonstrates that sWUE consistently decreases after the precipitation maximum point.

In all locations except for the A-Extreme the mean locations have higher sWUE values. This is also apparent in the projected climates for corn, but not as evident for soy or cotton. Soy values are lower than corn due in part to soy being a less efficient C3 crop (Dietzel et al. 2016).

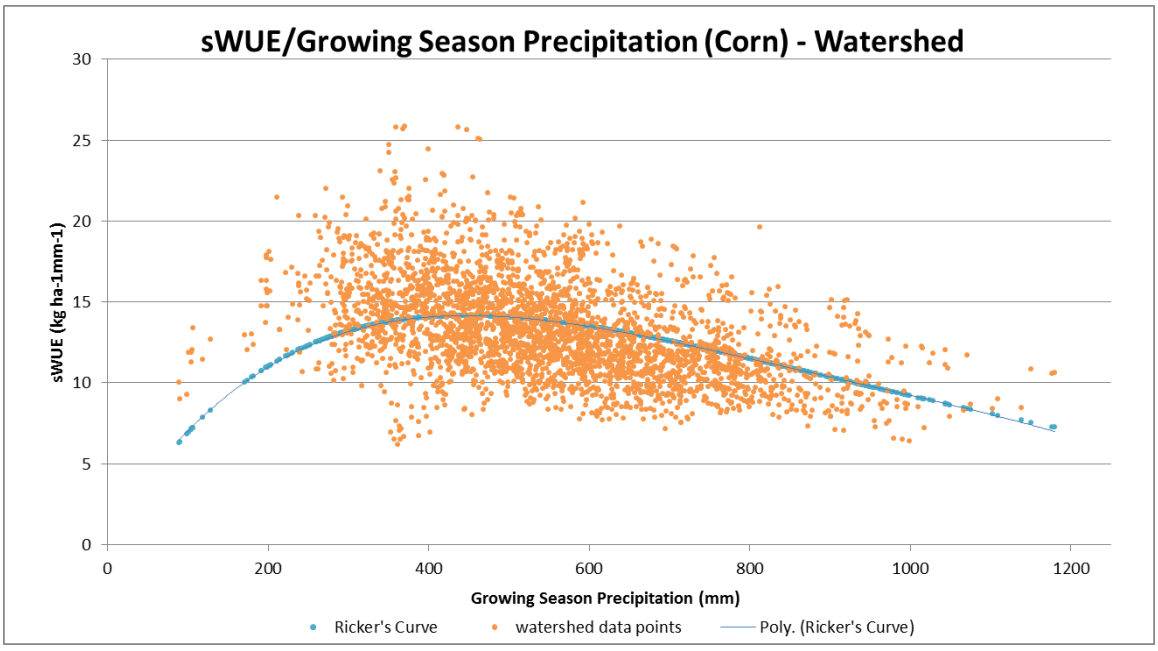


Figure 5-29: sWUE/Corn Growing Season Precipitation for the entire Obion Watershed

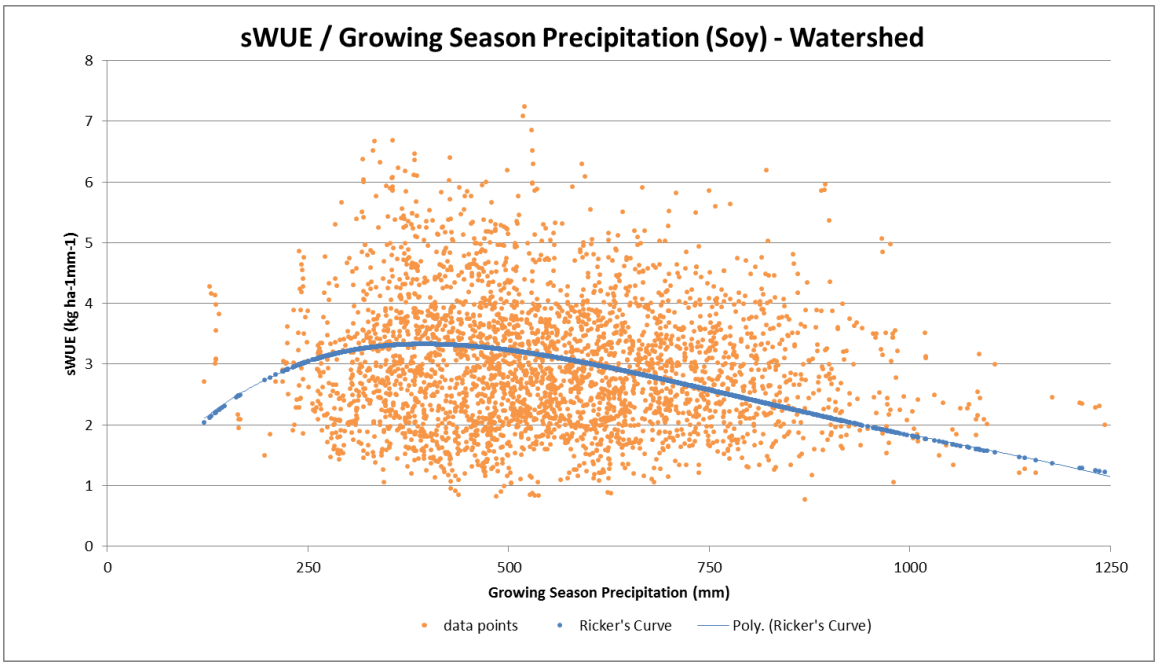


Figure 5-30: sWUE/Soy Growing Season Precipitation for the entire Obion Watershed

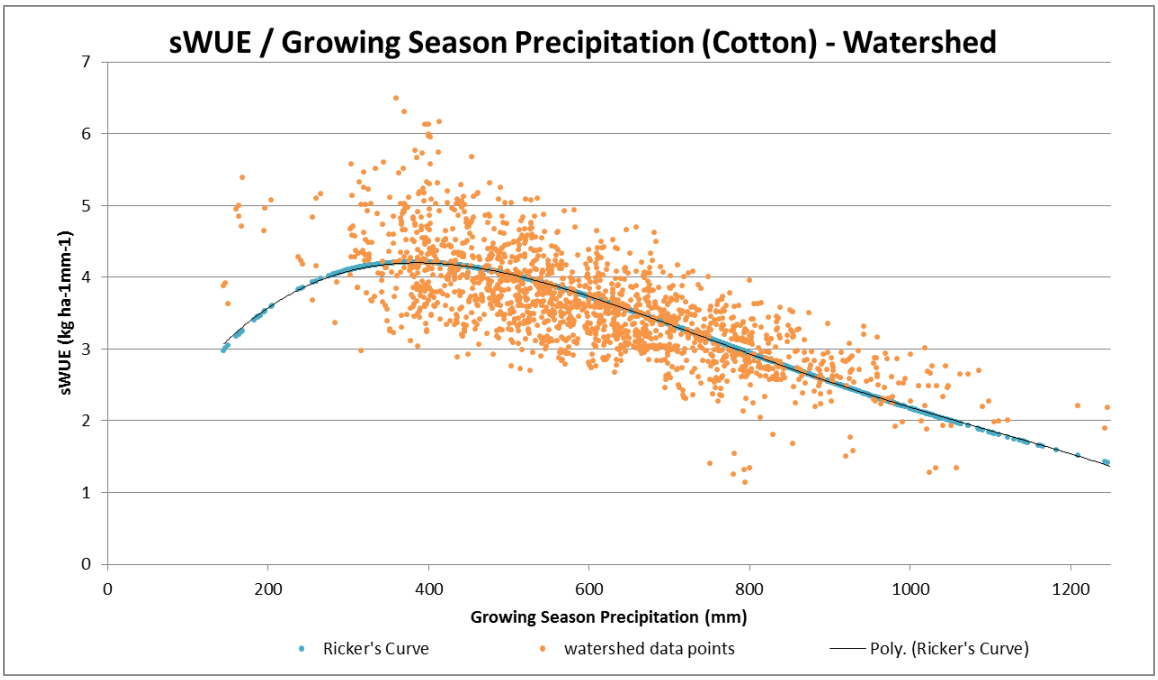


Figure 5-31: sWUE/Cotton Growing Season Precipitation for the entire Obion Watershed

Table 5-1: Maximum Precipitation Point on Curve Corresponding to Optimal Utilization of Water

Crop	Maximum Precipitation Point on Curve (mm)	sWUE (kg ha-1 mm-1)
Corn	447	14.15
Soybean	395	3.32
Cotton	381	4.21

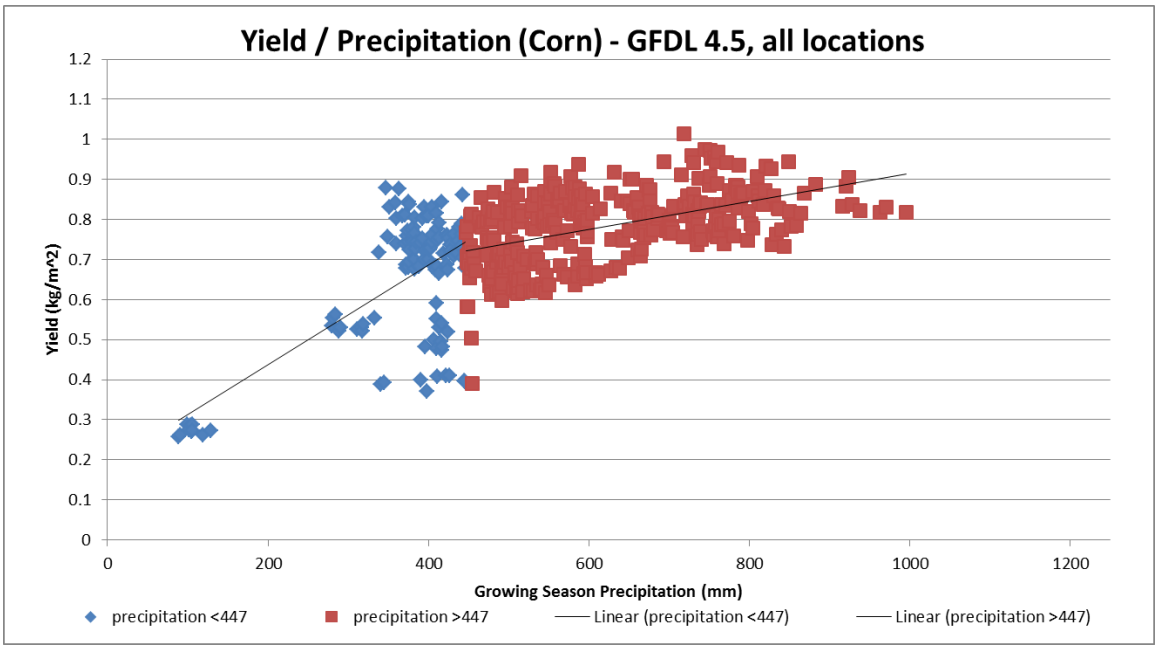


Figure 5-32: Yield / Corn Growing Season Precipitation for GFDL 4.5 projection

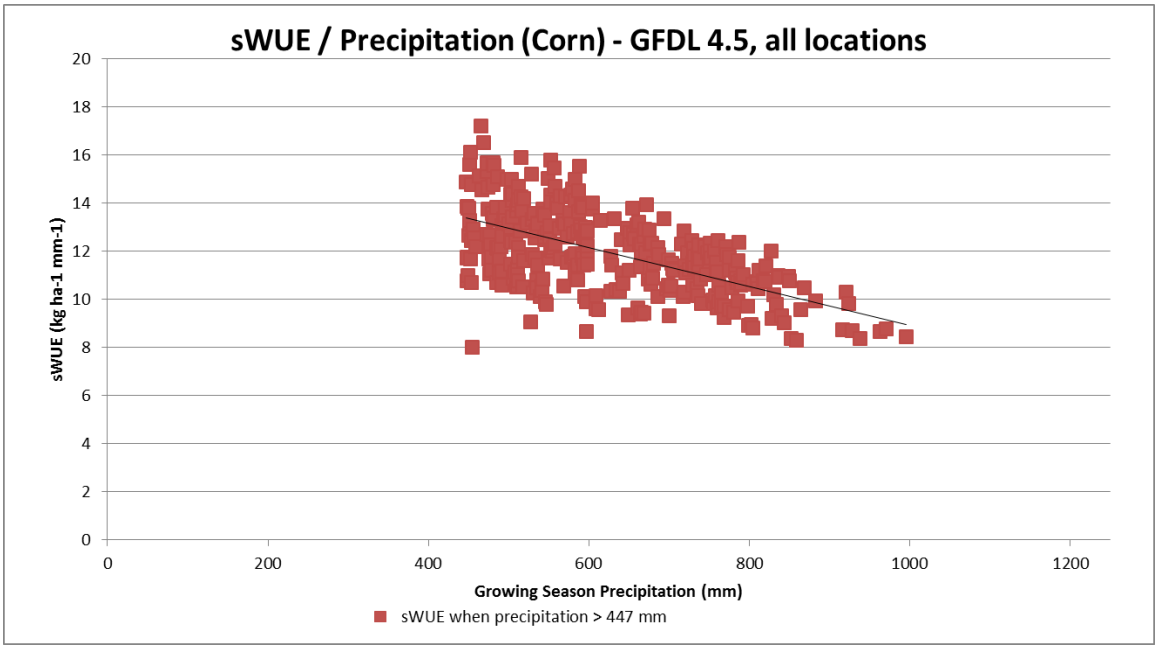


Figure 5-33: sWUE / Corn Growing Season Precipitation for GFDL 4.5 projection

The sWUE values for the past climates and the projected climates are also compared, as seen in Figure 5-34 - Figure 5-39, with three categories of sWUE, high (green), middle (yellow), and low (red). Although many factors are involved, this categorization allows for a rough estimate to see if the shape and slope are dominant factors in the outcome. Each comparison approximately aligns, with expected variations occurring due to the impending variable climate. The predicted order is then compared with each crop's observed past sWUE values for each location (Table 5-2), noting that this estimate is within range of the expected outcome.

Comparing ranges of corn values of 13.0-14.4 $\frac{\text{kg}}{\text{ha}*\text{mm}}$ to approximately 10-15 $\frac{\text{kg}}{\text{ha}*\text{mm}}$ for (Dietzel et al. 2016) and soy ranges of 3.0-4.3 $\frac{\text{kg}}{\text{ha}*\text{mm}}$ to approximately 2-3.5 $\frac{\text{kg}}{\text{ha}*\text{mm}}$ for (Dietzel et al. 2016). (Dietzel et al. 2016)'s sWUE data resulted in being four times greater than soy, which also occurred in the Obion Watershed. Variations are expected including different study sites, the comparison site is located in Boone County, Iowa, but approximate ranges are to be expected.

Table 5-2: Ordering of predicted sWUE of each location based on slope and shape

lower sWUE – higher sWUE	Shape	Slope	Location
	Linear & Mild Concave	> 6 % (linear) > 1 % (concave)	B-Extreme
	Convex (entire shape)	> 2 %	E-Extreme
	Mild S shape (convex on top)	> 0.1 %	C-Mean
	Linear	> 0.1 %	C-Extreme
			E-Mean
	Linear	> 2 %	D-Extreme
	Mild S shape (convex on the bottom)	> 5 %	B-Mean
	Linear	> 3 %	A-Mean
			A-Extreme
			D-Mean

A final table (Table 5-3) is presented with the predicted levels based on shape/ slope and the sWUE categories. This estimate shows that the shape and slope alone are able to demonstrate a rough estimate of the predicted values.

The sWUE equation performs an evaluation of the yield over a defined area per water used and lost. Between locations, precipitation values do not vary greatly across the Obion River watershed, but do vary between years. Modifying the original equation and normalizing it for precipitation results in an evaluation of the yield over a defined area that also takes into account the water that is in the soil and that the plant uses.

Figure 2-1 shows the water cycle of the crop, including precipitation, ET (which is the combination of transpiration and soil evaporation), runoff, drainage (lateral and vertical losses), actual plant use, and water contained in the soil, and precipitation.

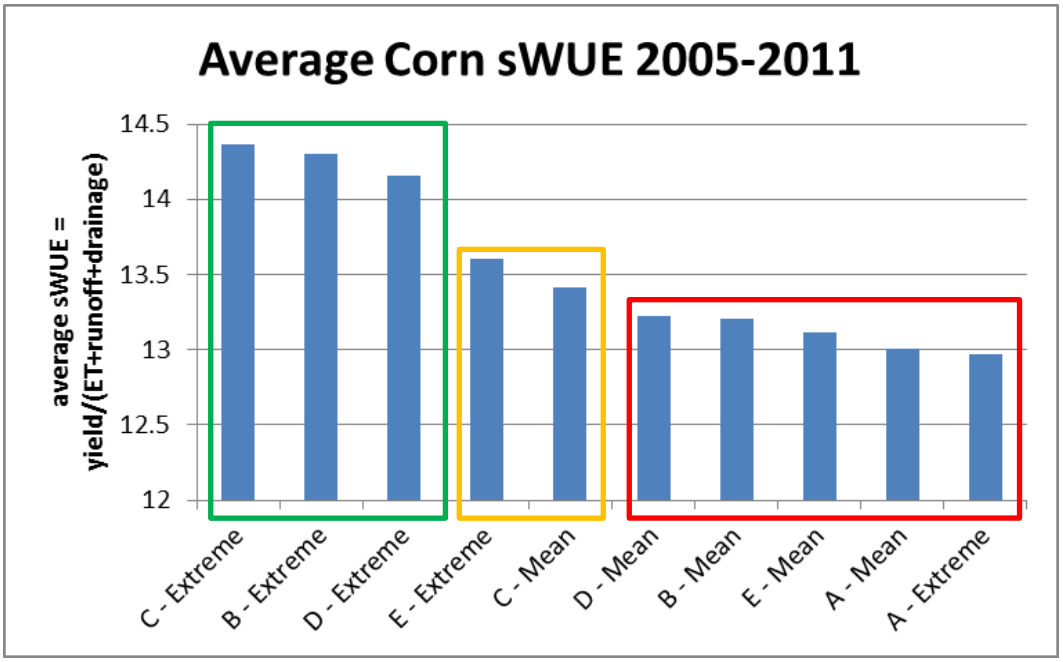


Figure 5-34: Average corn sWUE values for past 2005-2011

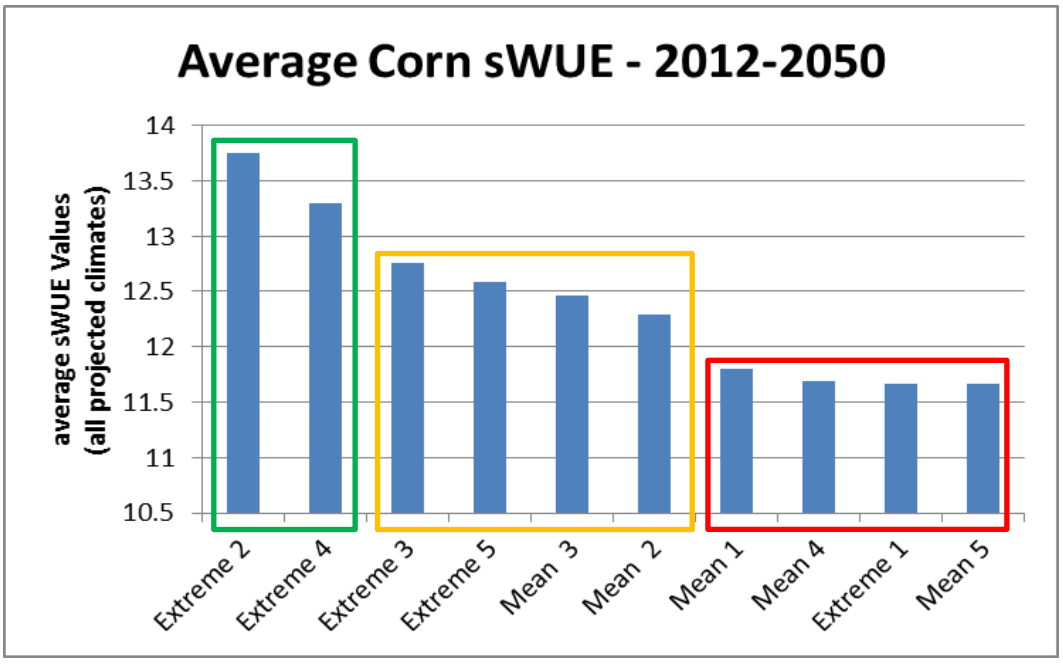


Figure 5-35: Average corn sWUE values for all projected future climate

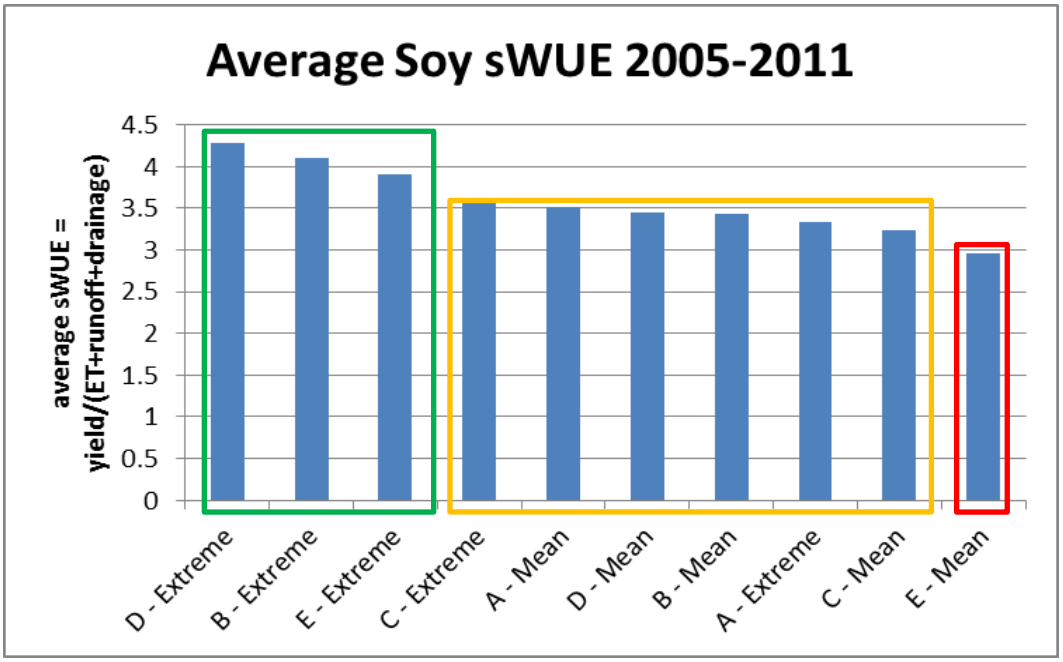


Figure 5-36: Average soy sWUE for past 2005-2011

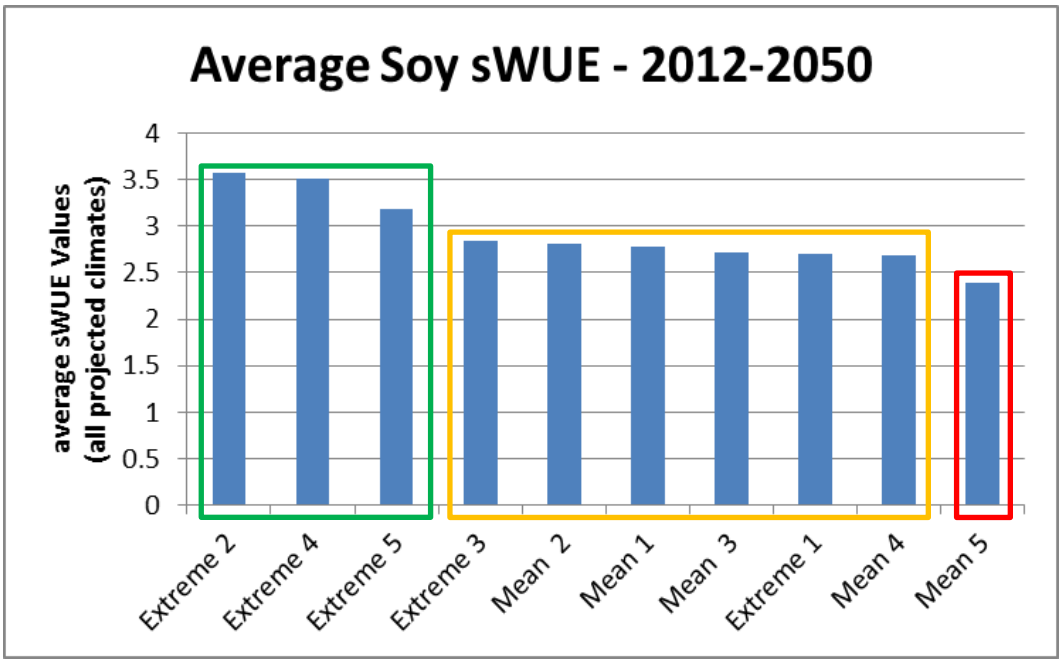


Figure 5-37: Average soy sWUE values for all future projected climates

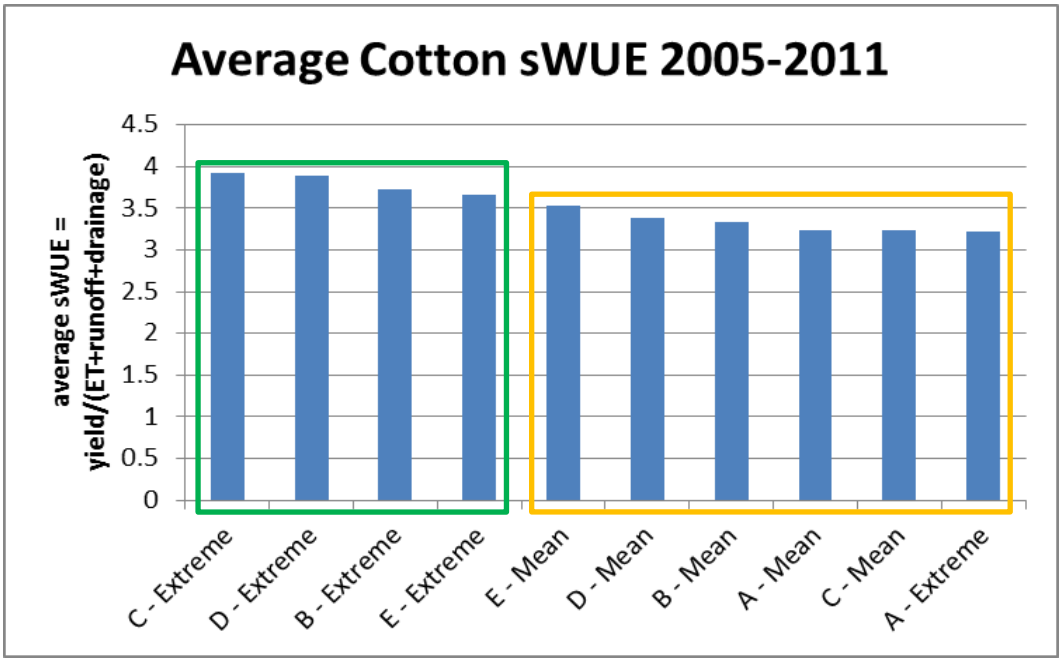


Figure 5-38: Average cotton sWUE for past 2005-2011

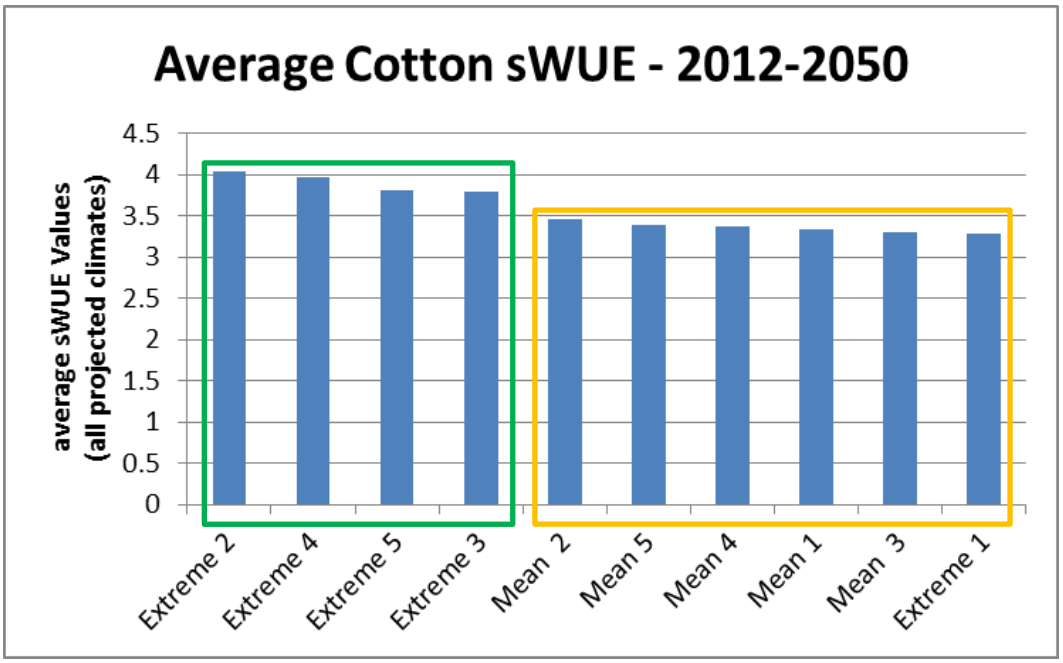


Figure 5-39: Average cotton sWUE Values for all future projected climates

Table 5-3: Predicted and sWUE values based on shape and slope

	Predicted level sWUE Based on Criteria	sWUE Value		
Location	Shape & Slope	Corn	Soy	Cotton
A-Extreme	low	low	middle	middle
B-Extreme	high	high	high	high
C-Extreme	middle	middle	middle	high
D-Extreme	middle	high	high	high
E-Extreme	high	middle	high	high
A-Mean	low	low	middle	middle
B-Mean	middle	middle	middle	middle
C-Mean	high	middle	middle	middle
D-Mean	low	low	middle	middle
E-Mean	middle	low	low	middle

The addition of runoff, drainage, and ET over the precipitation for each growing season allows for normalization of each year since the expected water input to the area presents as precipitation. This modification causes sWUE values to align with expected results between years (Figure 5-40 - Figure 5-42) with projected results shown in Figure 5-43 - Figure 5-45 and Table 5-4 - Table 5-6.

$$modified\ sWUE\left(\frac{kg}{ha}\right) = \frac{yield\left(\frac{kg}{m^2}\right) * \frac{10{,}000\ m^2}{1\ ha}}{\frac{ET\ (mm) + runoff\ (mm) + drainage\ (mm) of\ growing\ season}{precipitation\ (mm)}} \quad (5\text{-}2)$$

The impact of each climate scenario on the water use efficiency is demonstrated by looking at the overall maximum and minimum of all the locations (Figure 5-34 - Figure 5-39) which are the B-Extreme and E-Mean respectively and their slopes. Appendix A.3 displays the modified sWUE (MsWUE) graphs for all the projected climate scenarios.

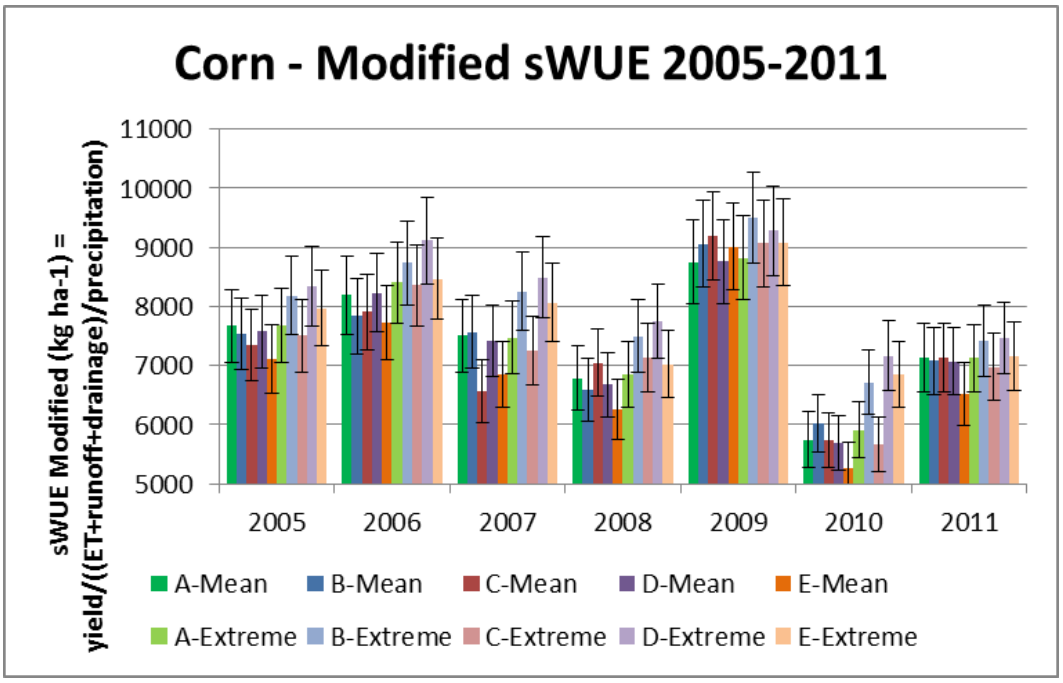


Figure 5-40: Modified corn sWUE for past climate of 2005-2011

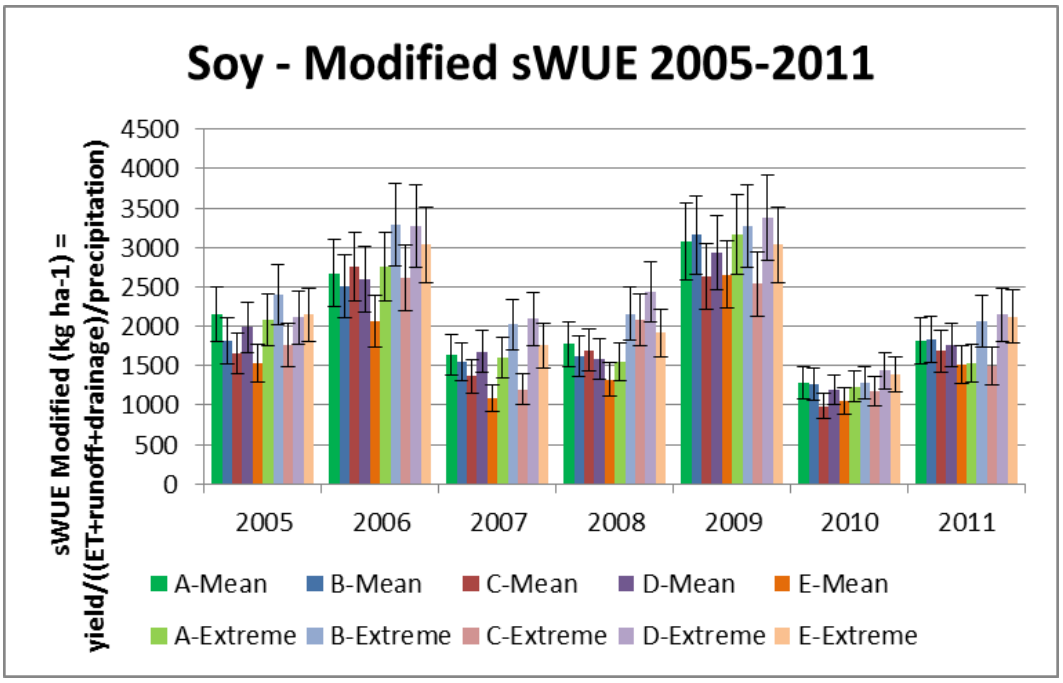


Figure 5-41: Modified soy sWUE for past climate of 2005-2011

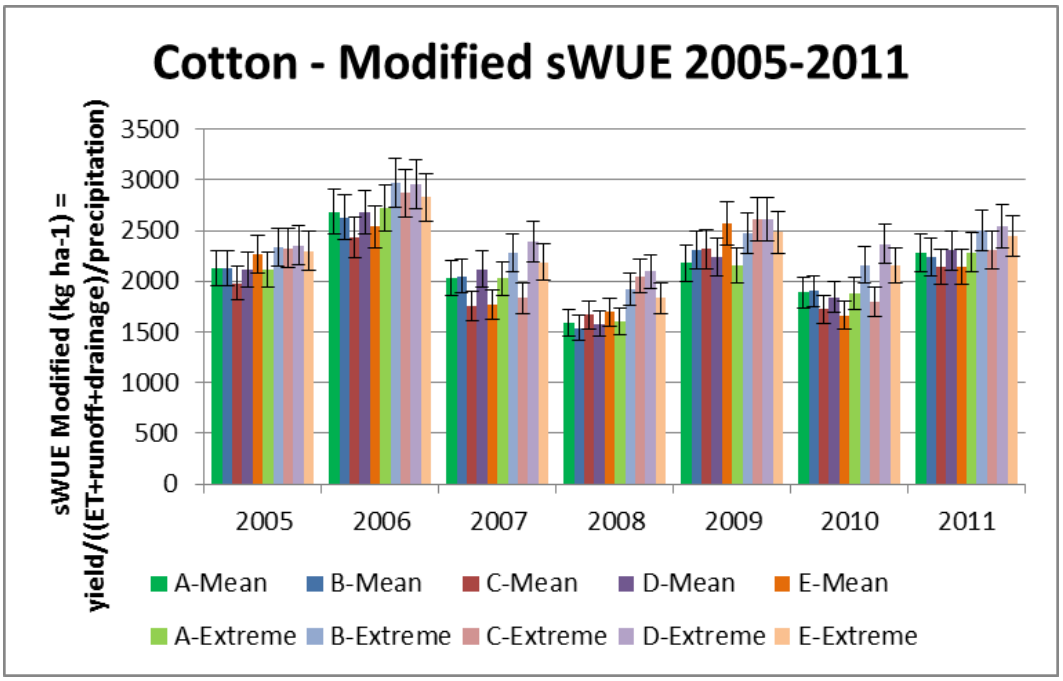


Figure 5-42: Modified cotton sWUE for past climate of 2005-2011

Table 5-4: Climate projections of modified sWUE (kg ha-1) slopes for corn

	Location	Climate Projection							
		GFDL 4.5	GFDL 8.5	HadG 4.5	HadG 8.5	IPSL 4.5	IPSL 8.5	MIRO 4.5	MIRO 8.5
High	B-Extreme	-36	-21	-78	-74	-38	-67	-31	-70
Low	E-Mean	-39	-26	-72	-66	-32	-62	-35	-65

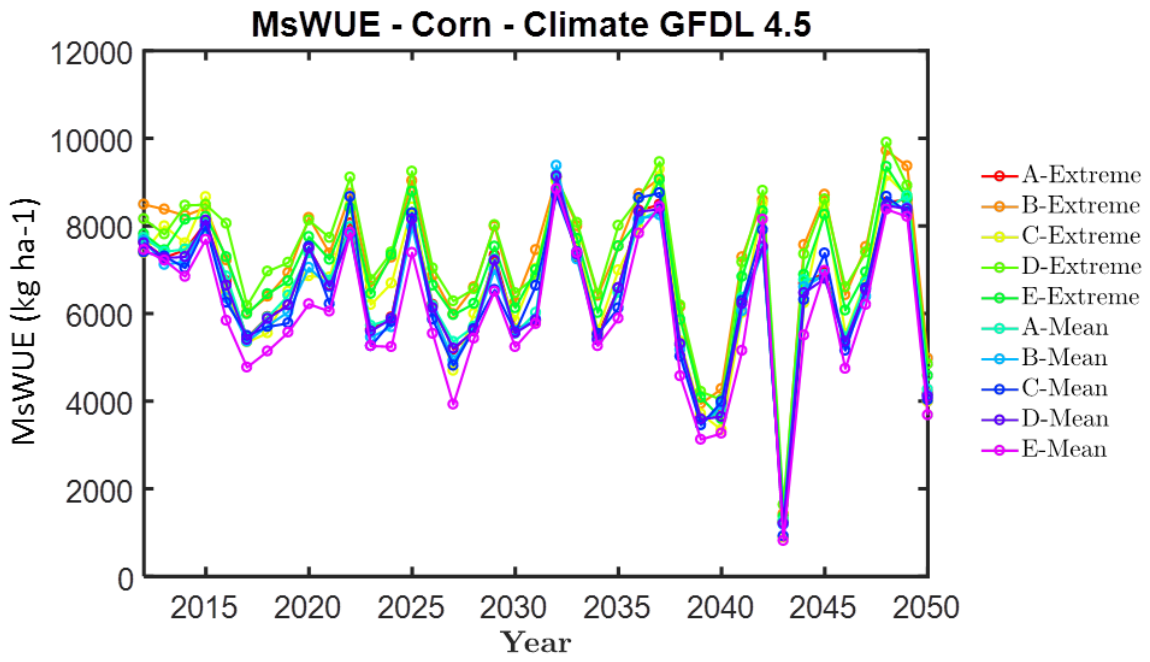


Figure 5-43: Climate GFDL 4.5 modified sWUE (kg ha-1) for corn

Table 5-5: Climate Means of modified sWUE (kg ha-1) slopes for soy

	Location	Climate Projection							
		GFDL 4.5	GFDL 8.5	HadG 4.5	HadG 8.5	IPSL 4.5	IPSL 8.5	MIRO 4.5	MIRO 8.5
High	B-Extreme	-12	-11	-32	-35	-24	-28	-15	-33
Low	E-Mean	-9.7	-8	-20	-20	-16	-20	-12	-23

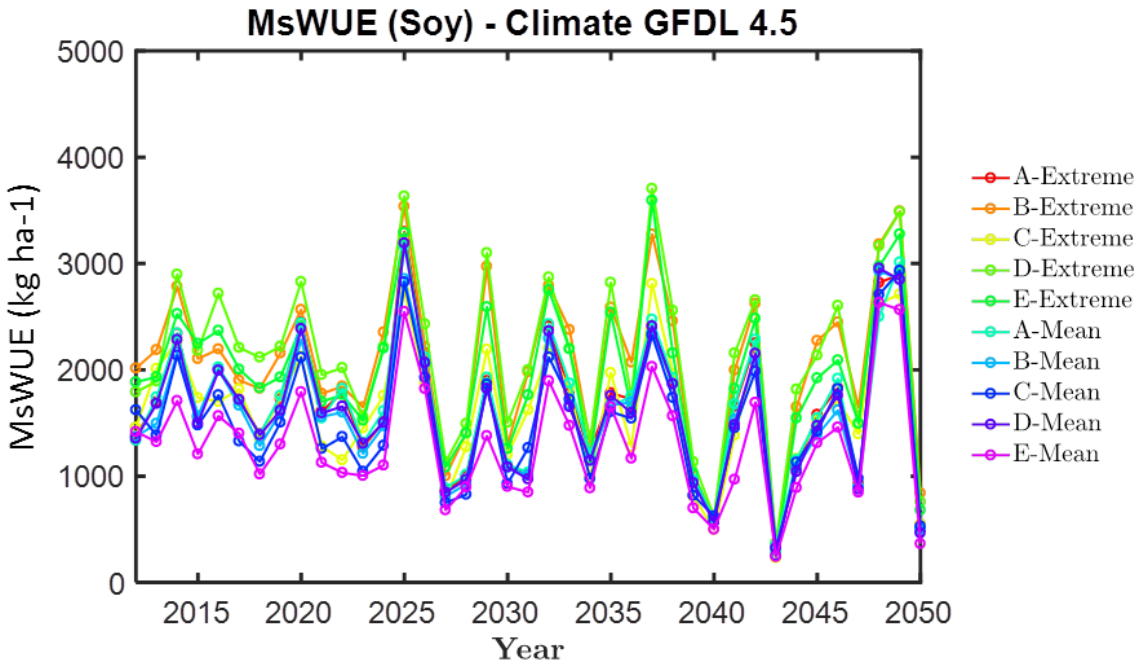


Figure 5-44: Climate GFDL 4.5 of modified sWUE (kg ha-1) for soy

Table 5-6: Climate slope of modified sWUE (kg ha-1) for cotton

	Location	Climate Projection							
		GFDL 4.5	GFDL 8.5	HadG 4.5	HadG 8.5	IPSL 4.5	IPSL 8.5	MIRO 4.5	MIRO 8.5
High	B-Extreme	-6.4	-1.9	-12	-14	-1.7	-6.9	-3.1	-9.6
Low	E-Mean	-8	-5.4	-17	-15	-7.8	-12	-8.6	-16

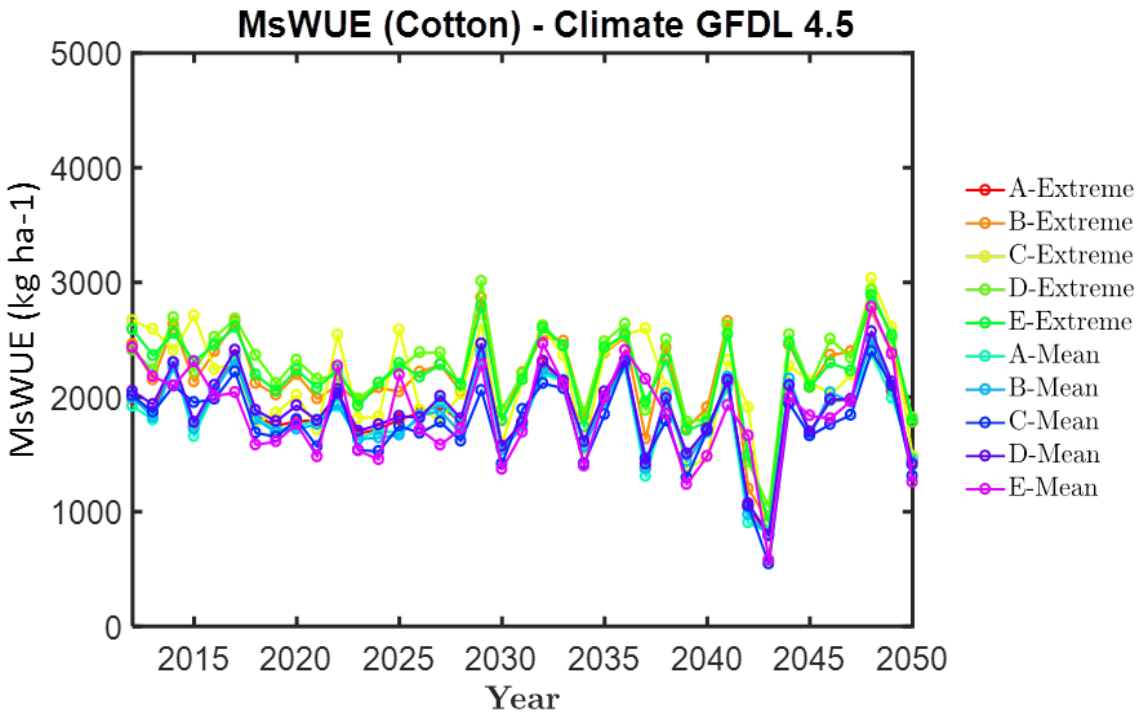


Figure 5-45: Climate GFDL 4.5 of modified sWUE (kg ha-1) for cotton

The frequency of the modified sWUE values (Figure 5-46 - Figure 5-48) for all locations and climate projections display a normal distribution for corn and cotton and skewness for soy. The statistics for all locations and all climate projections together are in Table 5-7. Table 5-8 - Table 5-10 and Appendix A.4 contain the same data, but divided by each climate projection. Both variations show the same pattern.

Soy's response behavior differs from corn with overall lower sWUE values, noting that soy is a legume. Dietzel et al. (2016) mentions that one reason for the overall lower soy values are the differing types of plants, with corn a C4 plant and soy a C3 plant.

During this same study during the driest years of testing soy had less variability and used water more efficiently. They concluded that during the drier years soy was more likely to be inefficient due to system water loss then decrease in yields.

This is a possible explanation for the bell-shaped distribution for corn and skewness for soy. Distributions were made with SPSS software, (SPSS Statistics for Windows 2013). The water use efficiency is influenced by precipitation and temperature. Growing season precipitation for each crop is presented in Table 4-10 - Table 4-12.

Yield Potential

Projected crop yields, in Figure 5-1 - Figure 5-3, provide an example of all the datasets. The overall crop yields for corn and soy have a projected decrease, cotton also has an anticipated decrease, but at a smaller rate. Despite this decrease in yields determing if crops could benefit from the addition of irrigation can be estimated based on yield potential. Lobell et al. (2009) compared various studies, including corn crops in Nebraska, with a resulting yield potential of 15 $Mg\ ha^{-1}$ for rainfed corn.

Yield potentials are values based on ideal growing conditions, with rainfed systems having a typical yield potential of approximately 50%. Whereas typical irrigated major systems have a yield potenital of approximately 80%. Projected climates for an example location of A-Mean have a potential yield percentage ranging from 44-48% (Figure 5-49), showing that all scenerios would benefit from the addition of precision agriculture.

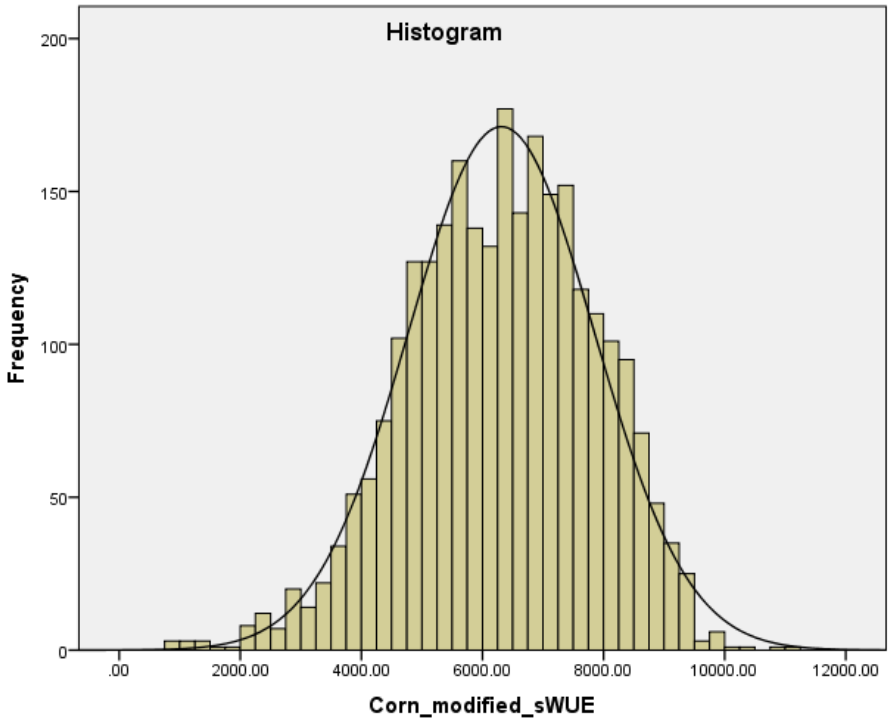


Figure 5-46: Modified corn sWUE values (kg ha-1) for all locations and climate projections

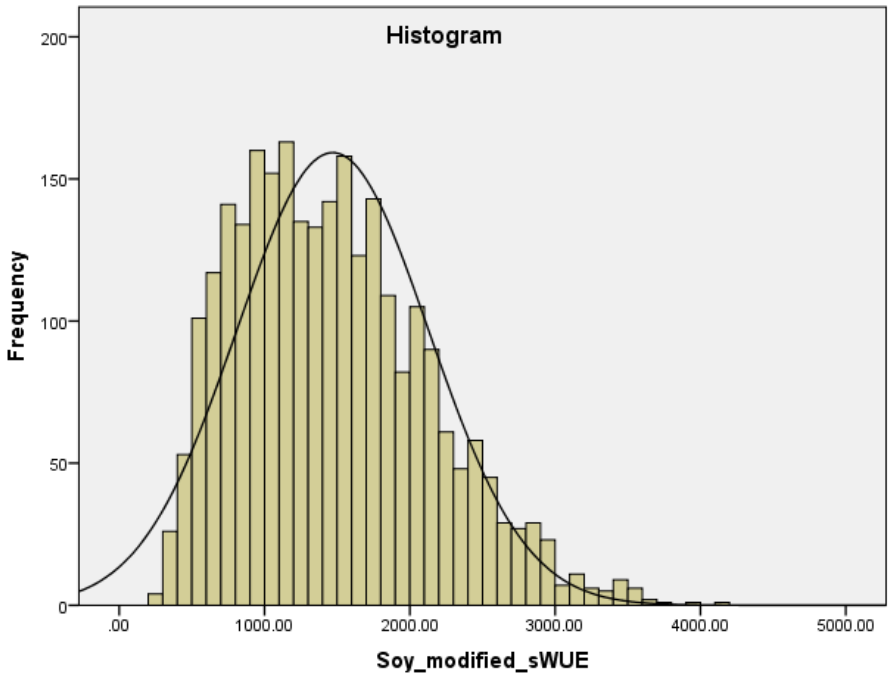


Figure 5-47: Modified soy sWUE values (kg ha-1) for all locations and climate projections

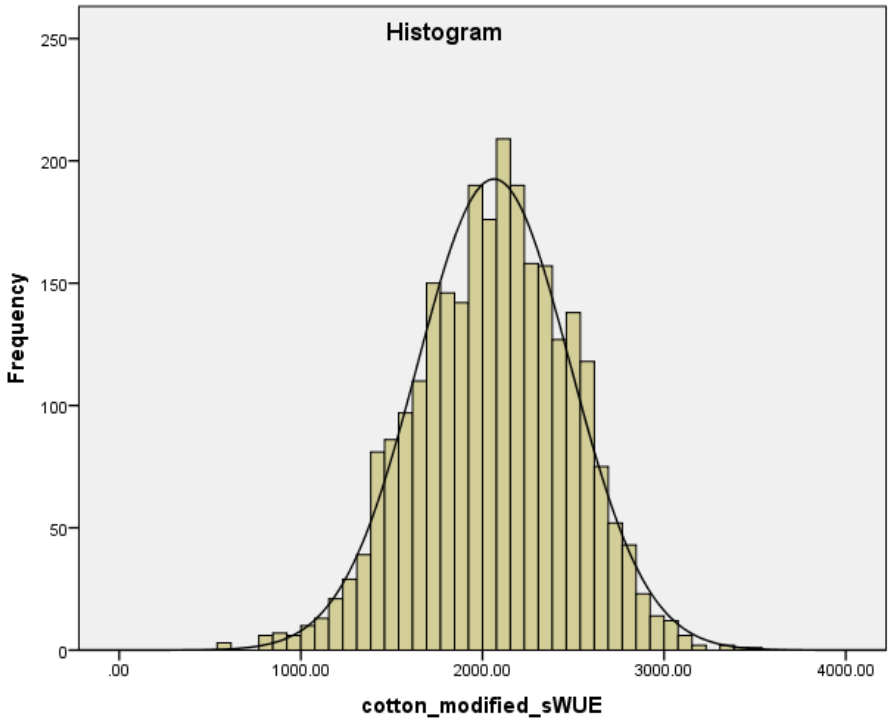


Figure 5-48: Modified cotton sWUE values (kg ha-1) for all locations and climate projections

Table 5-7: Distribution statistics for all locations and all climates for each crop, annual values

Statistics

		Corn_modified_sWUE	Soy_modified_sWUE	cotton_modified_sWUE
N	Valid	2640	2640	2640
Mean		6311.4847	1468.8369	2062.8162
Median		6379.7966	1400.3318	2079.9887
Std. Deviation		1537.91206	661.22845	420.63552
Skewness		-.243	.615	-.155
Std. Error of Skewness		.048	.048	.048
Kurtosis		-.117	.034	-.062
Std. Error of Kurtosis		.095	.095	.095
Minimum		813.27	231.06	545.58
Maximum		11031.34	4133.59	3534.40

Table 5-8: Corn distribution statistics for all locations for each projected climate, annual values

Statistics

	corn MsWUE GFDL4.5	corn MsWUE Had4.5	corn MsWUEI PSL4.5	corn MsWUE MIR4.5	corn MsWUE GFDL8.5	corn MsWUE Had8.5	corn MsWUEI PSL8.5	corn MsWUE MIR8.5
N Valid	330	330	330	330	330	330	330	330
Mean	6522.642	5845.875	6672.620	6681.133	6750.779	5730.342	5981.273	6307.209
Median	6584.775	5722.135	6899.010	6587.590	7098.710	5511.440	6151.055	6320.380
Std. Deviation	1744.963	1414.975	1327.222	1080.137	1791.983	1428.397	1542.455	1481.213
Skewness	-.777	.003	-.335	.081	-.445	.089	-.220	.094
Std. Error of Skewness	.134	.134	.134	.134	.134	.134	.134	.134
Kurtosis	.971	-.131	-.521	-.710	-.691	-.490	-.290	.041
Std. Error of Kurtosis	.268	.268	.268	.268	.268	.268	.268	.268
Minimum	813.27	2237.81	2848.33	4109.38	2197.74	2223.43	1821.64	2548.89
Maximum	9904.39	9389.51	9410.64	9406.33	10109.20	9090.61	9421.67	11031.34

Table 5-9: Soy distribution statistics for all locations for each projected climate, annual values

Statistics

	soy MsWUE GFDL4.5	soy MsWUE Had4.5	soy MsWUE IPSL4.5	soy MsWUE MIR4.5	soy MsWUE GFDL8.5	soy MsWUE Had8.5	soy MsWUE IPSL8.5	soy MsWUE MIR8.5
N Valid	330	330	330	330	330	330	330	330
Mean	1680.109	1278.674	1453.706	1621.824	1768.723	1205.633	1336.210	1405.811
Median	1645.860	1206.370	1375.850	1523.130	1668.070	1092.285	1301.795	1274.215
Std. Deviation	746.425	569.434	611.118	529.864	784.780	570.384	558.183	657.723
Skewness	.359	.510	.494	.454	.414	.702	.403	.787
Std. Error of Skewness	.134	.134	.134	.134	.134	.134	.134	.134
Kurtosis	-.313	-.674	-.186	-.551	-.458	-.267	-.394	.320
Std. Error of Kurtosis	.268	.268	.268	.268	.268	.268	.268	.268
Minimum	231.06	407.27	366.58	631.57	355.68	319.80	351.37	319.25
Maximum	3704.21	2989.88	3459.08	3022.86	4133.59	2858.63	3179.14	3499.02

Table 5-10: Cotton distribution statistics for all locations for each projected climate, annual values

Statistics

	cotton MsWUE GFDL4.5	cotton MsWUE Had4.5	cotton MsWUE IPSL4.5	cotton MsWUE MIR4.5	cotton MsWUE GFDL8.5	cotton MsWUE Had8.5	cotton MsWUE IPSL8.5	cotton MsWUE MIR8.5
N Valid	330	330	330	330	330	330	330	330
Mean	1937.503	1984.974	2133.180	2193.604	2027.255	2027.515	2083.5621	2114.934
Median	1950.585	1991.330	2142.750	2159.310	2052.995	2026.420	2117.280	2124.575
Std. Deviation	427.107	429.493	365.504	366.039	406.989	468.702	413.979	422.428
Skewness	-.384	-.031	.014	.033	-.185	.001	-.286	.035
Std. Error of Skewness	.134	.134	.134	.134	.134	.134	.134	.134
Kurtosis	.693	-.453	-.211	-.201	-.428	-.074	-.499	-.418
Std. Error of Kurtosis	.268	.268	.268	.268	.268	.268	.268	.268
Minimum	545.58	937.50	972.73	1271.94	941.46	791.80	1000.24	1135.10
Maximum	3034.14	3012.40	3149.82	3161.19	2942.39	3402.58	2942.45	3534.40

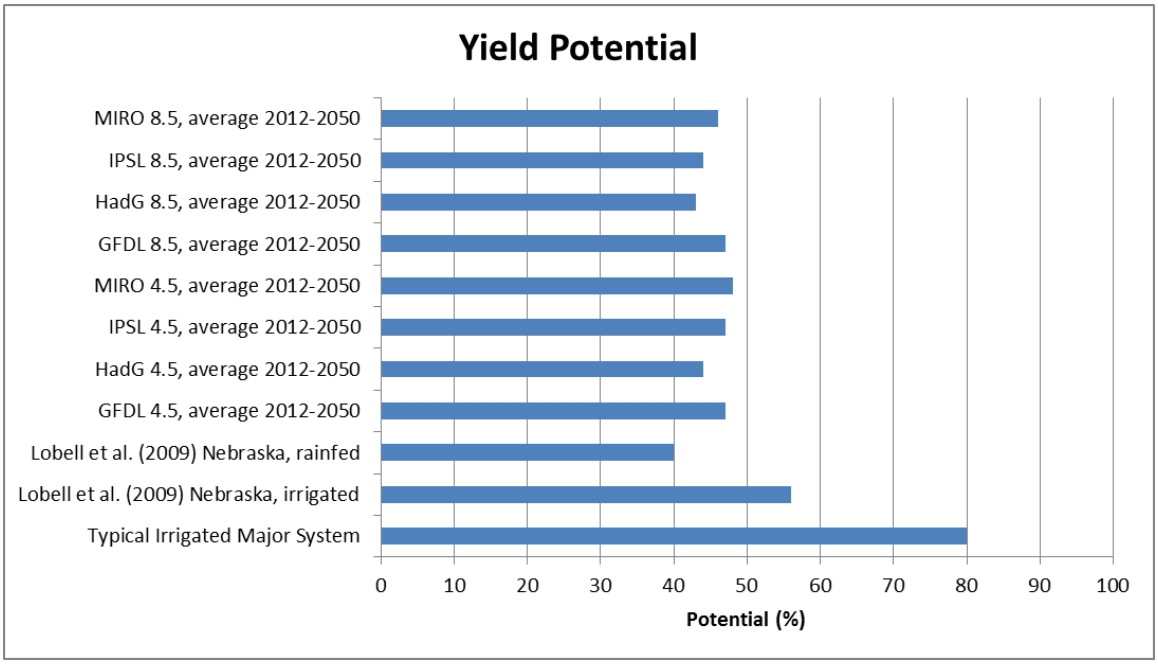


Figure 5-49: Average yield potential

Hypothesis 2

Soil Organic Carbon

The changes that occur in SOC depend on the inputs of litter and the outputs due to erosion, respiration, and degradation of the current SOC stocks (Figure 5-50). In this study SOC stocks are projected under different climate scenarios using daily data from 1980 to 2050 to ensure runoff and erosion reach a state of equilibrium (Papanicolaou and Abaci, 2008).

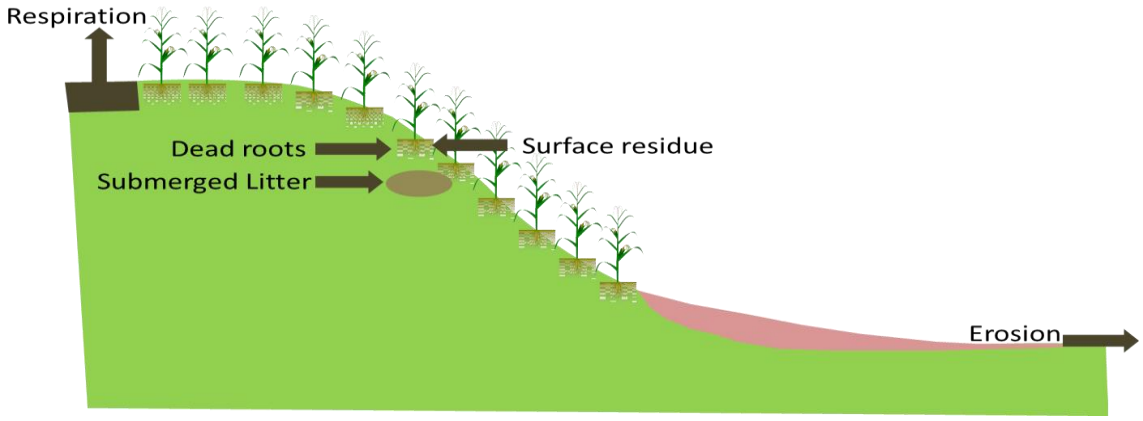


Figure 5-50: Parts of the SOC time-step including crop input, respiration, and erosional effects

Respiration

The respiration component of the SOC mass balance equation (Eq. 2-18) is a dominating factor controlling of soil carbon stocks. Respiration is quantified using a first order decomposition constant that is a weighted average of the different carbon pools (e.g., labile, recalcitrant). This decomposition rate is adjusted considering soil moisture (*wfunc*), soil temperature (*tfunc*), and anaerobic conditions (*A*).

With the projected temperature increases (Figure 4-11 and Figure 4-12), soil temperature must be considered in the projected degradation of SOC. Soil moisture is also important, as different hillslope profiles and locations (i.e., upslope; downslope) will have different respiration rates.

Consideration for anaerobic conditions is needed since microbial activity diminishes as the microbes become dormant under excess soil water conditions. Depending on the soil texture and presence of a fragipan, future projections often experienced periods of high soil water content where anaerobic conditions occurred.

Figure 5-51 depicts the respiration during a low yield year (year 2043), which experienced both water and temperature stresses. The trend in Figure 5-51 is expected, with increases during the summer months with higher temperatures and decreases correlating to cooler, winter months. The C-Mean and E-Mean locations have lower values, as these locations are on the western side of the watershed along the Mississippi River. Due to the composition of their soils and low slopes, drainage in these soils is poor. The water-logged conditions inhibit respiration. This difference between locations is not due to temperature, since locations within the watershed do not vary greatly in temperature.

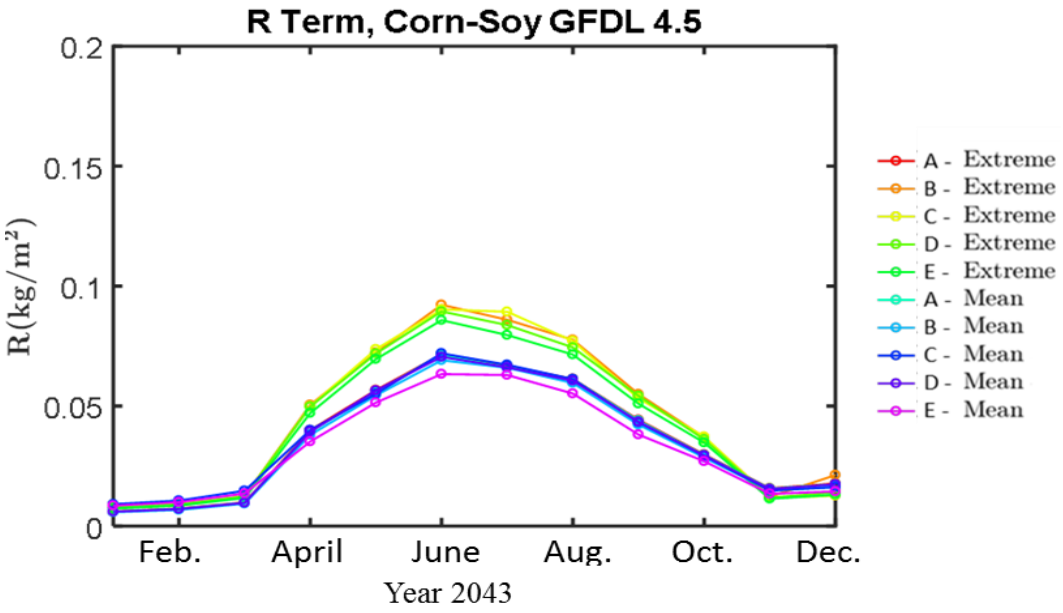


Figure 5-51: R Term for the months of year 2043 in GFDL 4.5 Corn-Soy rotation

Erosional Factor

Papanicolaou et al. (2015b) have shown the ER is a dynamic parameter, which has a large influence on SOC stocks in intensively managed hillslopes. A comparison of ER in the upslope and downslope section of each hillslope shows that downslope sections typically have an ER of approximately 1.0 and upslope regions, depending on the profile, tend to have higher values, which are attributed to the contribution of rainsplash (Papanicolaou et al., 2015b). Once runoff reaches the downslope sections it is more concentrated. A hillslope can also have a small amount of overall erosion leaving its profile, but this might not take into account the deposition of eroded material occurring throughout the hillslope. This analysis showed insignificant differences in all of the locations except C-Mean. A separate upslope and downslope ER are then determined for this location. As seen in the example of Figure 5-52, erosion losses did contribute to decreases of SOC, but only certain rain events have significant amounts. The low erosion may be attributed to propensity of no-till in the watershed (near 90%).

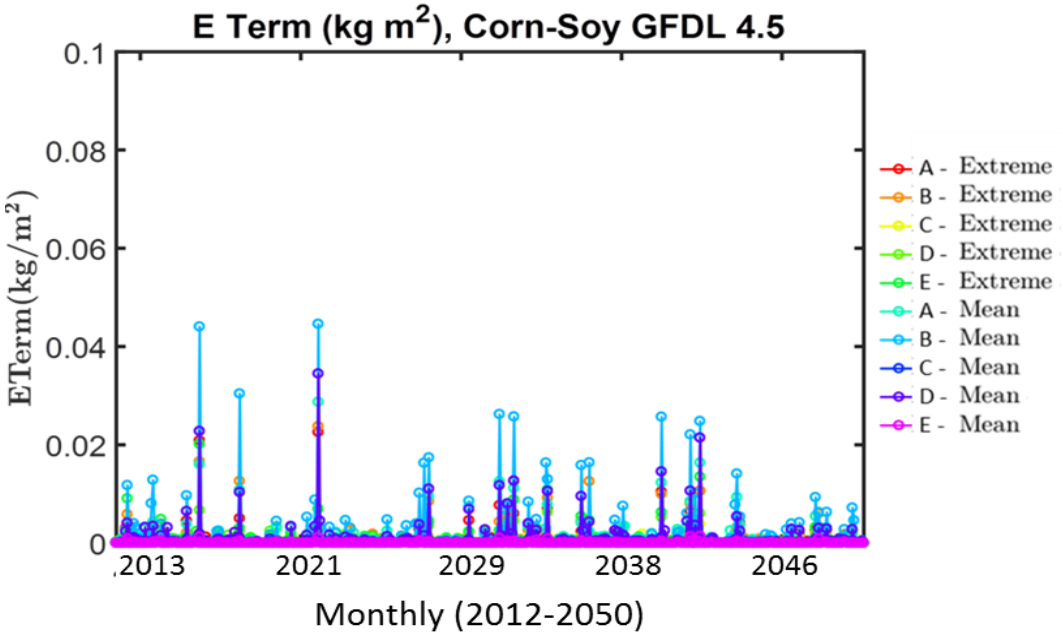


Figure 5-52: Monthly E Term values for GFDL 4.5 Corn-Soy rotation

Crop residue contributes to the SOC stocks in three forms: the residue that occurs on the surface, the submerged residue, and the dead roots (Figure 5-53). A small addition of litter occurs on the surface during the plant's life, this is when stresses result in the dropping of leaves or the premature dying of plants. The larger addition takes place at harvest when the plant remains are scattered on the soil surface. During planting, this residue is partially incorporated beneath the surface.

No-till involves a minimum amount of incorporation of residue during the planting process. Figure 5-54 highlights these steps while also showing the differences between corn and soy. The amount of additional litter from a corn harvest is significantly higher compared to soy.

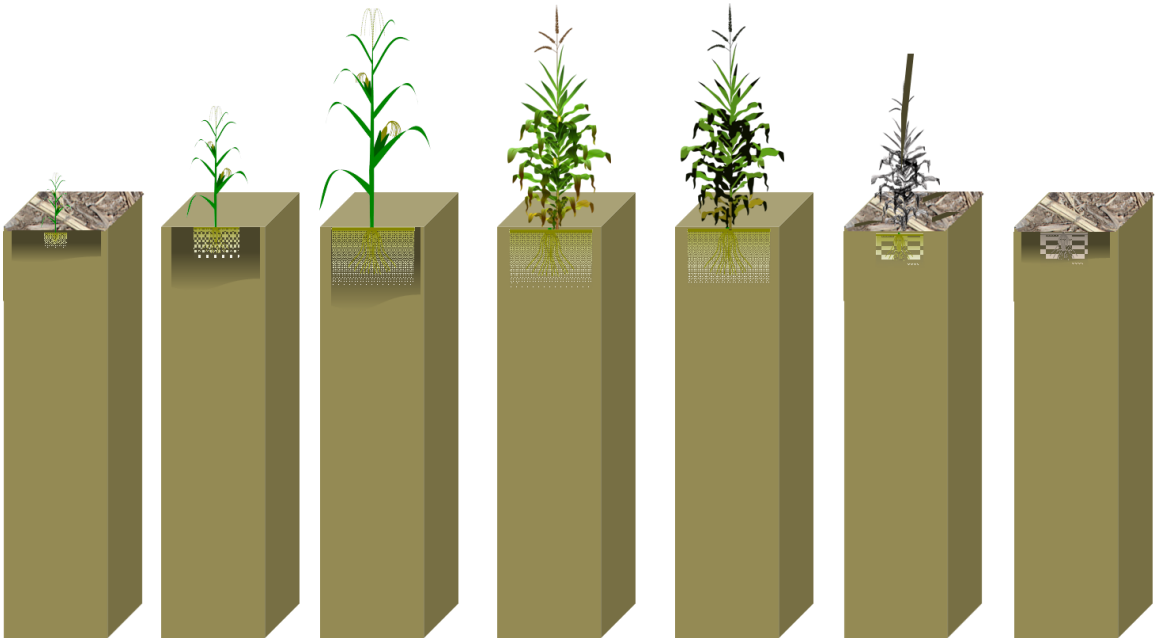


Figure 5-53: Stages of plant cycle showing surface residue, submerged residue, and dead roots

Other contributions are the plant roots, which the model terminates immediately at harvest. The additions of the dead roots for corn are also significantly higher than for soy and cotton (Figure 5-54).

All three types, namely surface residue, dead roots, and submerged residue, decompose over time before incorporation. WEPP calculates different decomposition based on the soil moisture and temperature.

Decomposition rates are also dependent on the type of residue, for example leaves decompose at a faster rate than the stalks. The daily change in these values, converted to SOC, provide the input needed to sustain soil health.

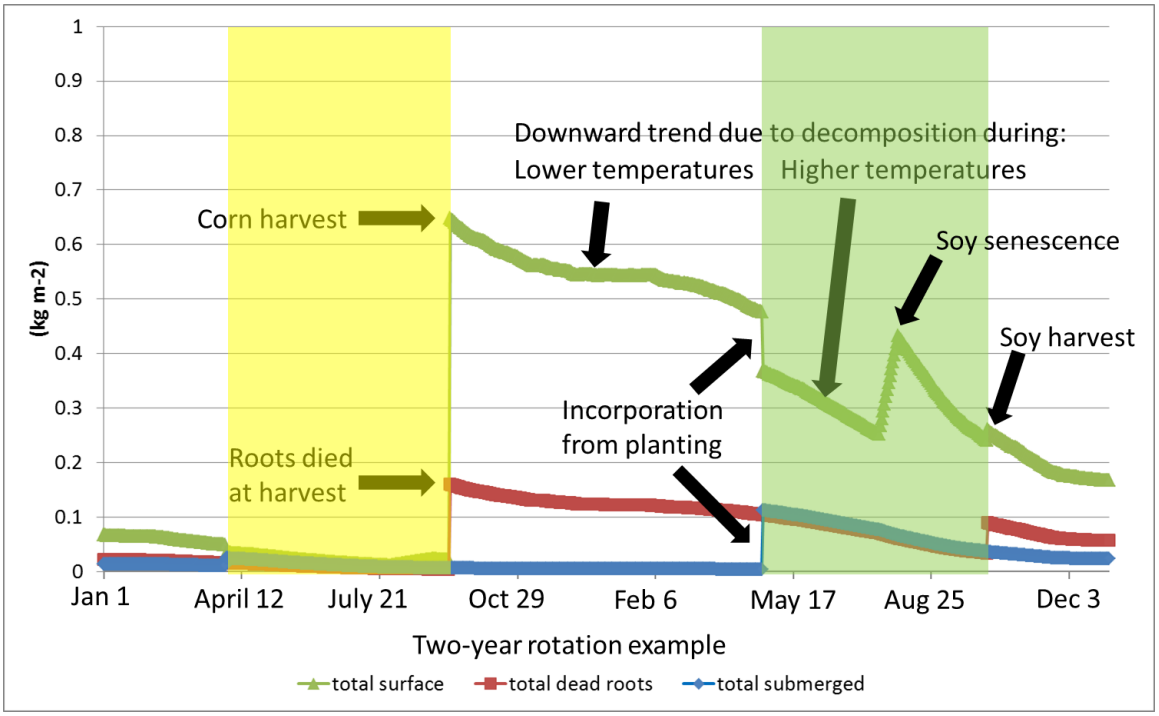


Figure 5-54: Example of the three types of litter, submerged, dead roots, and surface

Soil Organic Carbon

At each time step, the SOC from the previous time step and the additions from the change in crop residue are considered with the erosional and respiration losses occurring on the current SOC stocks. The results for climate projection GFDL 4.5 (Figure 5-55 - Figure 5-58) show a decreasing trend in SOC and percent organic matter

for both managements, Corn-Soy and Cotton-Soy. The stair-step effect seen in Figure 5-55 - Figure 5-58 is attributed to the 2-year rotation schedule for each management (corn-soy or cotton-soy).

Further evaluation into each of the individual terms is shown in Figure 5-59. The estimated SOC is graphed on the left axis and each of the associated terms are graphed on the right axis. Since these terms oscillate, in part due to changes in climate, management, temperature, and in order to show the overall contributions, they are graphed on a cumulative basis during the 2012-2050 time period. Erosion (E term) provides a small amount to the decrease in SOC, whereas respiration (R term) and litter (F term) provide large amounts of change. Comparing respiration to litter shows that over time the amount of loss from respiration supersedes the gain contributing from litter. Adding the losses from erosion compounds this negative effect, resulting in a decrease in SOC.

The downward trend in SOC was somewhat unexpected as long-term no-till management practices should have an expected increase in SOC. The no-till management, in fact does keep the erosional losses of SOC low; however, no-till does not protect the soil from the combined effects of increased respiration and decreased crop yields, which are products of the climate modifications. This is in part due to the slower rate of decomposition resulting from no-till.

Intensities in storm events, with more projected periods of droughts and floods, contribute to a downward shift in crop yields (Figure 5-1 - Figure 5-3) from crop related stresses. These decreases in yields contribute to a decrease in litter and roots. In addition, projected increases in temperatures accelerate the respiration component of SOC and decomposition rate of litter. The resultant decrease in SOC is attributed to these changes. Figure 5-60 - Figure 5-63 shows an example of one of the locations, E-Mean, and the average SOC values per decade for each climate projection and management. All climate projections and locations depict a decrease in SOC.

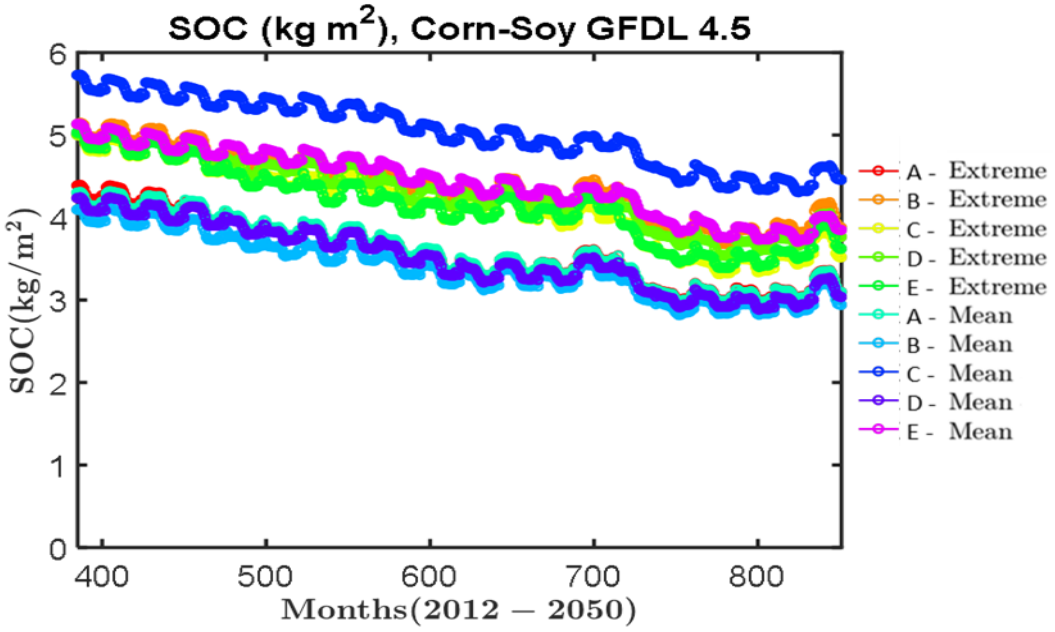


Figure 5-55: Monthly SOC for GFDL 4.5, Corn-Soy management for 2012-2050

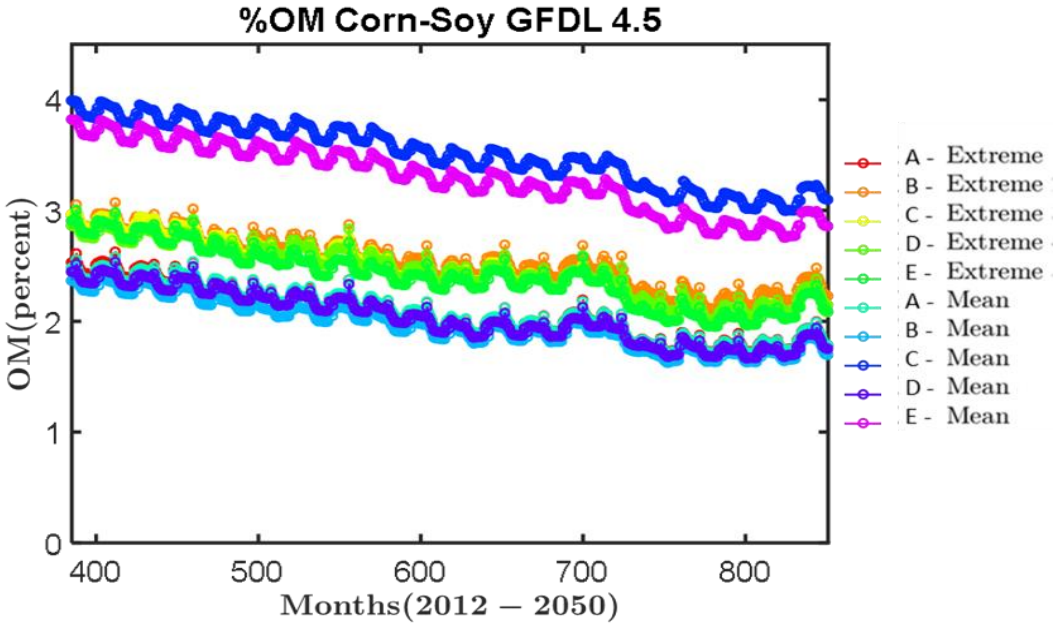


Figure 5-56: Monthly % OM for GFDL 4.5, Corn-Soy management for 2012-2050

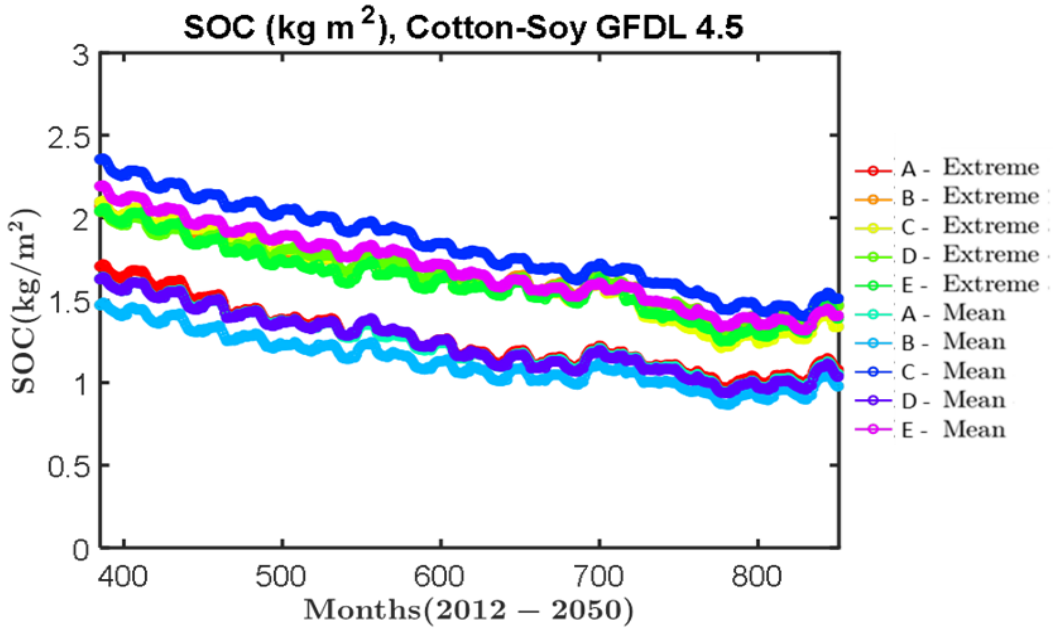


Figure 5-57: Monthly SOC for GFDL 4.5, Cotton-Soy management for 2012-2050

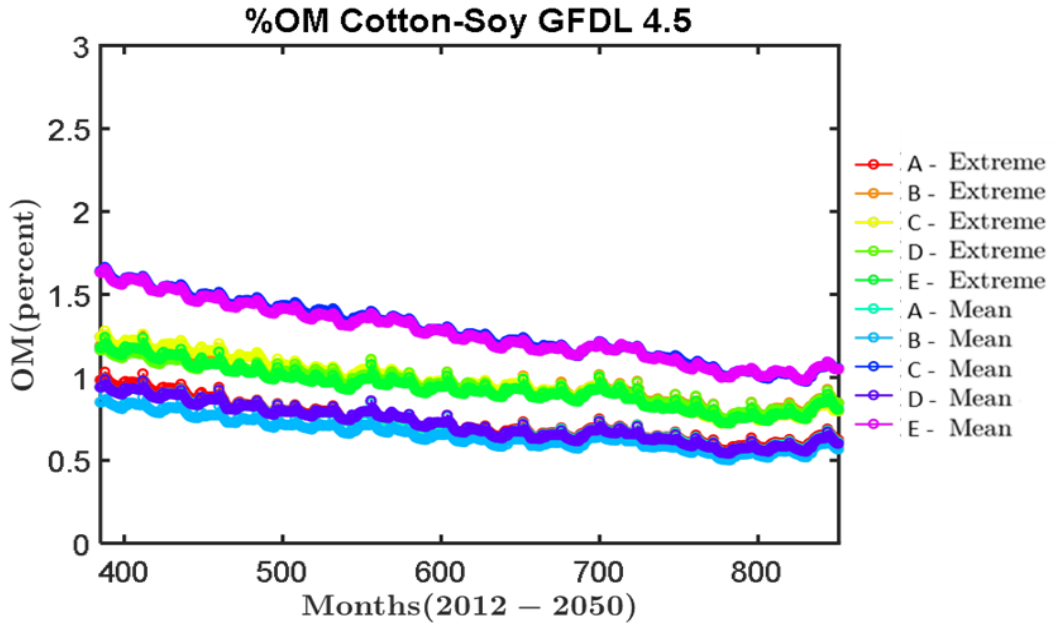


Figure 5-58: Monthly % OM for GFDL 4.5, Cotton-Soy management for 2012-2050

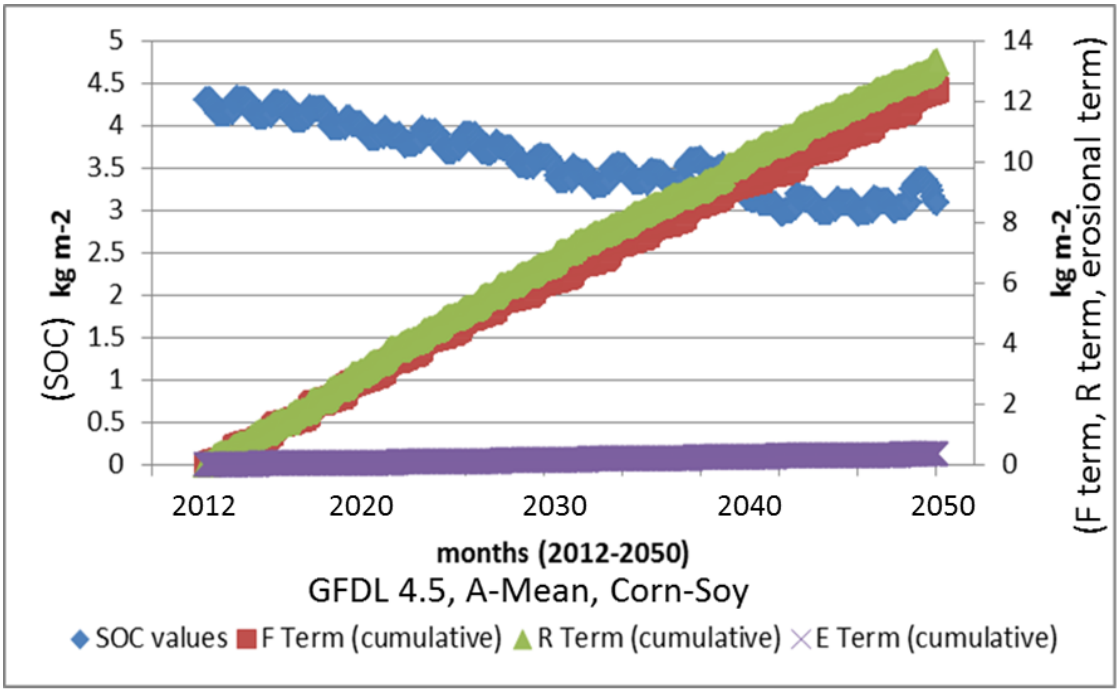


Figure 5-59: Evaluation of SOC terms

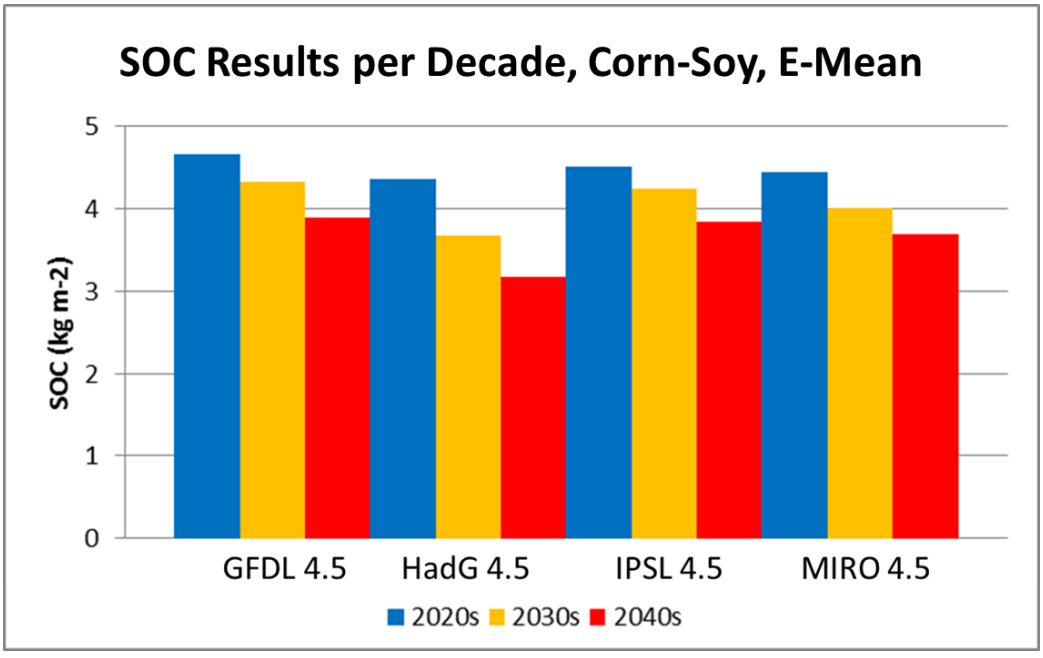


Figure 5-60: SOC results per decade for Corn-Soy, E-Mean, and 4.5 RCPs

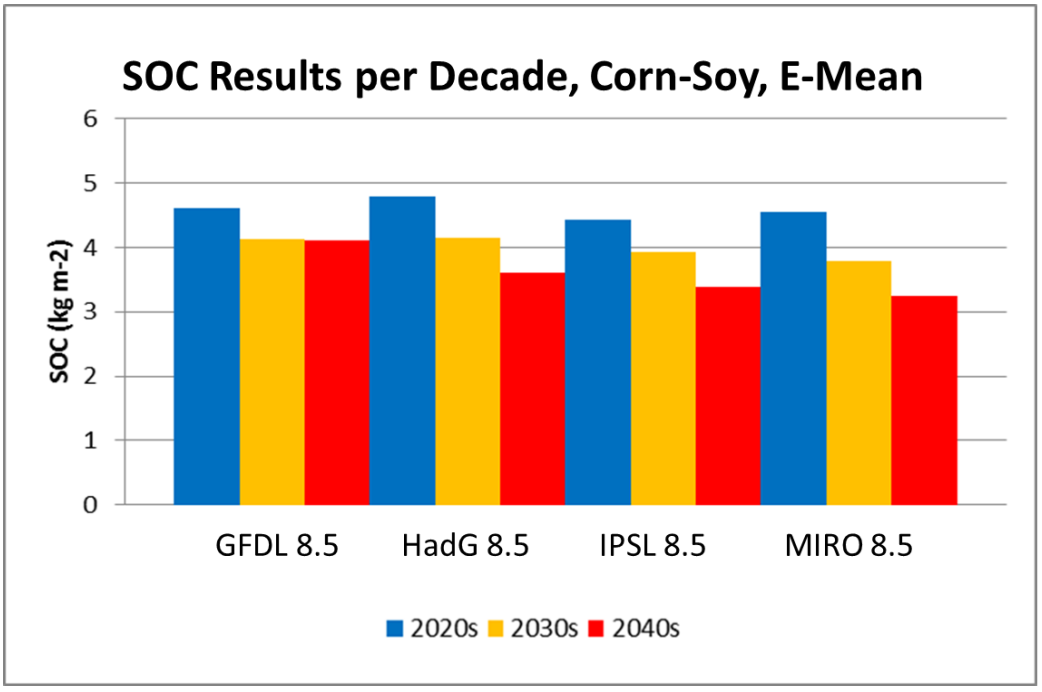


Figure 5-61: SOC results per decade for Corn-Soy, E-Mean, and 8.5 RCPs

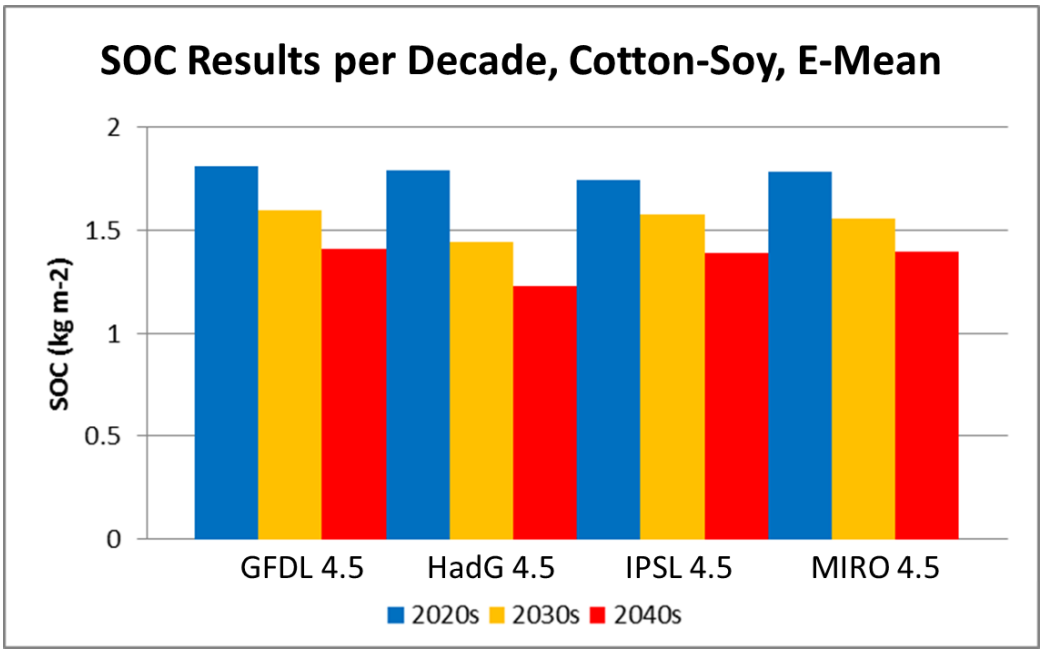


Figure 5-62: SOC results per decade for Cotton-Soy, E-Mean, and 4.5 RCPs

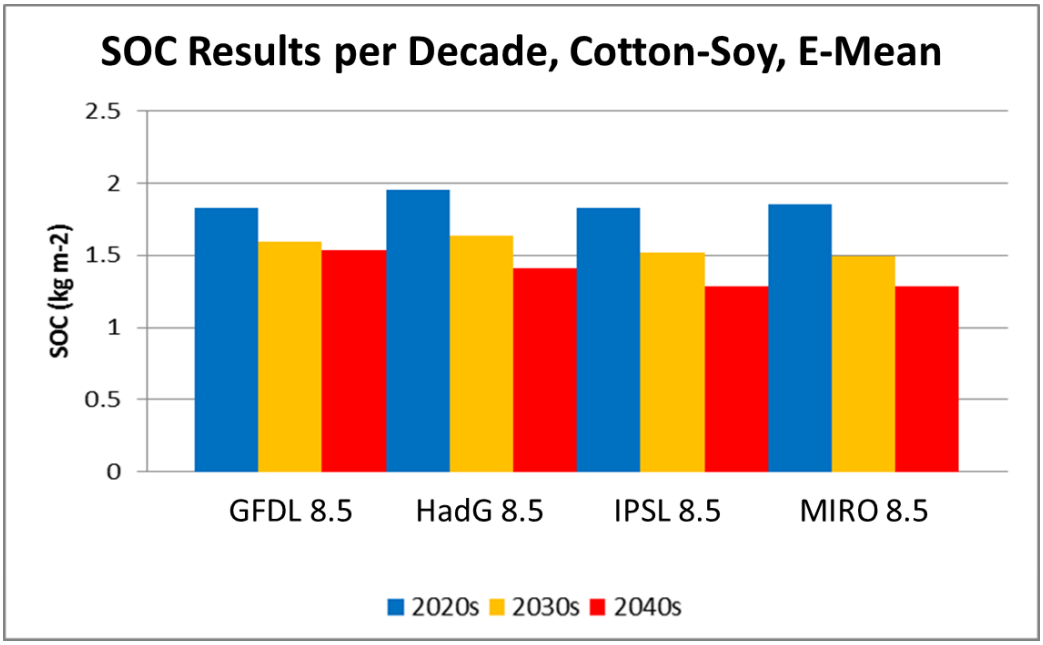


Figure 5-63: SOC results per decade for Cotton-Soy, E-Mean, and 8.5 RCPs

By converting SOC to a percentage of OM for GFDL 8.5 and utilizing Figure 5-64, estimates of a percentage of water by volume of 3.4%, 3.1%, and 3.1% for corn-soy and 1.4%, 1.2%, and 1.1% for cotton-soy for decades 2020s, 2030s, and 2040s respectively are calculated.

In Figure 5-64, as the percentage of OM decreases the range between the field capacity and the wilting point becomes smaller. A decrease in SOC correlates not only a decrease in the percentage of soil water, but at a faster rate of its decline, demonstrating the importance of maintaining and improving SOC levels.

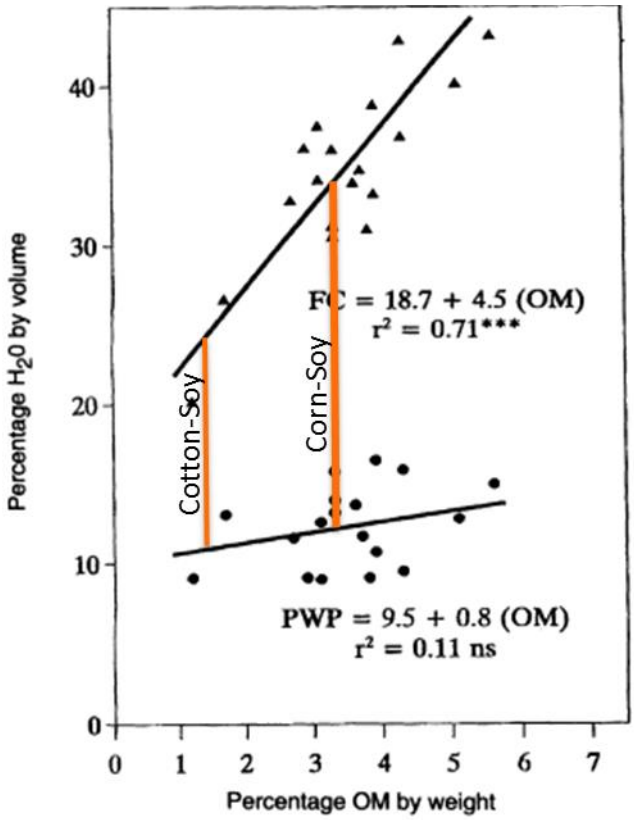


Figure 5-64: Percentage of water by volume (Hudson, 1994)

CHAPTER SIX
CONCLUSION AND RECOMMENDATIONS

The impending climate change is predicted to negatively impact agriculture without any changes to current management practices. Effects from more frequent extreme fluxes in precipitation and increases in temperature necessitate identifying a means of alleviation by utilizing available resources. Solutions should also create an improvement to current water and soil quality. Developing the link between soil moisture availability and crop yields provides a connection to not only improving current conditions, but also handling future outcomes.

The utilization of the land for the purposes of providing sustenance is predominantly regarded as positive if the outcome is the largest quantity of attainable yield. Achieving these maximum quantities and then sustaining and improving on them would help alleviate the concerns that providing for an increased world population incurs. Although a single guided focus of yields deters from this goal since the entire system is affected by soil and water quality and ultimately future yields. This is where a systems level approach to water utilization aids in assessing if the continuation of our current management practices, amidst the impending climate, would change the level of utilization.

Projections indicate that precipitation events will have an overall decrease, but it is not precipitation alone that dictates the water availability. Storm events are predicted to be more intense with longer periods of droughts and flooding. Flooding leads to more frequent times of runoff. These events also, in addition to increases in temperature, result in crop stresses that effect the yield outcome, with current projections indicating a decrease in crop yields.

Results also indicate an overall decrease in system utilization for corn and soy and to a smaller extent, cotton. Since yields are the largest driver of sWUE values and overall

precipitation is decreasing during the growing season, decreased efficiency is likely due to crop stresses which are affecting its yields. Stresses also include those arising from the temperature increases. Cotton's results indicate that although it is still influenced, it is better suited to the upcoming adaptations.

Climate changes are also expected to affect SOC, with increased storm intensities perpetuating erosional losses, longer periods of time between storm events increasing crop stresses which result in decreased litter inputs. In addition, temperature increases are projected to increase crop stresses, increase the respiration related SOC degradation, and accelerate litter decomposition rates. Resulting in projected decreases of SOC for both corn-soy and cotton-soy managements. Correlations between the percent of OM and water holding capacities result in a decrease of available water to crops. This can have negative impacts to projected crop yields.

By improving on our current focus, in order to foresee impending concerns, through targeted irrigation during times of stress, implementing management practices that improve soil quality, and adjusting regions of crop suitability can each help alleviate future concerns. Additional potential research such as implementing cover crops to the existing rotation, analyzing targeted precision agriculture, and controlled environmental experimentation could further drive the system towards a positive direction.

LIST OF REFERENCES

Abaci, Ozan, and AN Papanicolaou. 2009. 'Long-term effects of management practices on water-driven soil erosion in an intense agricultural sub-watershed: monitoring and modelling', Hydrological processes, 23: 2818-37.
Abendroth, Lori, Roger Elmore, Robert G Hartzler, Clarke McGrath, Daren S Mueller, Gary P Munkvold, Richard Pope, Marlin E Rice, Alison E Robertson, and John E Sawyer. 2009. 'Corn Field Guide', Extension and Outreach Publications. 26. http://lib.dr.iastate.edu/extension_pubs/26.
Alberts, GA, Nearing, MA, Weltz, MA, Risse, LM, Pierson, FB, Zhang, XC, Laflen, JM, and Simanton, JR, 1995, Soil component: in USDA-Water Erosion Prediction Project: Hillslope Profile and Watershed Model Documentation (DC Flanagan and MA Nearing, eds.), NESRL Rept. No. 10, USDA-ARS National Soil Erosion Research Laboratory, West Lafayette, Indiana.
Allen, Richard G, Luis S Pereira, D Raes, and M Smith. 1998. 'FAO Irrigation and drainage paper No. 56', Rome: Food and Agriculture Organization of the United Nations, 56: e156.
Angel, James R, Melissa Widhalm, Dennis Todey, Ray Massey, and Larry Biehl. 2017. 'The U2U corn growing degree day tool: Tracking corn growth across the US Corn Belt', Climate Risk Management, 15: 73-81.
Archontoulis, Sotirios V, and Fernando E Miguez. 2015. 'Nonlinear regression models and applications in agricultural research', Agronomy Journal, 107: 786-98.
Arnold, JG, Weltz MA, Alberts EE, and Flanagan, DC, 1995, Plant growth component: in USDA- Water Erosion Prediction Project: Hillslope Profile and Watershed Model Documentation (DC Flanagan and MA Nearing, eds.), NSERL Report No. 10, USDA-ARS National Soil Erosion Research Laboratory, West Lafayette, Indiana.
Ascough, J., Baffaut, C., Nearing, M.A., Liu, B.Y. 1997. 'The WEPP Watershed Model: I. Hydrology and Erosion', Transactions of the ASAE. VOL. 40(4):921-933.
Bauer, Philip, DW Faircloth, Diane Rowland, and GL Ritchie. 2012. 'Water-sensitivity of cotton growth stages', Cotton Irrigation Management of Humid Regions, Cotton Incorporated. p: 17-20.
Brouwer, C, and M Heibloem. 1986. 'Irrigation water management: irrigation water needs', Training manual, 3.
Casteel S. (2010) Soybean physiology: how well do you know soybeans? Purdue University, USA. Available online at: https://www.agry.purdue.edu/ext/soybean/Arrivals/10SoyDevt.pdf. Accessed on 05/2016.
DehghaniSanij, Hossein, Tahei Yamamoto, and Velu Rasiah. 2004. 'Assessment of evapotranspiration estimation models for use in semi-arid environments', Agricultural water management, 64: 91-106.
Dermisis, D., Abaci, O., (Thanos) Papanicolaou, A. N. and Wilson, C. G. (2010), Evaluating grassed waterway efficiency in southeastern Iowa using WEPP. Soil Use and Management, 26: 183–192.

Dietzel, R., Matt Liebman, Robert Ewing, Matt Helmers, Robert Horton, Meghann Jarchow, and Sotirios Archontoulis. 2016. 'How efficiently do corn-and soybean-based cropping systems use water? A systems modeling analysis', Global change biology, 22: 666-81.
Environmental Systems Research Institute, ESRI. 2017. Redlands, CA.
Flanagan, DC, JR Frankenberger, and JC Ascough II. 2012. 'WEPP: Model use, calibration, and validation', Transactions of the ASABE, 55: 1463-77.
Flanagan, D.C. and Livingston, S.J. (Eds.), 1995. Water erosion prediction project (WEPP) version 95.7 user summary. NSERL Report No. 11, National Soil Erosion Research Laboratory, USDA-Agricultural Research Service, West Lafayette, Indiana, 139pp.
Flinchum, W.T. 2001. 'Corn production in Tennessee', Agricultural Extension Service publication No. PB443. University of Tennessee, Knoxville. TN.
Flinchum, W.T., Buschermohle, M.J., Denton, H.P., Farmer, C.M., Gerloff, D.C., McNeil, S.G., Newman, M.A., Rhodes, G.N., Seward, R.W., Wills Jr., J.B., . 2013. 'Soybean Production in Tennessee, PB1608. University of Tennessee, Knoxville, TN'.
Foster, GR, Flanagan, DC, Nearing, MA, Lane, LJ, Risse, LM, and Finkner, SC, 1995, Hillslope erosion component: in USDA-Water Erosion Prediction Project: Hillslope Profile and Watershed Model Documentation (DC Flanagan and MA Nearing, eds.), USDA-ARS, NSERL Report No. 10.
Gustafson, David, Michael Hayes, Emily Janssen, David B Lobell, Stephen Long, Gerald C Nelson, Himadri B Pakrasi, Peter Raven, G Philip Robertson, and Richard Robertson. 2015. 'Pharaoh's dream revisited: an integrated US Midwest field research network for climate adaptation', BioScience, 66: 80-85.
Hamilton, SK, MZ Hussain, AK Bhardwaj, B Basso, and GP Robertson. 2015. 'Comparative water use by maize, perennial crops, restored prairie, and poplar trees in the US Midwest', Environmental Research Letters, 10: 064015.
Hatfield, Jerry L, and John H Prueger. 2015. 'Temperature extremes: effect on plant growth and development', Weather and Climate Extremes, 10: 4-10.
Houborg, R., M.Rodell, B.Li, R.Reichle, and B. F.Zaitchik (2012), Drought indicators based on model-assimilated Gravity Recovery and Climate Experiment (GRACE) terrestrial water storage observations, Water Resour. Res., 48, W07525, doi:10.1029/2011WR011291.
Hudson, Berman D. 1994. 'Soil organic matter and available water capacity', Journal of Soil and Water Conservation, 49: 189-94.
Kranz, W., Irmak, S., von Donk, S.J., Yonts, C.D., Martin, D.L. 2008. 'Irrigation Management for Corn', NebGuide, G1850.
Laflen, John M, and Dennis C Flanagan. 2013. 'The development of US soil erosion prediction and modeling', International Soil and Water Conservation Research, 1: 1-11.

Lee, Chad, Herbek, James, Murdock, Llyod, Schwab, Green, Greg J.D., and Martin, James, Plant and Soil Sciences;, Ric and Johnson Bessin, Doug, Entomology; Hershman, Donald and Vincelli, Paul, Plant Pathology;, and Tim Stombaugh, Biosystems and Agricultural Engineering; Riggins, Steve, Agricultural Economics 2007. 'Corn and Soybean Production Calendar', ID-159, Cooperative Extension Service, University of Kentucky College of Agriculture, Lexington KY, 40546.

Liang, Xu, Dennis P Lettenmaier, Eric F Wood, and Stephen J Burges. 1994. 'A simple hydrologically based model of land surface water and energy fluxes for general circulation models', Journal of Geophysical Research: Atmospheres, 99: 14415-28.

Lobell DB, Cassman KG, Field CB. 2009. Crop yield gaps: Their importance, magnitudes and causes. Annu Rev Environ Resour 34:179–204.

Lohmann, D., Raschke, E., Nijssen, B., and Lettenmaier, D. P.: 1998a, 'Regional Scale Hydrology: I. Formulation of the VIC-2L Model Coupled to a Routing Model',Hydrol. Sci. J. 43, 131–141.

MACA, Multivariate Adaptive Constructed Analogs. 2016. Accessed [accessed 2016]. https://maca.northwestknowledge.net.

Main, C. 2012. 'Cotton production in Tennessee. Agricultural Extension Service publication. University of Tennessee, Knoxville. TN, 12-0109 W288 4/12.

MATLAB. 2017. Natick, Massachusetts: The MathWorks Inc. R2017a.

McClure A., 2009. 'Planting Corn for Grain in Tennessee', Agricultural Extension Service publication. University of Tennessee, Knoxville, TN, W077 2/09.

McClure A., Cannon, K. 2016. 'Tennessee Corn Quick Facts', The University of Tennessee Agricultural Extension Service, 16-0163 W 368, 6/16.

McClure, A., Salmeron, M., Verbree, D., Purcell L. 2016. 'Soybean Yield Response: Planting Date and Maturity Groups in Tennessee', Agricultural Extension, Knoxville, TN.

Metherell, A.K., L.A. Harding, C.V. Cole, and W.J. Parton. 1993. CENTURY Soil organic matter model environment. Technical documentation. Agroecosystem version 4.0. Great Plains System Research Unit Technical Report No.4. USDA-ARS, Fort Collins, Colorado, USA.

NASS, USDA. 2010. 'Field crops: Usual planting and harvesting dates', USDA National Agricultural Statistics Service, Agriculural Handbook, 628.

Nearing, M. A., Liu, B. Y., Risse, L.M. and Zhang, X. (1996), Curve Numbers and Green-Ampt Effective Hydraulic Conductivities. JAWRA Journal of the American Water Resources Association, 32: 125–136.

Nicks, AD, Lane, LJ, and Gander, GA, 1995, Weather generator: in USDA-Water Erosion Prediction Project: Hillslope Profile and Watershed Model Documentation (DC Flanagan and MA Nearing, eds.), USDA-ARS NSERL Report No. 10.

Neild, R.E., and Newman, J.E. 1987. Growing season characteristics and requirements in the Corn Belt (Cooperative Extension Service, Iowa State University).

Papanicolaou, A.N. and Abaci, O. 2008. Upland erosion modeling in a semi-humid environment via the water erosion prediction project model. J of Irrigation and Drainage Engineering, Ms. No. IRENG-07-5256R1, p 127.
Papanicolaou, A.N., Wacha, K., Abban, B., Wilson, C.G., Hatfield, J., Stanier, C., and Filley, T.. 2015b. 'From soilscapes to landscapes: A landscape-oriented approach to simulate soil organic carbon dynamics in intensively managed landscapes', Journal of Geophysical Research: Biogeosciences, 120: 2375-401.
Papanicolaou, A.N., Sanford, J., Dermisis, D., and Mancilla, G.. 2010. 'A 1-D morphodynamic model for rill erosion', Water Resources Research, 46.
Papanicolaou, A.N., Elhakeem, M., Wilson, C.G., Burras, C.L., West, L.T., Hangsheng, H.L., Clark, B., and Oneal, B.E. 2015a. 'Spatial variability of saturated hydraulic conductivity at the hillslope scale: Understanding the role of land management and erosional effect', Geoderma, 243: 58-68.
Papanicolaou, Group:, Papanicolaou, A. N., Wilson, C.G., Wilson, Abban, B., and Ghaneeizad, S.M. 2017.
Parton, WJ, Stewart, JWB, Cole, CV. Dynamics of C, N, P, and S in grassland soils: a model. Biogeochem. 1988; 5: 109-131.
Raper, T. 2014. 'Tennessee Cotton Quick Facts', The University of Tennessee Agricultural Extension Service, 15-0073 09/14.
Robinson, E. 2004. 'Early still best for cotton planting', Delta Farm Press.
Sadras, Victor O, Patricio Grassini, and Pasquale Steduto. 2011. 'Status of water use efficiency of main crops', The state of world's land and water resources for food and agriculture (SOLAW). FAO, Rome and Earthscan, London. Available from http://www. fao. org/fileadmin/templates/solaw/files/thematic_reports/TR_07_web. pdf.
Sanford, Ward E, and David L Selnick. 2013. 'Estimation of Evapotranspiration Across the Conterminous United States Using a Regression With Climate and Land-Cover Data', JAWRA Journal of the American Water Resources Association, 49: 217-30.
Savabi, MR, and JR Williams. 1995. 'Water balance and percolation: in USDA-Water Erosion Prediction Project: Hillslope Profile and Watershed Model Documentation (DC Flanagan and MA Nearing, eds.), USDA-ARS NSERL Report No. 10', WEPP Document.
Senay, Gabriel B, Stefanie Bohms, Ramesh K Singh, Prasanna H Gowda, Naga M Velpuri, Henok Alemu, and James P Verdin. 2013. 'Operational evapotranspiration mapping using remote sensing and weather datasets: A new parameterization for the SSEB approach', JAWRA Journal of the American Water Resources Association, 49: 577-91.
Sivapalan, M. and Woods, R. A. (1995), Evaluation of the effects of general circulation models' subgrid variability and patchiness of rainfall and soil moisture on land surface water balance fluxes. Hydrol. Process., 9: 697–717. doi:10.1002/hyp.3360090515

Southworth, Jane, JC Randolph, M Habeck, OC Doering, RA Pfeifer, D Gangadhar Rao, and JJ Johnston. 2000. 'Consequences of future climate change and changing climate variability on maize yields in the midwestern United States', Agriculture, Ecosystems & Environment, 82: 139-58.

SPSS Statistics for Windows, IBM Corp. IBM. 2013. Armonk, NY: IBM Corp.

Stocker, Thomas F, Dahe Qin, Gian-Kasper Plattner, M Tignor, Simon K Allen, Judith Boschung, Alexander Nauels, Yu Xia, Vincent Bex, and Pauline M Midgley. 2013. "Climate Change 2013: The Physical Science Basis. Contribution of Working Group I to the Fifth Assessment Report of the Intergovernmental Panel on Climate Change, 1535 pp." In.: Cambridge Univ. Press, Cambridge, UK, and New York.

Stott, DE, Alberts, EE, and Weltz, MA, 1995, Residue decomposition and management: in USDA- Water Erosion Prediction Project: Hillslope Profile and Watershed Model Documentation (DC Flanagan and MA Nearing, eds.), USDA-ARS NSERL Report No. 10.

Survey, Soil. 2016. 'Natural Resources Conservation Service, United States Department of Agriculture. Web Soil Survey', Accessed Accessed [Dec. 2016]. http://websoilsurvey.nrcs.usda.gov/.

Sykes, V. R., R. H. Blair, and M. A. McClure. 2016. 'Corn Grain Hybrid Tests in Tennessee 2016', UT Extension, PB 1850.

Thompson, A., Hensley, D., Newman, M., Stewart, S., Patrick, R. 2006. 'Crop Profile for Soybeans in Tennessee', The Crop Profile/PMSP database is supported by USDA NIFA. https University of Wisconsin, Agronomy, Soybean Growth and Development, 2015 ://ipmdata.ipmcenters.org/documents/cropprofiles/TNsoybeans.pdf.

USDA. 2016. "USDA National Agricultural Statistics Service Cropland Data Layer, Available at USDA-NASS, Washington, DC." In.

USGS. 2016. 'United States Geological Survey Landsat Image data', Accessed Accessed [Nov. 2016]. available at URL http://landsat.usgs.gov.

Velpuri, Naga M, Gabriel B Senay, Ramesh K Singh, Stefanie Bohms, and James P Verdin. 2013. 'A comprehensive evaluation of two MODIS evapotranspiration products over the conterminous United States: Using point and gridded FLUXNET and water balance ET', Remote Sensing of Environment, 139: 35-49.

Verstraeten, Willem W, Frank Veroustraete, and Jan Feyen. 2008. 'Assessment of evapotranspiration and soil moisture content across different scales of observation', Sensors, 8: 70-117.

West, Tristram O, Craig C Brandt, Latha M Baskaran, Chad M Hellwinckel, Richard Mueller, Carl J Bernacchi, Varaprasad Bandaru, Bai Yang, Bradly S Wilson, and Gregg Marland. 2010. 'Cropland carbon fluxes in the United States: Increasing geospatial resolution of inventory-based carbon accounting', Ecological Applications, 20: 1074-86.

Wilson, Christopher G, Kenneth M Wacha, AN Papanicolaou, Heather A Sander, Violet B Freudenberg, Benjamin KB Abban, and Chang Zhao. 2016. 'Dynamic

assessment of current management in an intensively managed agroecosystem', Journal of Contemporary Water Research & Education, 158: 148-71.
Wright, D.L., Marois, J.J., Sprenkel, R.K. 2005. 'Cotton Growth and Development', Agronomy Department, UF/IFAS Extension, SS-AGR-238.
Wu, Z., Lu, G., Zhang, J., Yang, Y. Simulation of daily soil moisture using VIC model. Scientia Geographica Si- nica, 2007, 27(3): 359-364.
Xing, Zisheng, Lien Chow, Fan-Rui Meng, Herb W Rees, Lionel Steve, and John Monteith. 2008. 'Validating evapotranspiraiton equations using bowen ratio in New Brunswick, Maritime, Canada', Sensors, 8: 412-28.
Zipper, S.C., M.E. Soylu, E.G. Booth, and S.P. Loheide. 2015. Untangling the effects of shallow groundwater and soil texture as drivers of subfield scale yield variability. Water Resources Research. 51:6338-6358.

APPENDIX

A.1 Soil compositions

Table A.1.-1: Soil composition location A-Mean

Location	Soil Type	Layer	Depth (mm)	Sand (%)	Silt (%)	Clay (%)	Weighted OM (%)
A- Mean	Silt loam	1	50	17	70	13	1.3586
Soil Albedo: 0.3484	Silt loam	2	100	17	70	13	1.3586
Elevation: 100-106m	Silt loam	3	200	17	71	13	1.2493
CEC: 3.8	Silt loam	4	300	17	71	13	1.0997
	Silt loam	5	400	17	71	13	0.9500
	Silt loam	6	600	17	71	13	0.7230
	Silt loam	7	800	17	71	13	0.5329
	Silt loam	8	1000	17	71	13	0.4145
	Silt loam	9	1500	17	71	13	0.2059
	bedrock	10	2000	0	0	0	0

Table A.1-2: Soil composition location B-Mean

Location	Soil Type	Layer	Depth (mm)	Sand (%)	Silt (%)	Clay (%)	Weighted OM (%)
B-Mean	Silt loam	1	50	17	70	13	1.3891
Soil Albedo: 0.344	Silt loam	2	100	17	70	13	1.3891
Elevation: 125-140m	Silt loam	3	200	17	70	13	1.3516
CEC: 4.1	Silt loam	4	300	17	70	13	1.1826
	Silt loam	5	400	17	70	13	1.0136
	Silt loam	6	600	17	70	13	0.7243
	Silt loam	7	800	17	70	13	0.5325
	Silt loam	8	1000	17	70	13	0.3868
	Silt loam	9	1500	17	70	13	0.1614
	Silt loam	10	2000	17	70	13	0.0740

Table A.1-3: Soil composition location C-Mean

Location	Soil Type	Layer	Depth (mm)	Sand (%)	Silt (%)	Clay (%)	Weighted OM (%)
C-Mean	silty loam	1	50	21	48	32	2.2390
Soil Albedo: 0.245	silty loam	2	100	21	48	32	2.2390
Elevation: 87m	silty loam	3	200	21	48	32	2.0498
CEC: 20	silty loam	4	300	24	44	32	1.7744
	clay	5	400	23	42	35	1.4990
	Silty clay loam	6	600	28	41	31	1.0820
	Silty clay loam	7	800	33	37	31	0.7574
	Silty clay loam	8	1000	35	36	29	0.5517
	loam	9	1500	45	32	24	0.2290
	bedrock	10	2000	0	0	0	0.0000

Table A.1-4: Soil composition location D-Mean

Location	Soil Type	Layer	Depth (mm)	Sand (%)	Silt (%)	Clay (%)	Weighted OM (%)
D-Mean	Silt loam	1	50	18	69	13	1.4463
Soil Albedo: 0.336	Silt loam	2	100	18	69	13	1.4463
Elevation: 100-113m	Silt loam	3	200	18	69	13	1.3132
CEC: 3.8	Silt loam	4	300	18	68	15	1.1308
	Silt loam	5	400	17	68	15	0.9485
	Silt loam	6	600	17	68	15	0.6643
	Silt loam	7	800	17	68	15	0.4748
	Silt loam	8	1000	19	67	14	0.3358
	Silt loam	9	1500	21	66	13	0.1255
	bedrock	10	2000	0	0	0	0.0000

Table A.1-5: Soil composition location E-Mean

Location	Soil Type	Layer	Depth (mm)	Sand (%)	Silt (%)	Clay (%)	Weighted OM (%)
E-Mean	clay	1	50	22	31	47	2.2007
Soil Albedo: 0.249	clay	2	100	22	31	47	2.2007
Elevation: 77-80m	clay	3	200	20	31	48	1.9609
CEC: 38.5	clay	4	300	18	31	51	1.6323
	clay	5	400	18	31	52	1.3038
	clay	6	600	23	32	45	0.8535
	clay	7	800	30	29	41	0.7733
	clay	8	1000	34	30	37	0.5947
	clay	9	1500	35	29	36	0.0766
	bedrock	10	2000	0	0	0	0.0000

Table A.1-6: Soil composition location A-Extreme

Location	Soil Type	Layer	Depth (mm)	Sand (%)	Silt (%)	Clay (%)	Weighted OM (%)
A-Extreme	Silt loam	1	50	17	70	13	1.3866
Soil Albedo: 0.345	Silt loam	2	100	17	70	13	1.3866
Elevation: 101-114m	Silt loam	3	200	14	75	11	1.2734
CEC: 3.1	Silt	4	300	13	77	10	1.1183
	Silt	5	400	13	77	10	0.9632
	Silt	6	600	13	77	10	0.7253
	Silt	7	800	13	77	10	0.5373
	Silt	8	1000	13	77	10	0.4115
	Silt	9	1500	13	77	10	0.3271
	bedrock	10	2000	0	0	0	0.0000

Table A.1-7: Soil composition location B-Extreme

Location	Soil Type	Layer	Depth (mm)	Sand (%)	Silt (%)	Clay (%)	Weighted OM (%)
B-Extreme	Silt loam	1	50	25	63	12	1.3891
Soil Albedo: 0.344	Silt loam	2	100	25	63	12	1.3891
Elevation: 142-146m	Silt loam	3	200	24	62	14	1.3516
CEC: 4.1	Silt loam	4	300	22	58	20	1.1826
	Silt loam	5	400	20	58	22	1.0136
	Silt loam	6	600	20	58	22	0.7243
	Silt loam	7	800	20	58	22	0.5325
	Silt loam	8	1000	30	53	17	0.3868
	Silt loam	9	1500	40	49	12	0.1614
	Silt loam	10	2000	40	48	11	0.0835

Table A.1-8: Soil composition location C-Extreme

Location	Soil Type	Layer	Depth (mm)	Sand (%)	Silt (%)	Clay (%)	Weighted OM (%)
C-Extreme	Silt Loam	1	50	18	57	25	2.0246
Soil Albedo: 0.267	Silt Loam	2	100	18	57	25	2.0246
Elevation: 77-78m	Silt Loam	3	200	18	56	26	1.8322
CEC: 38	Other	4	300	23	45	32	1.5242
	Other	5	400	25	43	31	1.2163
	Other	6	600	28	44	29	0.7622
	Other	7	800	31	43	27	0.4952
	Other	8	1000	0	0	0	0.3205
	Other	9	1500	0	0	0	0.0936
	Bedrock	10	2000	0	0	0	0.0371

Table A.1-9: Soil composition location D-Extreme

Location	Soil Type	Layer	Depth (mm)	Sand (%)	Silt (%)	Clay (%)	Weighted OM (%)
D-Extreme	Silt loam	1	50	35	53	12	1.3706
Soil Albedo: 0.347	Silt loam	2	100	35	53	12	1.3706
Elevation: 109-119m	Silt loam	3	200	35	52	13	1.2537
CEC: 3.1	Silty clay loam	4	300	30	48	22	1.0936
	Clay loam	5	400	22	48	30	0.9334
	Clay loam	6	600	22	48	30	0.6944
	Clay loam	7	800	22	50	28	0.5054
	Clay loam	8	1000	31	45	23	0.3839
	loam	9	1500	45	40	14	0.1755
	loam	10	2000	52	34	14	0.1091

Table A.1-10: Soil composition location E-Extreme

Location	Soil Type	Layer	Depth (mm)	Sand (%)	Silt (%)	Clay (%)	Weighted OM (%)
E-Extreme	Silt loam	1	50	18	69	13	1.4477
Soil Albedo: 0.336	Silt loam	2	100	18	69	13	1.4477
Elevation: 119-109m	Silt loam	3	200	18	69	13	1.3143
CEC: 3.8	Silt loam	4	300	18	68	15	1.1316
	Silt loam	5	400	17	68	15	0.9488
	Silt loam	6	600	17	68	15	0.6644
	Silt loam	7	800	17	68	15	0.4745
	Silt loam	8	1000	19	67	14	0.3356
	Silt loam	9	1500	21	66	13	0.1253
	Silt loam	10	2000	0	0	0	0.0539

A.2 Calibrations

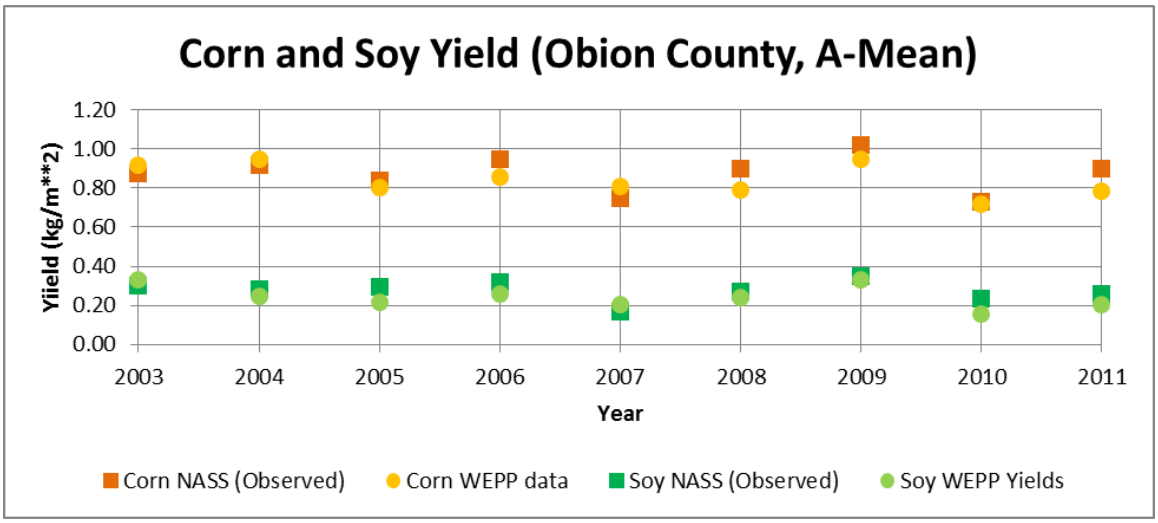


Figure A.2-1: A-Mean Corn and Soy Calibration

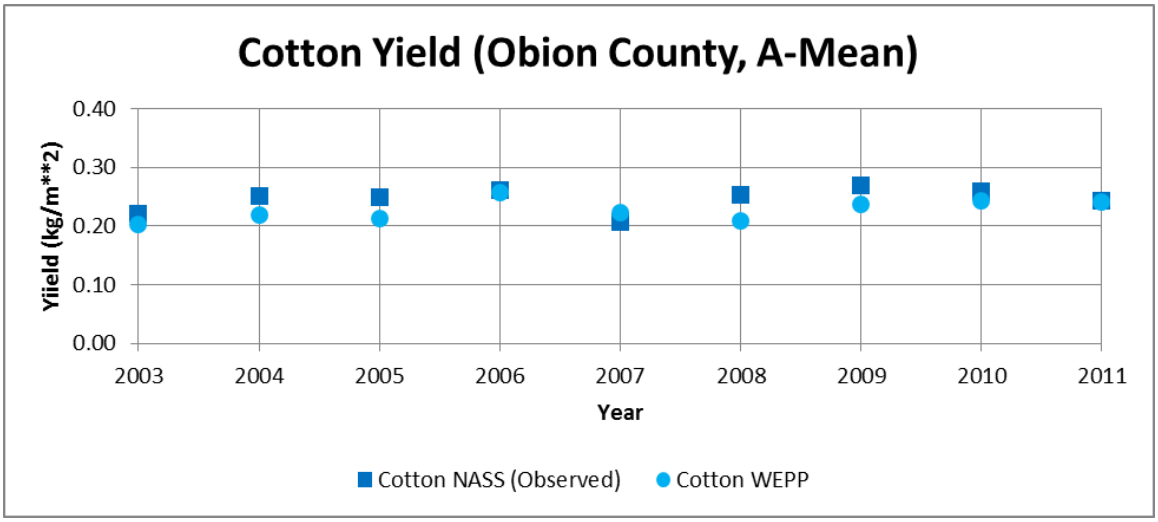


Figure A.2-2: A-Mean Cotton Calibration

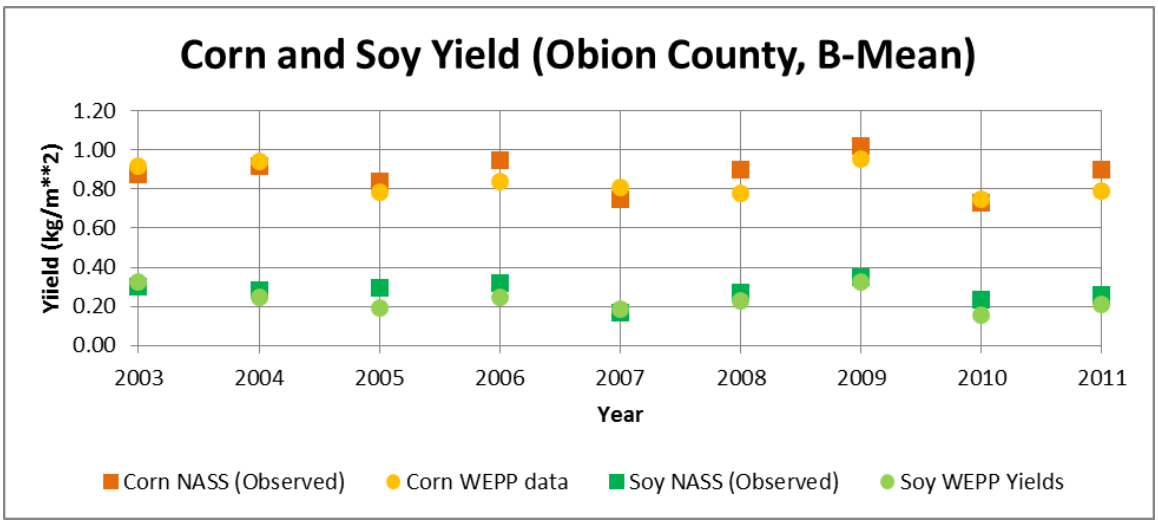


Figure A.2-3: B-Mean Corn and Soy Calibration

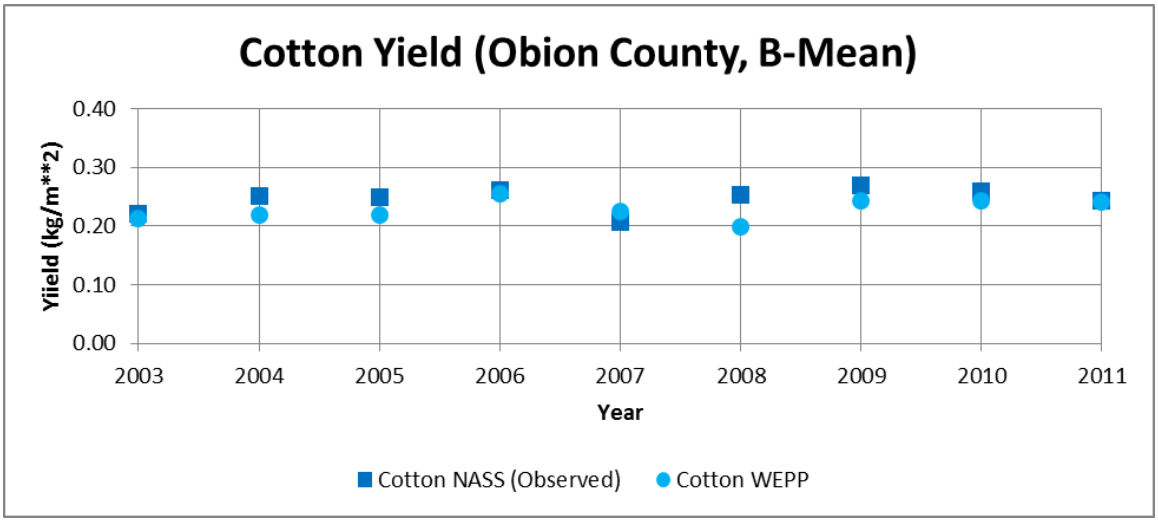


Figure A.2-4: B-Mean Cotton Calibration

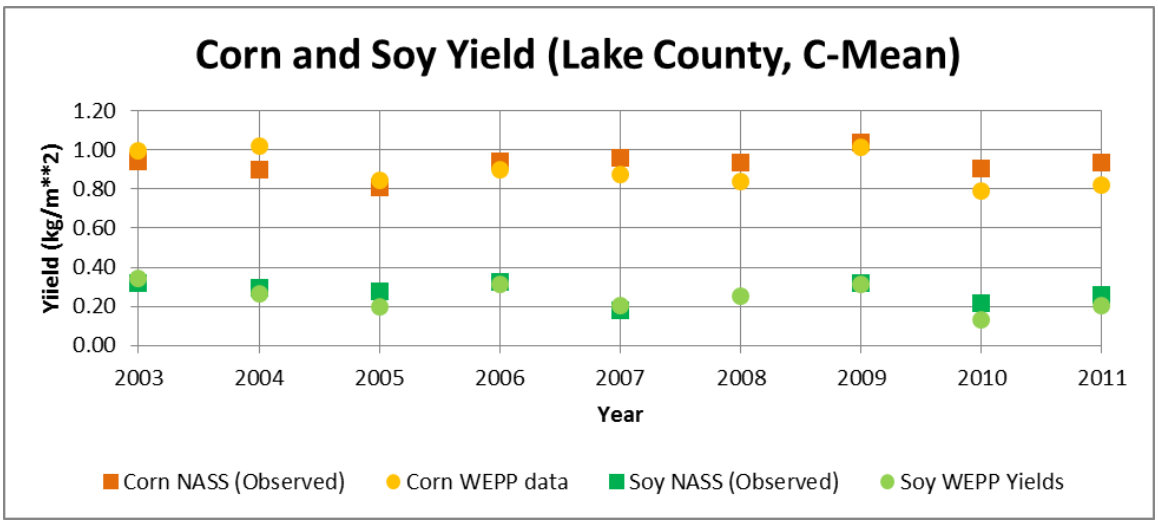


Figure A.2-5: C-Mean Corn and Soy Calibration

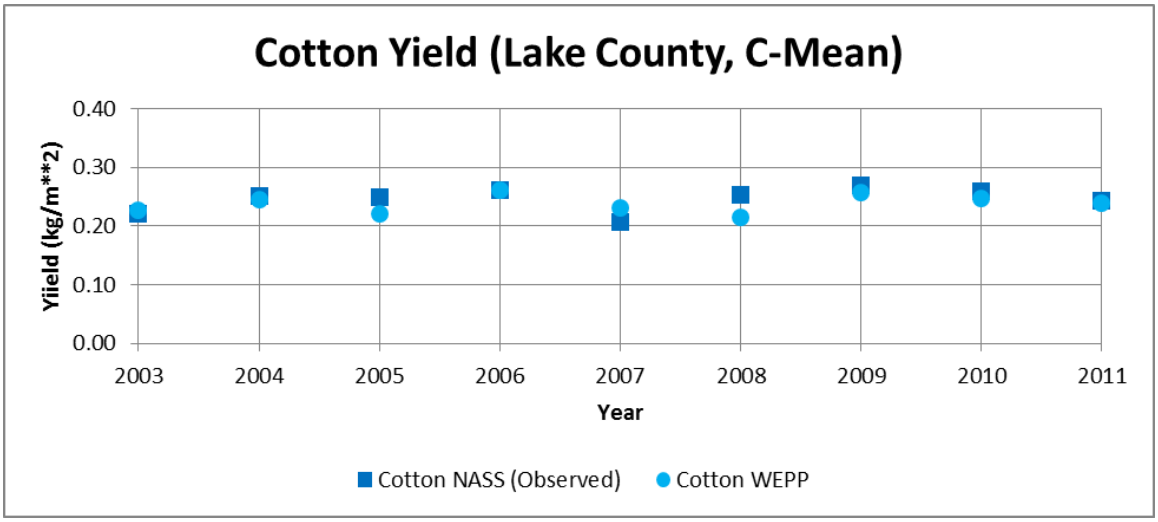


Figure A.2-6: C-Mean Cotton Calibration

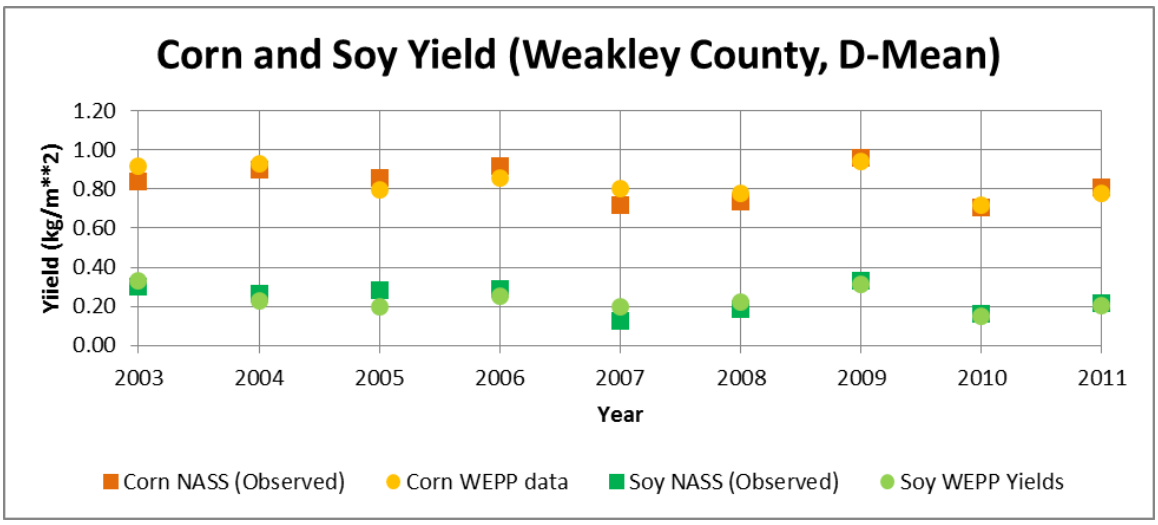


Figure A.2-7: D-Mean Corn and Soy Calibration

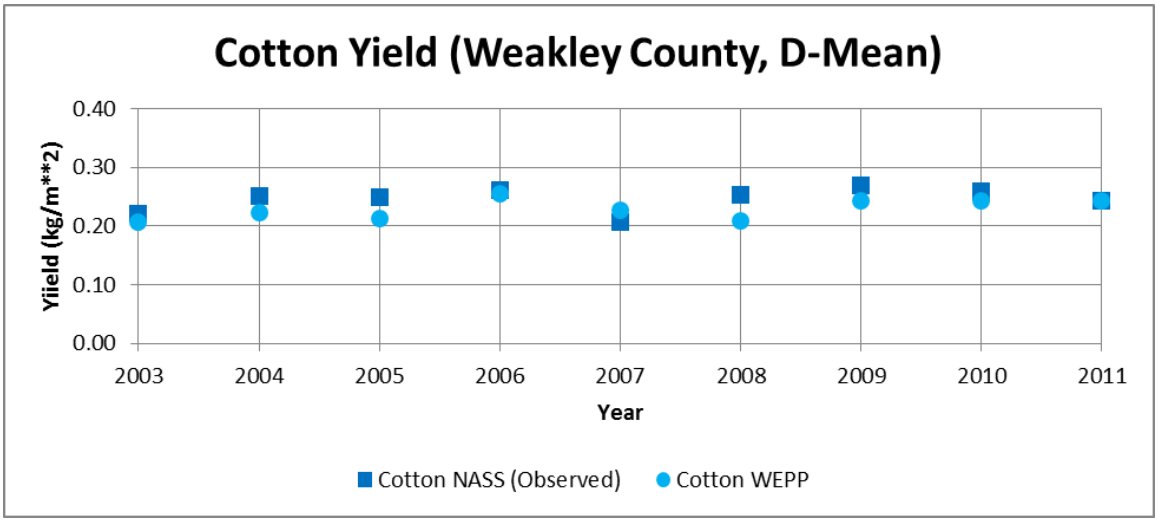


Figure A.2-8: D-Mean Cotton Calibration

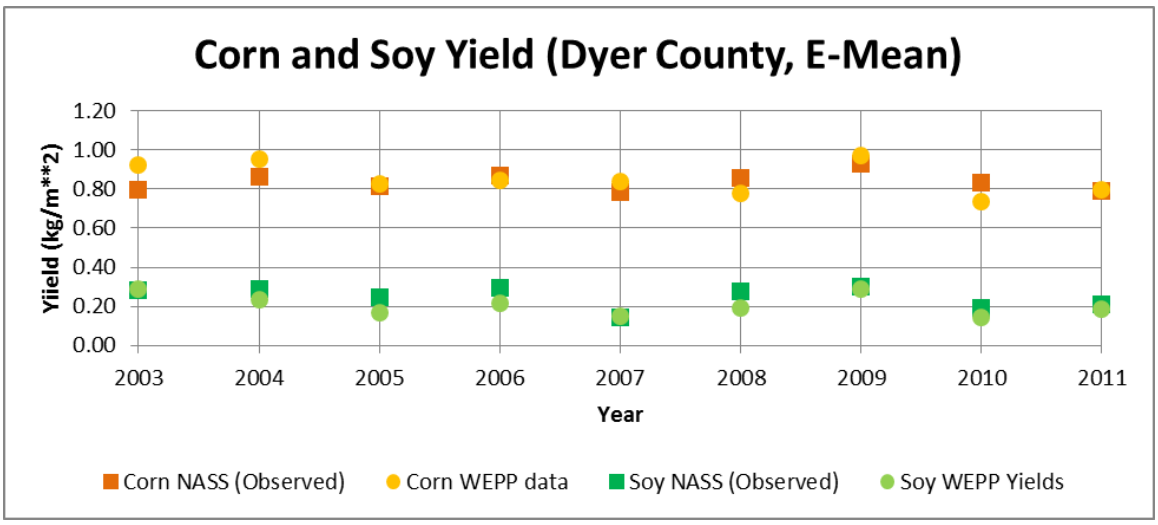


Figure A.2-9: E-Mean Corn and Soy Calibration

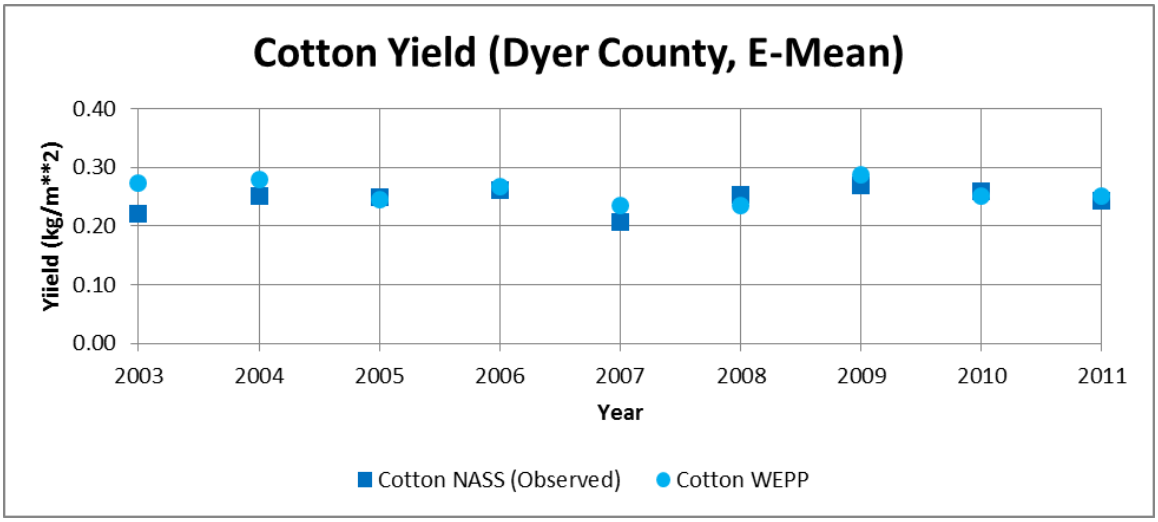


Figure A.2-10: E-Mean Cotton Calibration

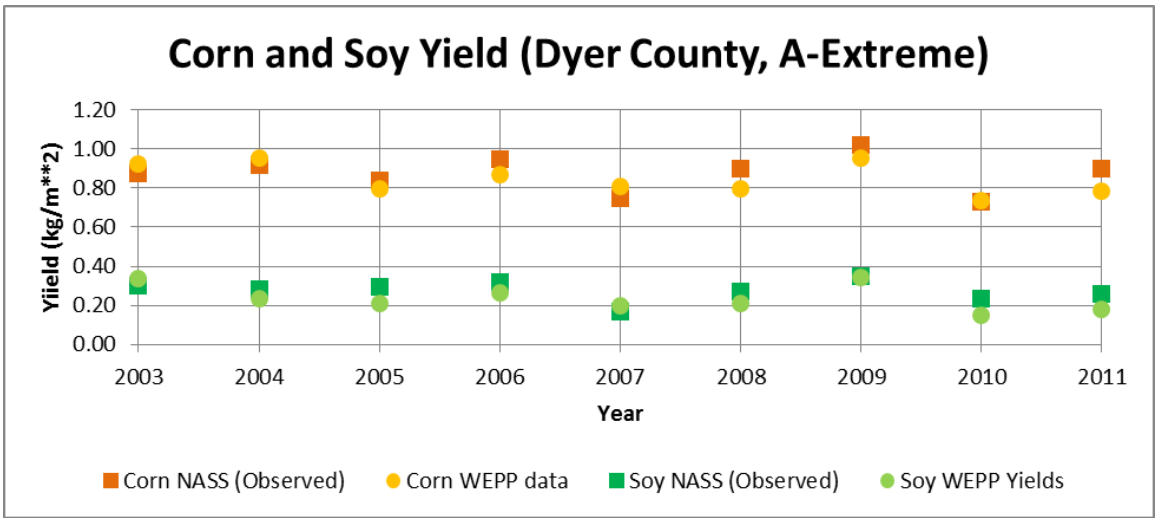


Figure A.2-11: A-Extreme Corn and Soy Calibration

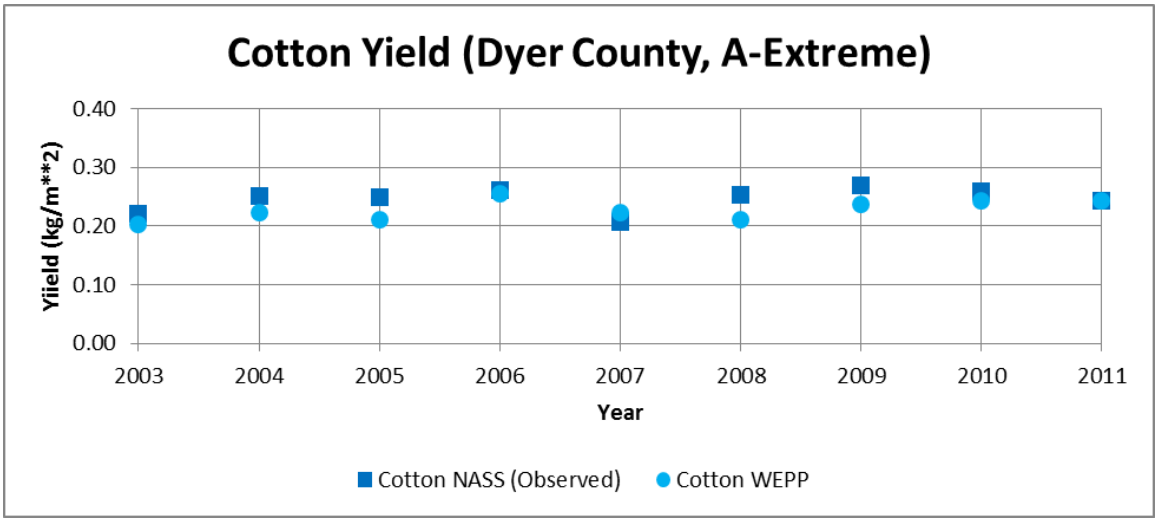


Figure A.2-12: A-Extreme Cotton Calibration

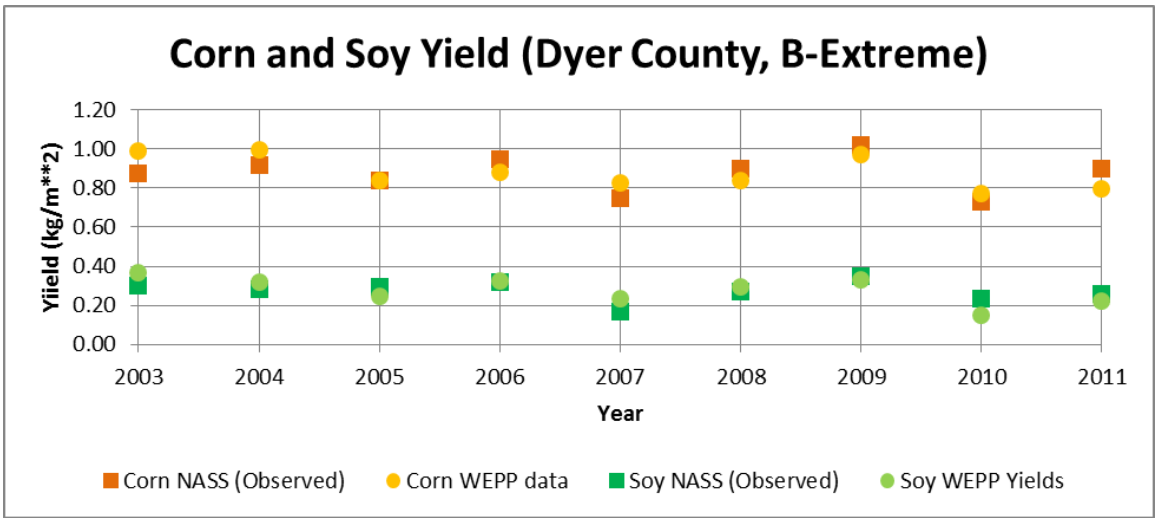


Figure A.2-13: B-Extreme Corn and Soy Calibration

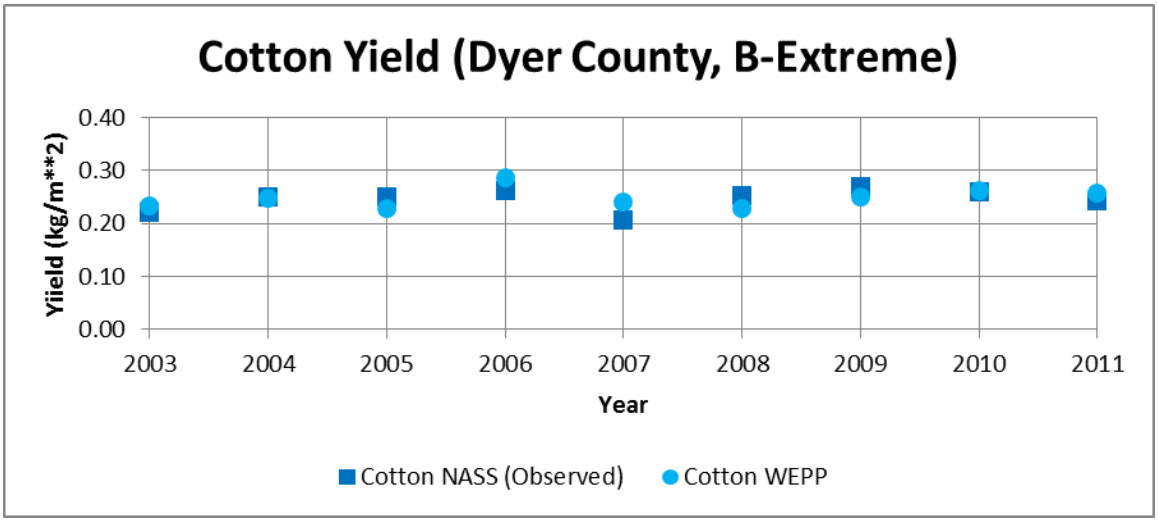


Figure A.2-14: B-Extreme Cotton Calibration

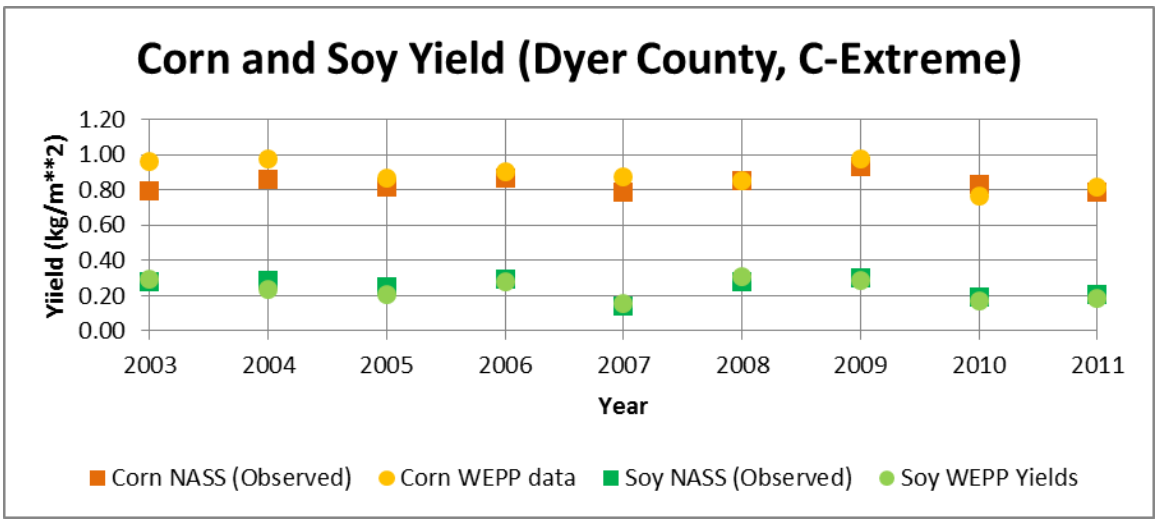


Figure A.2-15: C-Extreme Corn and Soy Calibration

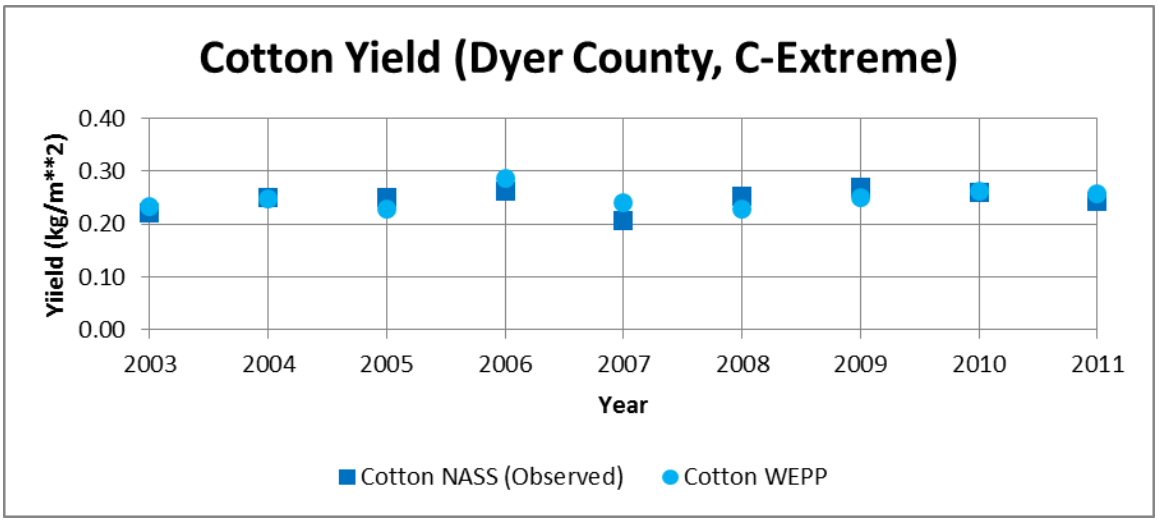


Figure A.2-16: C-Extreme Cotton Calibration

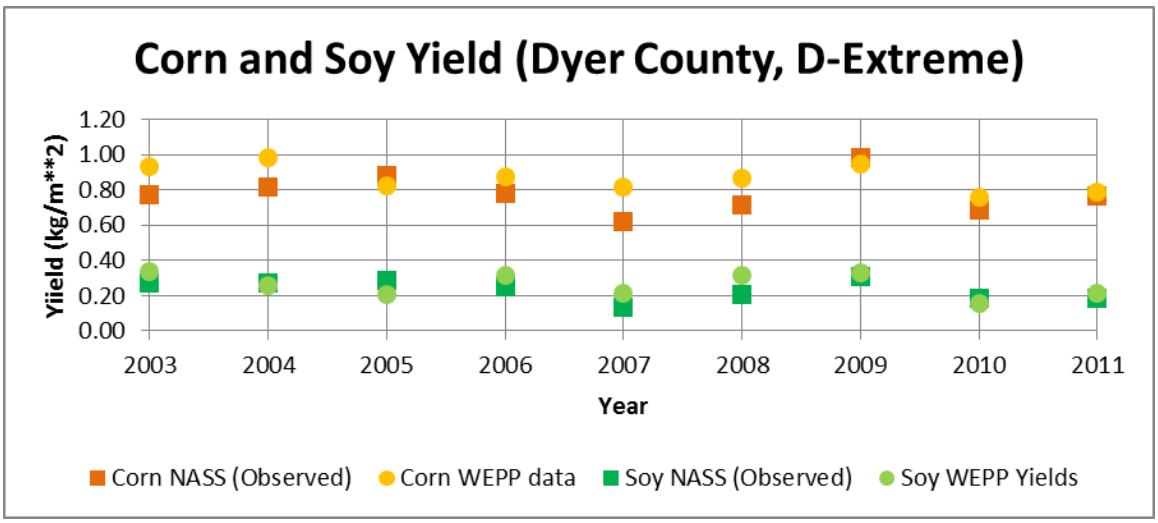


Figure A.2-17: D-Extreme Corn and Soy Calibration

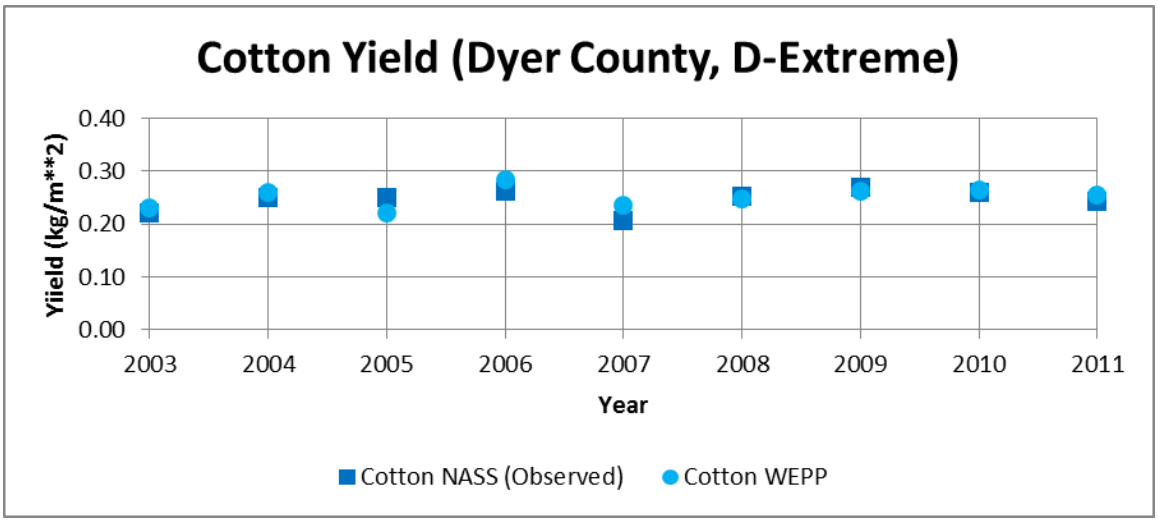


Figure A.2-18: D-Extreme Cotton Calibration

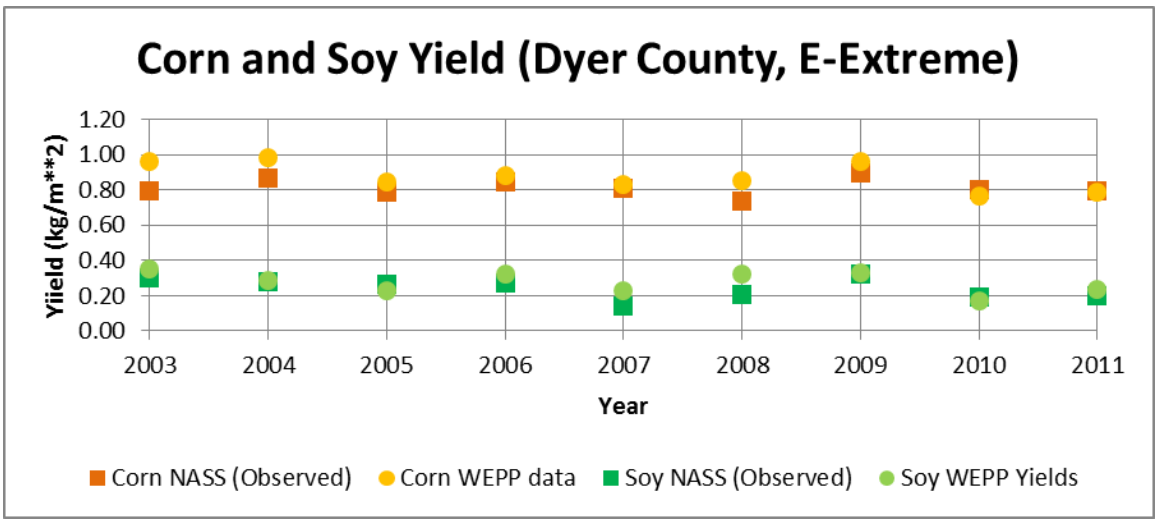


Figure A.2-19: E-Extreme Corn and Soy Calibration

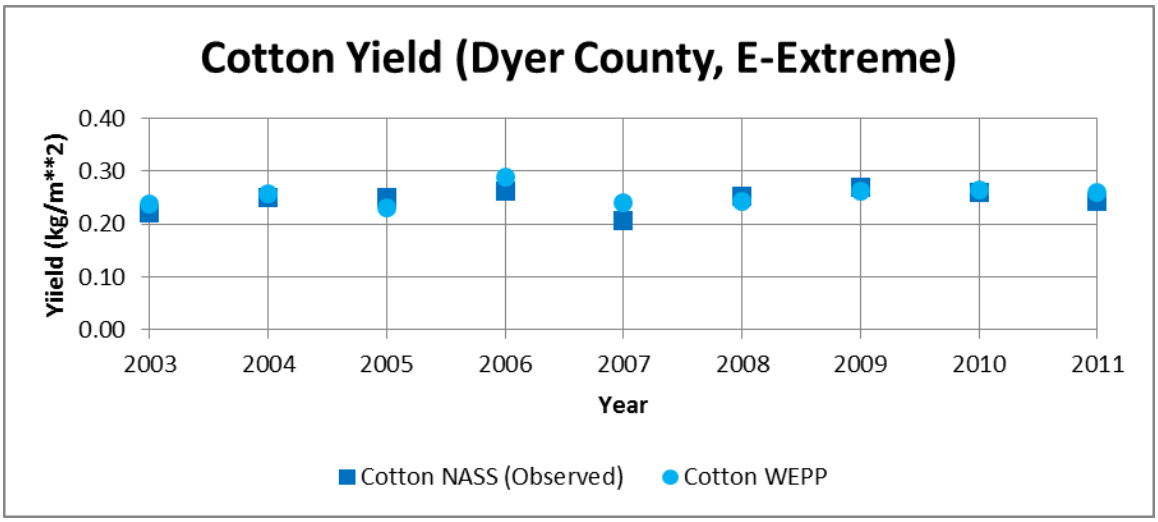


Figure A.2-20: E-Extreme Cotton Calibration

A.3 Modified sWUE = yields/((ET+runoff+drainage)/precipitation)

A.3.1 Corn

RCP 4.5

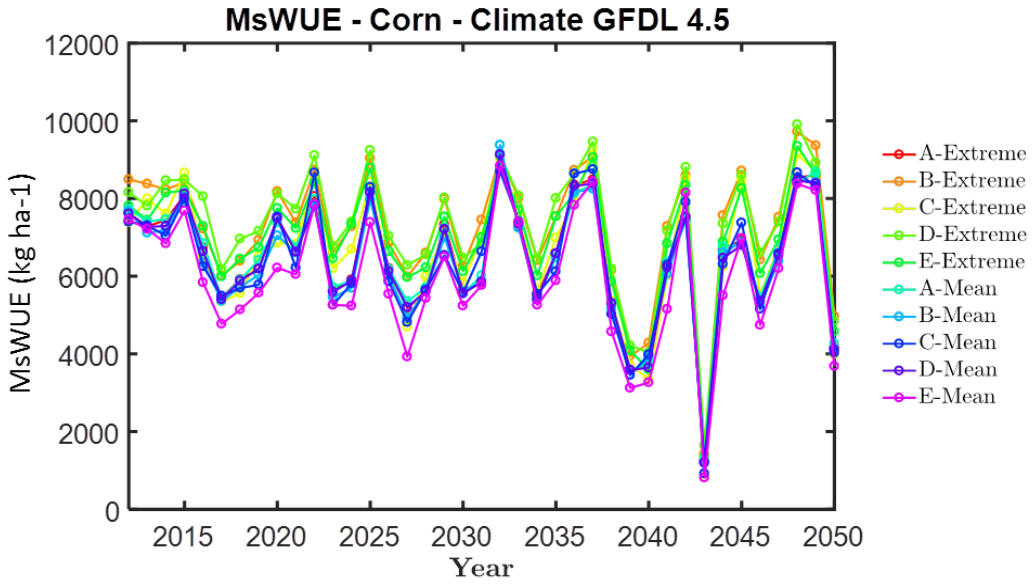


Figure A.3.1-1: Corn Modified sWUE for GFDL RCP 4.5

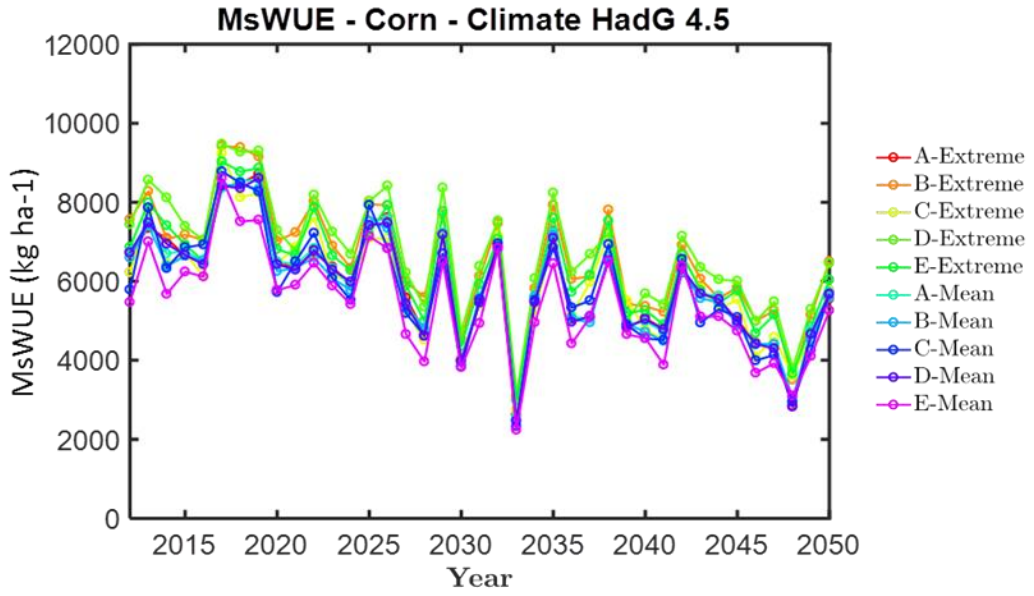


Figure A.3.1-2: Corn Modified sWUE for HadG RCP 4.5

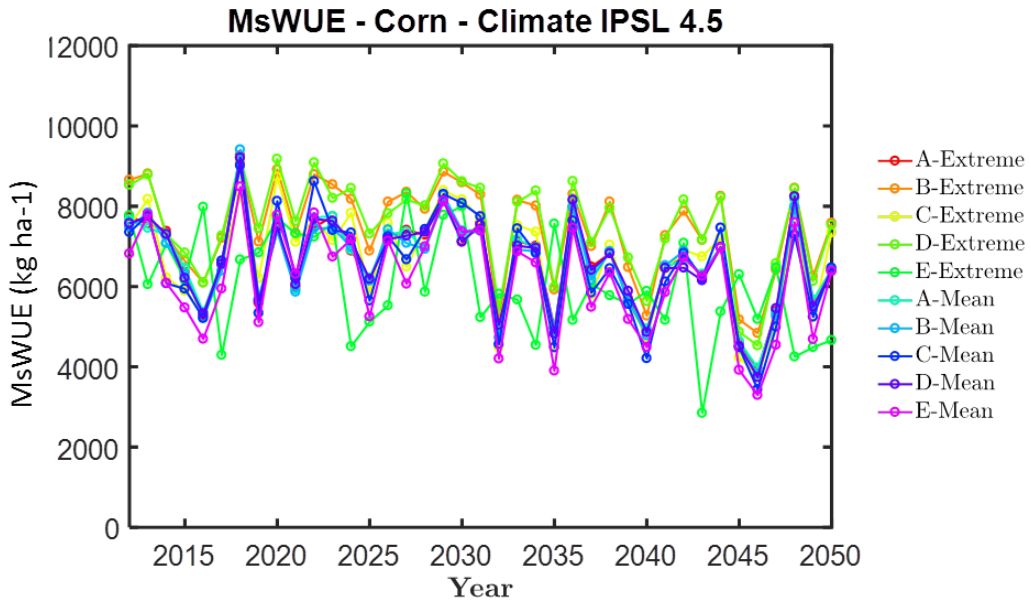


Figure A.3.1-3: Corn Modified sWUE for IPSL RCP 4.5

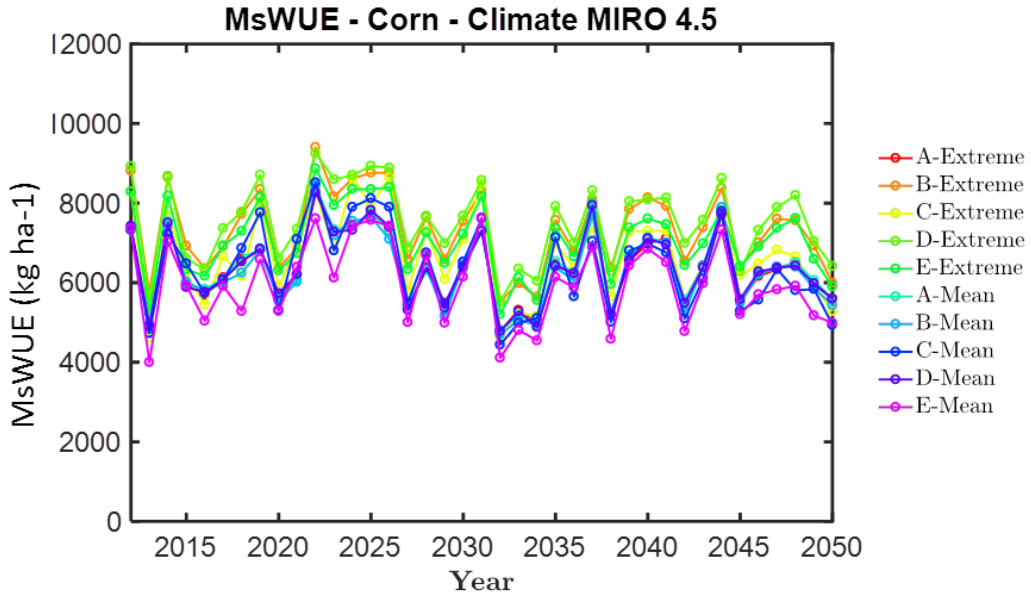


Figure A.3.1-4: Corn Modified sWUE for MIRO RCP 4.5

RCP 8.5

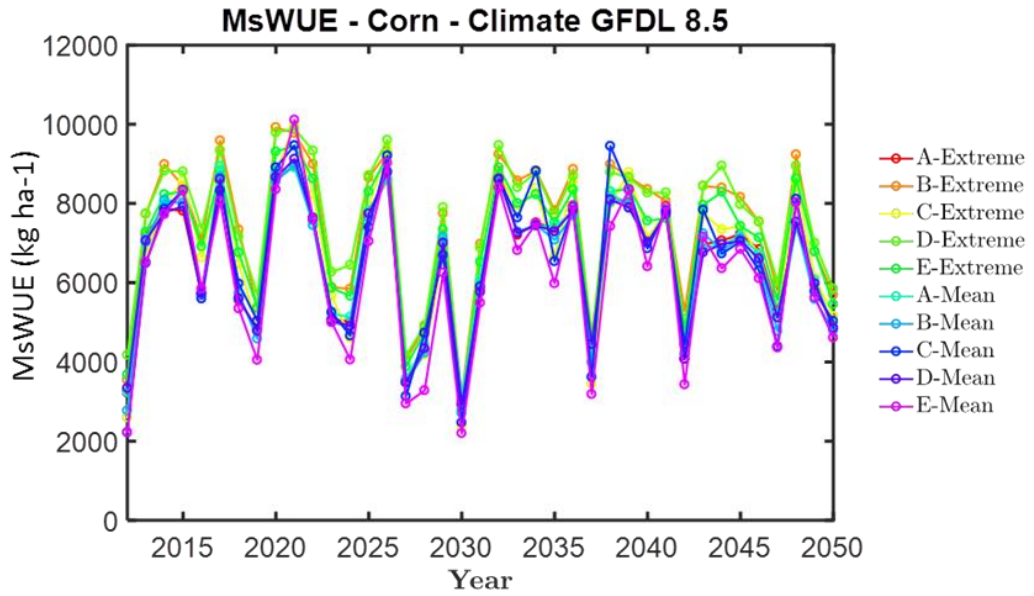


Figure A.3.1-5: Corn Modified sWUE for GFDL RCP 8.5

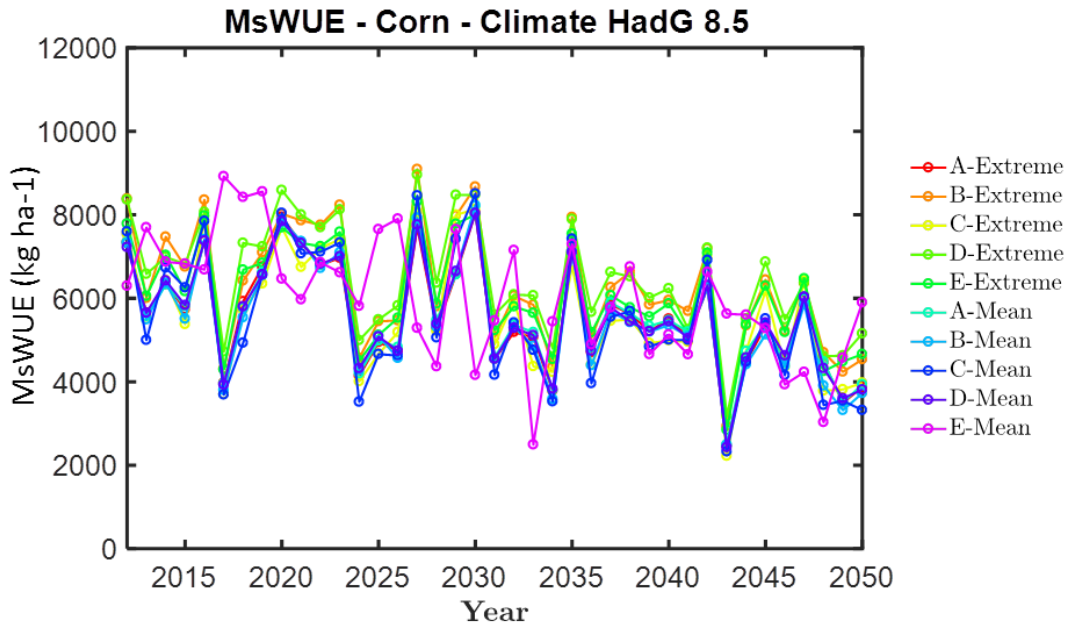


Figure A.3.1-6: Corn Modified sWUE for HadG RCP 8.5

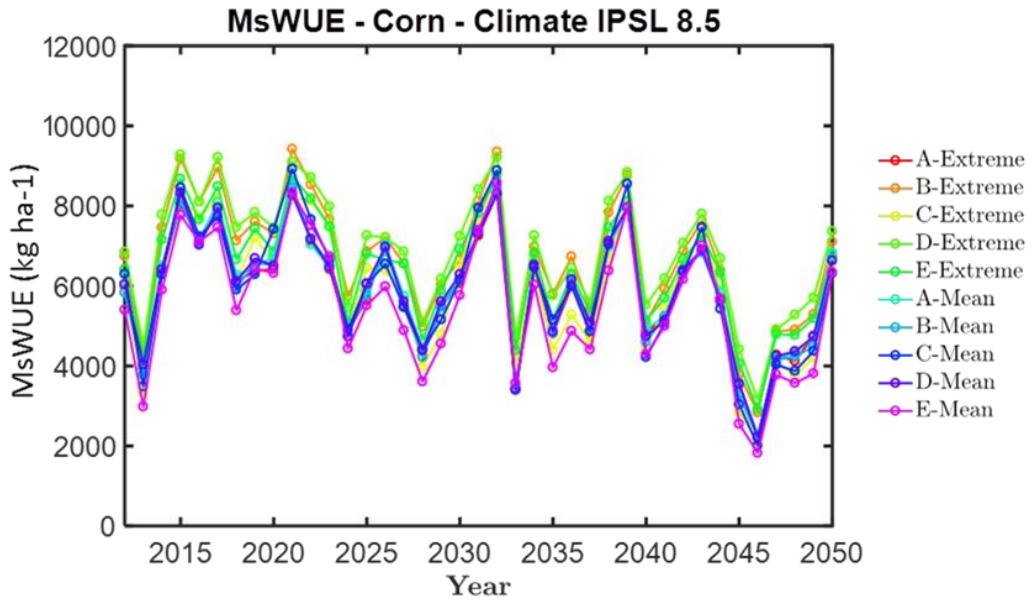


Figure A.3.1-7: Corn Modified sWUE for IPSL RCP 8.5

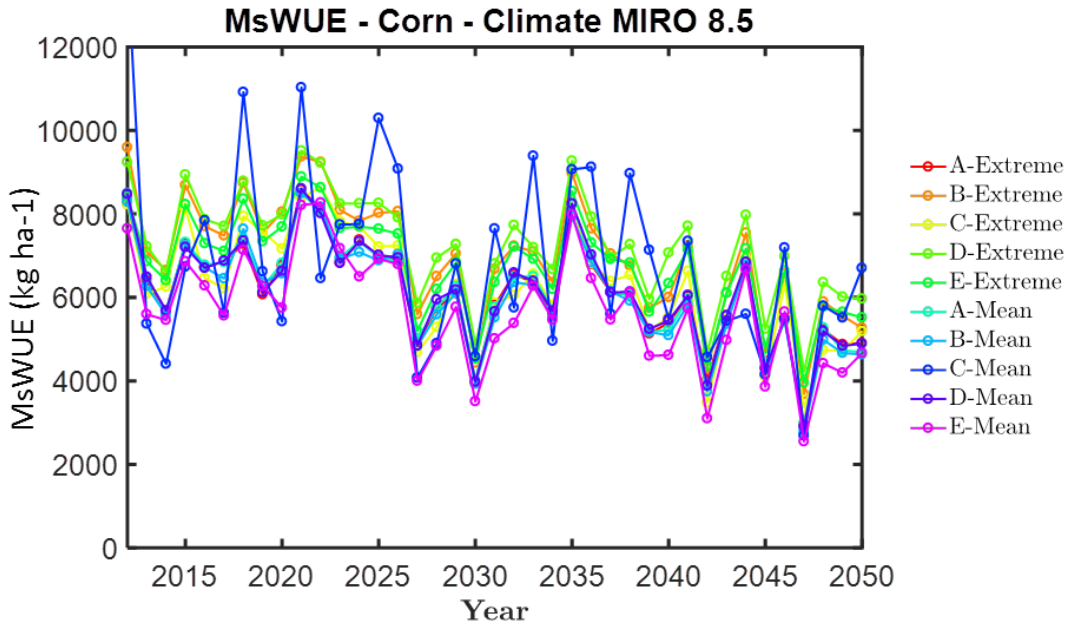


Figure A.3.1-8: Corn Modified sWUE for MIRO RCP 8.5

A.3.2 Soy

RCP 4.5

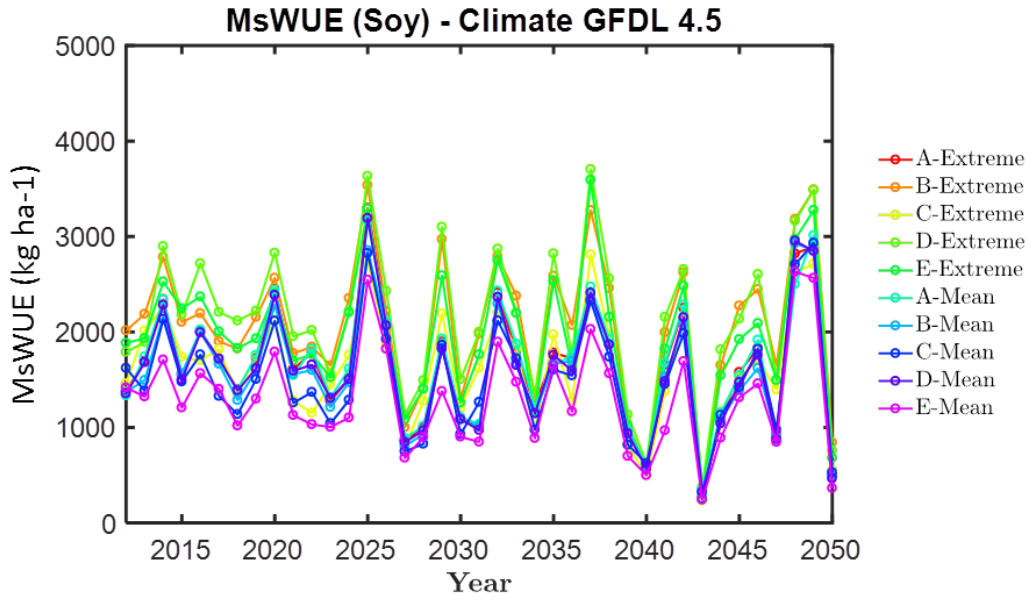


Figure A.3.2-1: Soy Modified sWUE for GFDL RCP 4.5

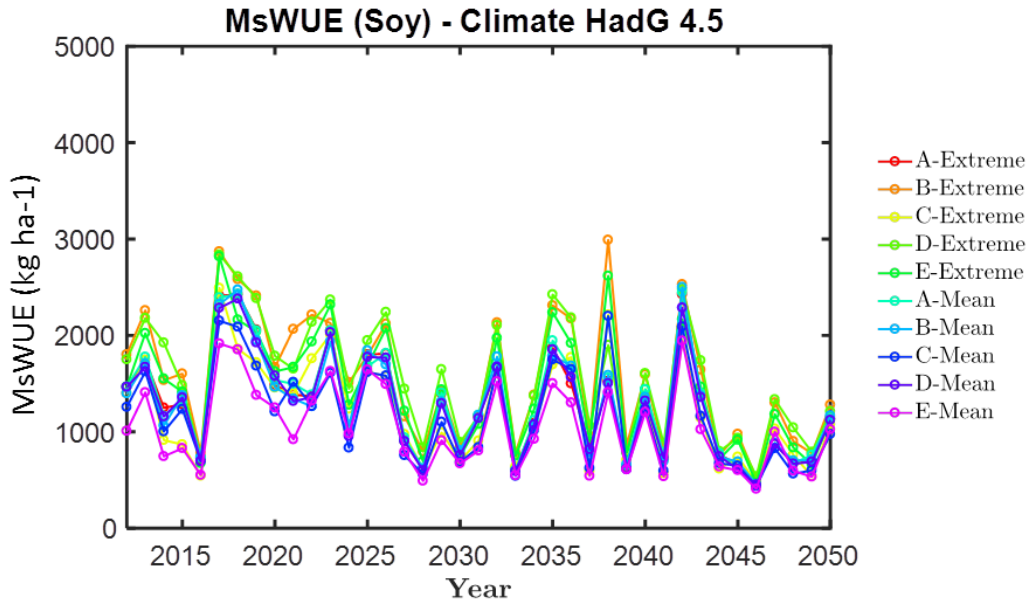


Figure A.3.2-2: Soy Modified sWUE for HadG RCP 4.5

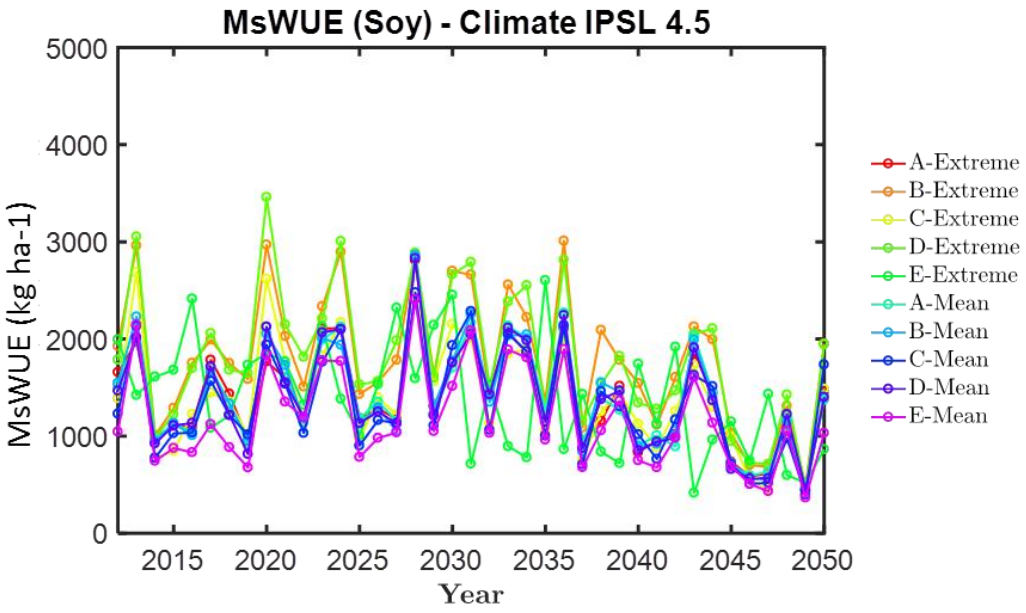


Figure A.3.2-3: Soy Modified sWUE for IPSL RCP 4.5

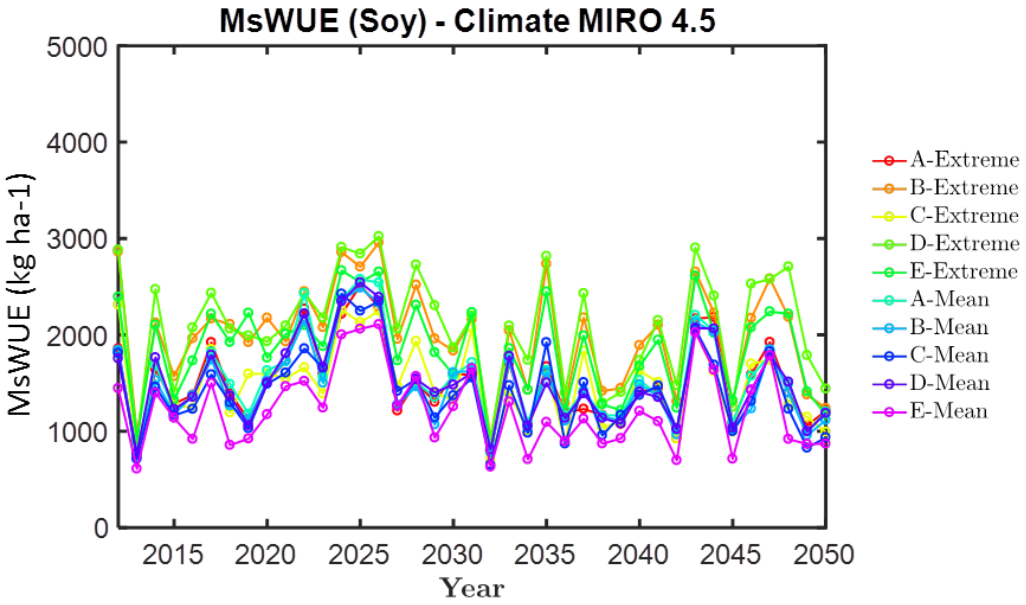


Figure A.3.2-4: Soy Modified sWUE for MIRO RCP 4.5

RCP 8.5

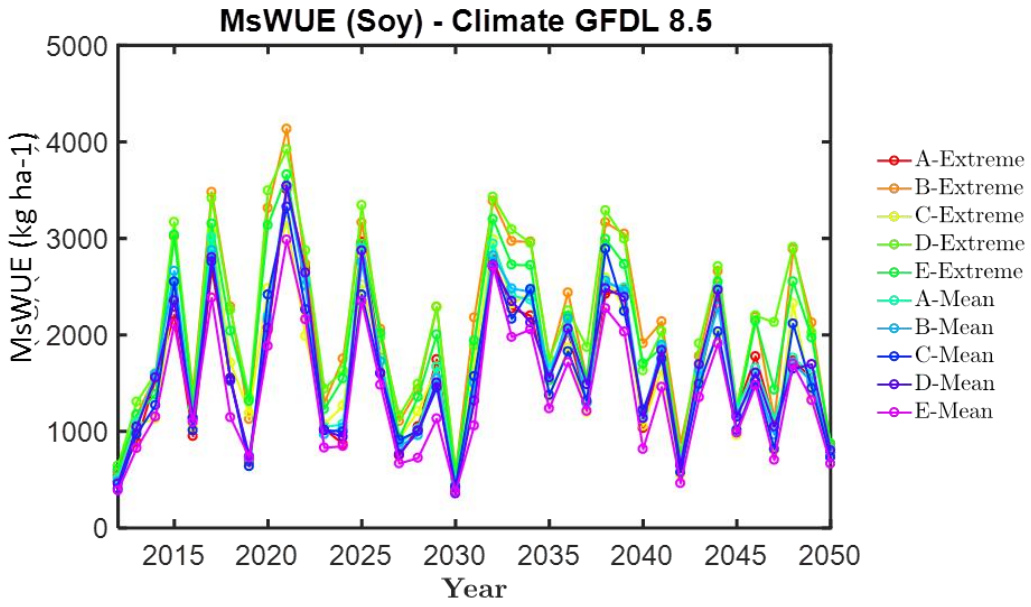


Figure A.3.2-5: Soy Modified sWUE for GFDL RCP 8.5

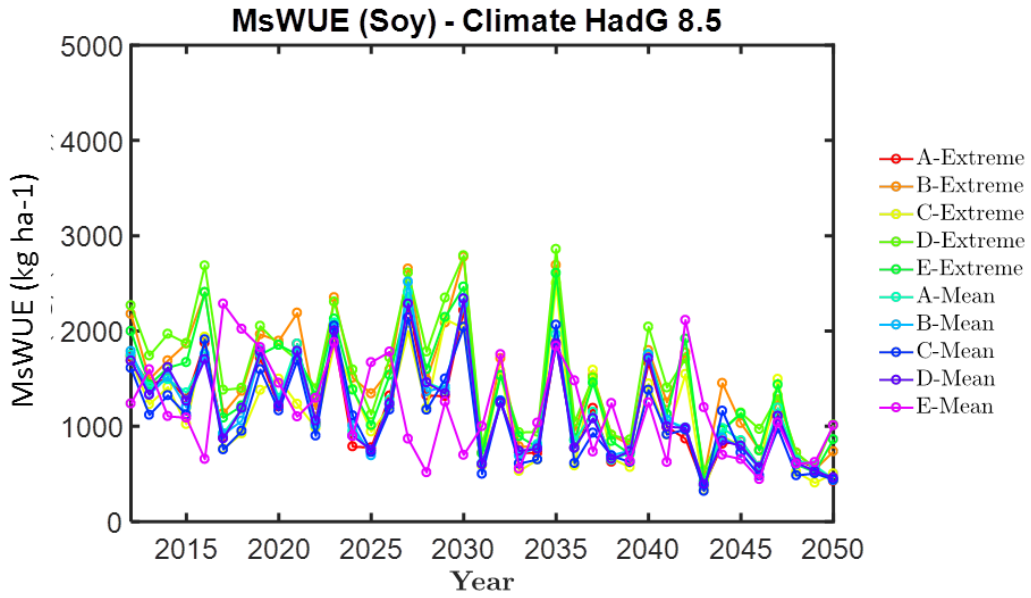


Figure A.3.2-6: Soy Modified sWUE for HadG RCP 8.5

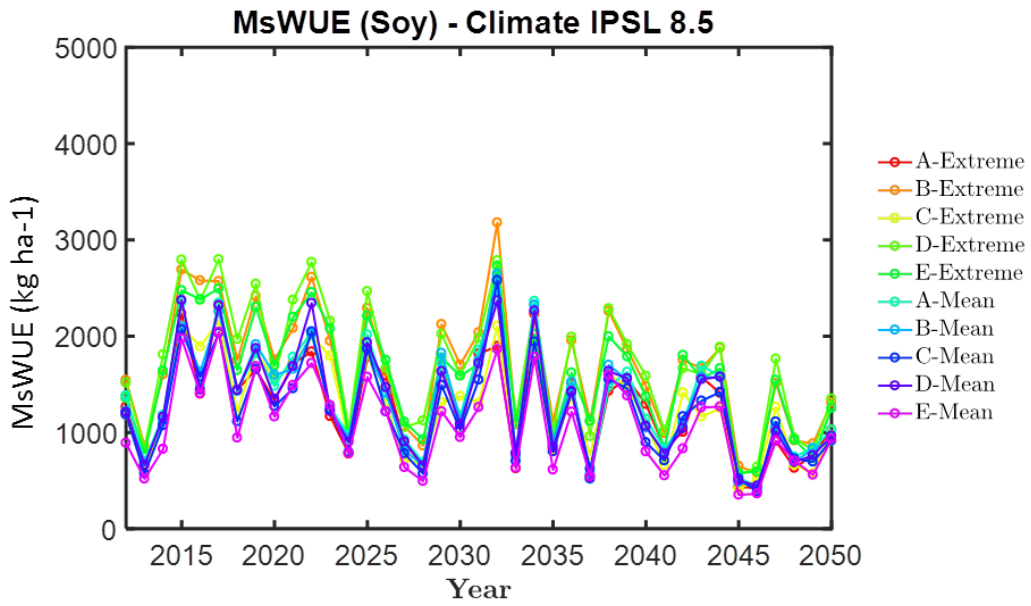


Figure A.3.2-7: Soy Modified sWUE for IPSL RCP 8.5

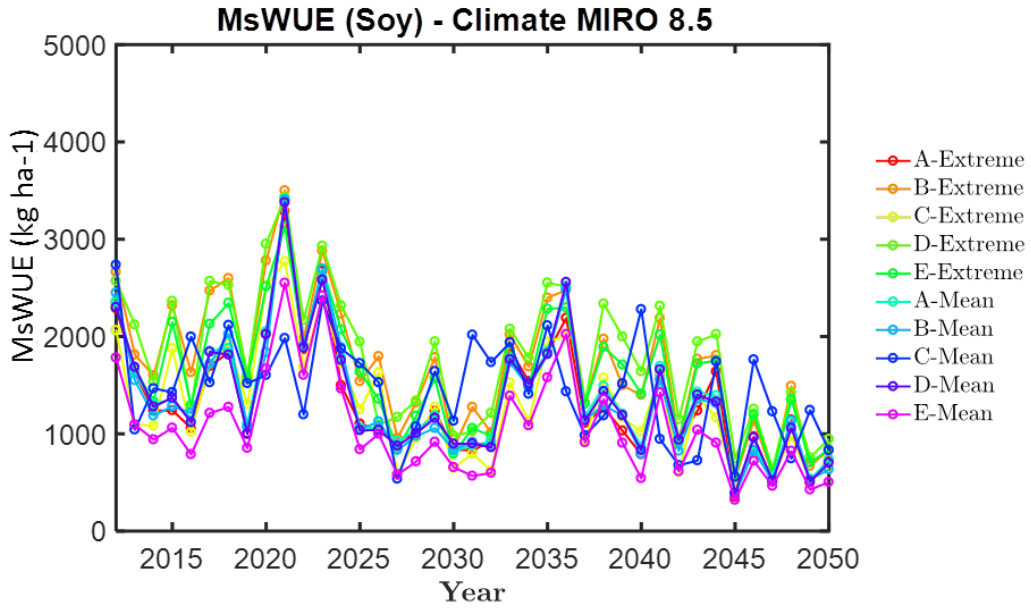


Figure A.3.2-8: Soy Modified sWUE for MIRO RCP 8.5

A.3.3 Cotton

RCP 4.5

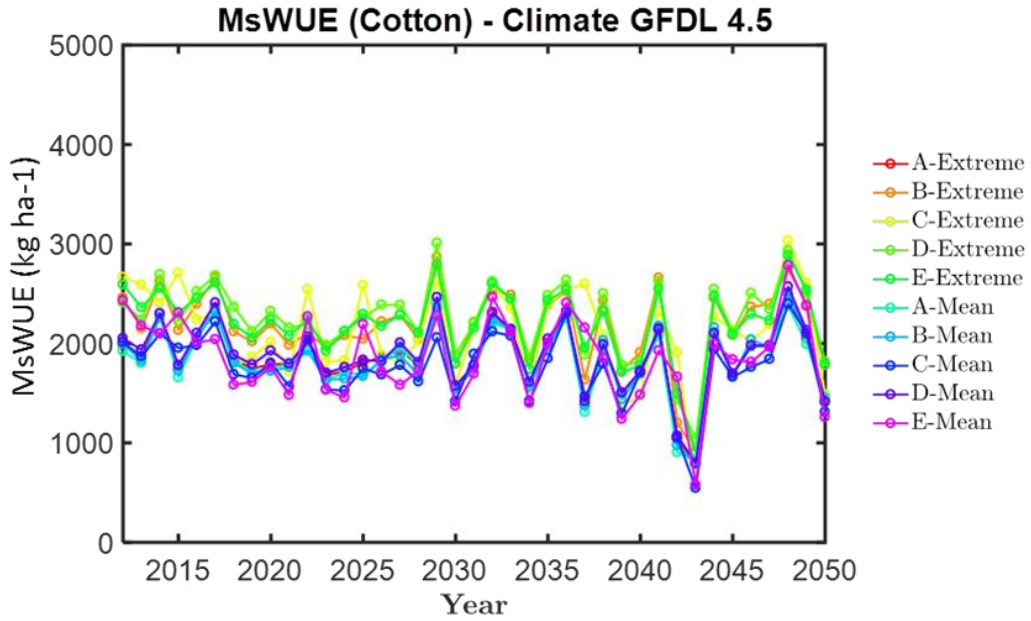


Figure A.3.3-1: Cotton Modified sWUE for GFDL RCP 4.5

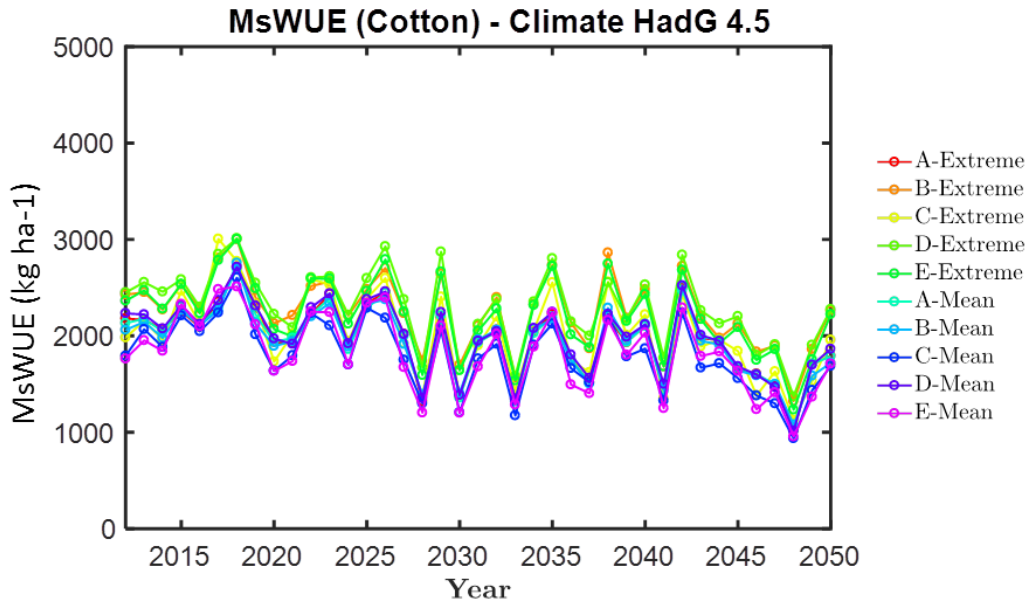


Figure A.3.3-2: Cotton Modified sWUE for HadG RCP 4.5

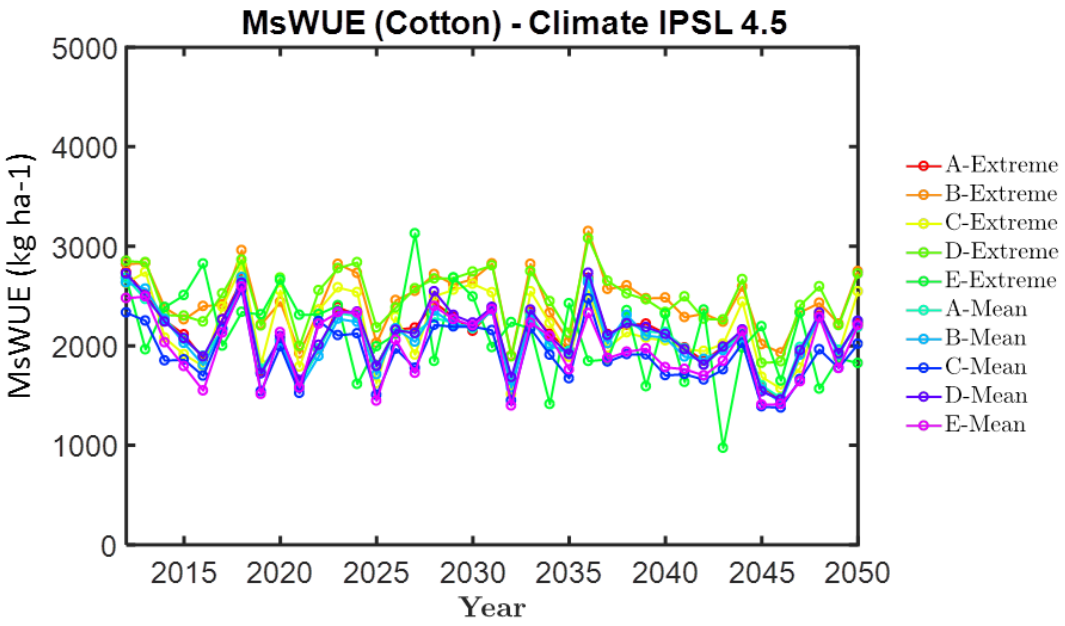


Figure A.3.3-3: Cotton Modified sWUE for IPSL RCP 4.5

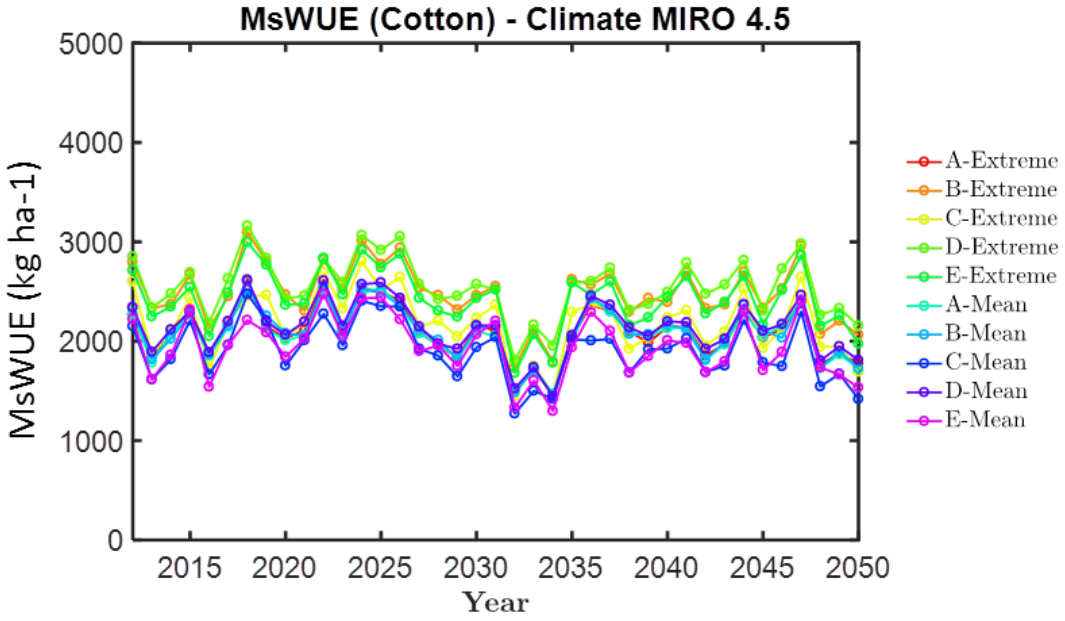


Figure A.3.3-4: Cotton Modified sWUE for MIRO RCP 4.5

RCP 8.5

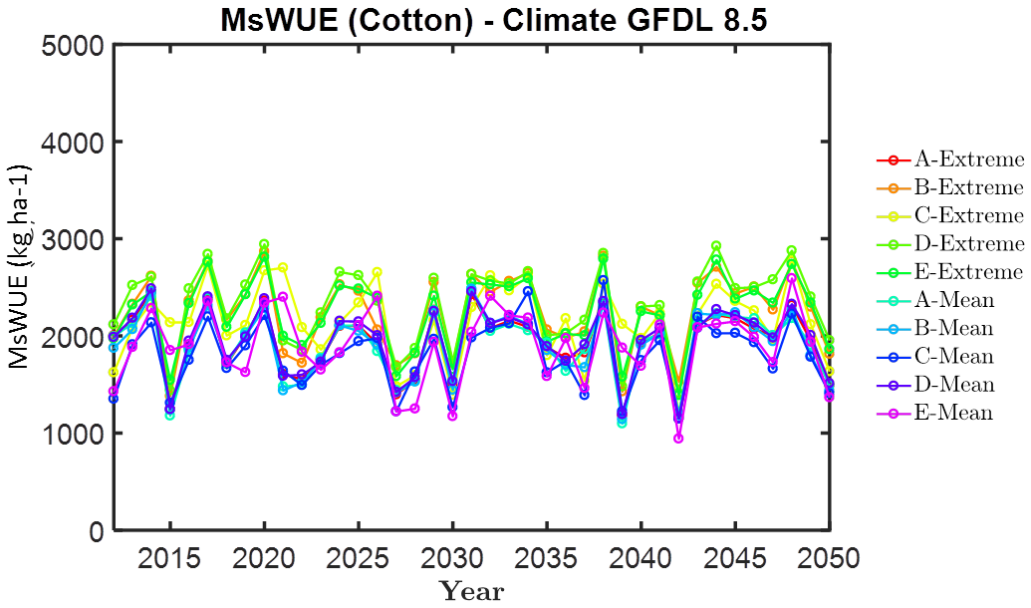


Figure A.3.3-5: Cotton Modified sWUE for GFDL RCP 8.5

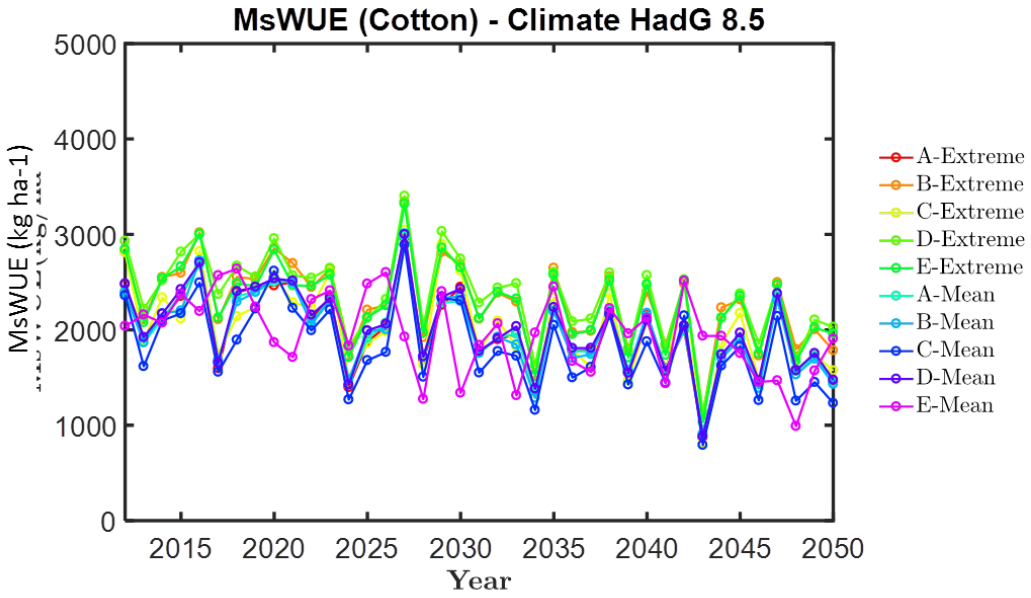


Figure A.3.3-6: Soy Modified sWUE for HadG RCP 8.5

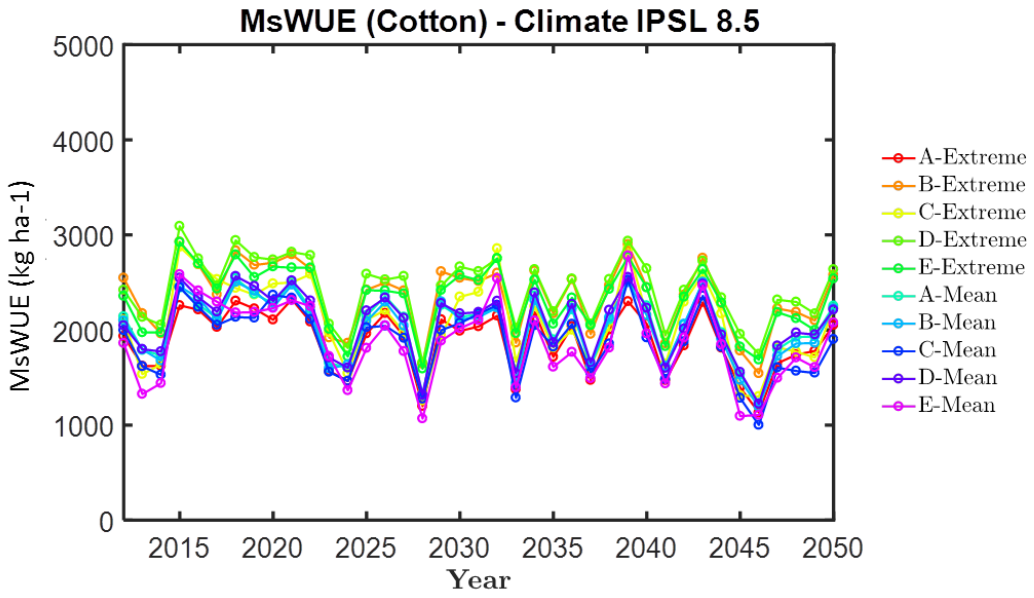


Figure A.3.3-7: Cotton Modified sWUE for IPSL RCP 8.5

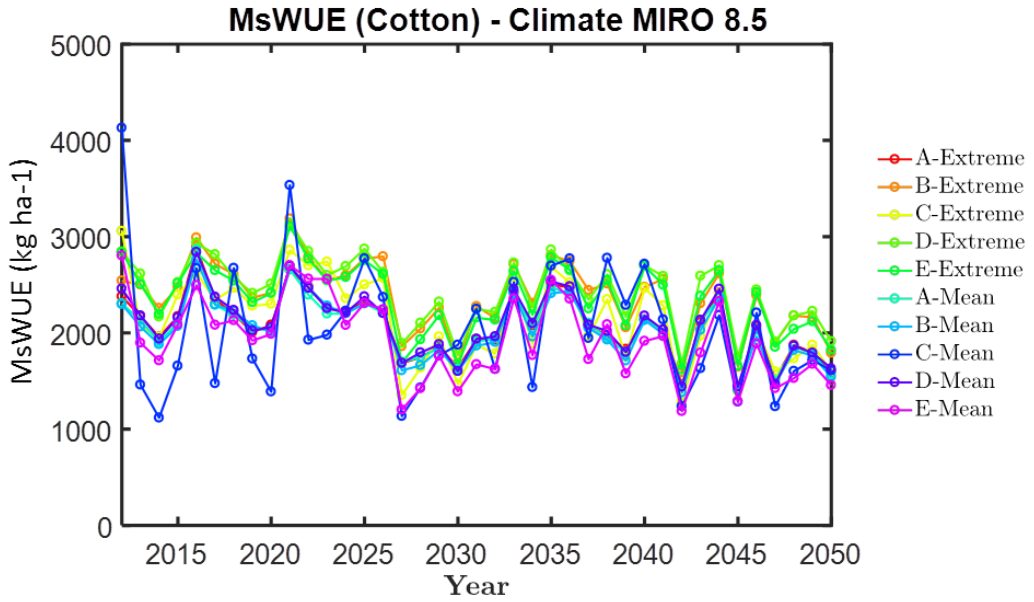


Figure A.3.3-8: Cotton Modified sWUE for MIRO RCP 8.5

A.4 sWUE Projected Climate Histograms

A.4.1 Corn

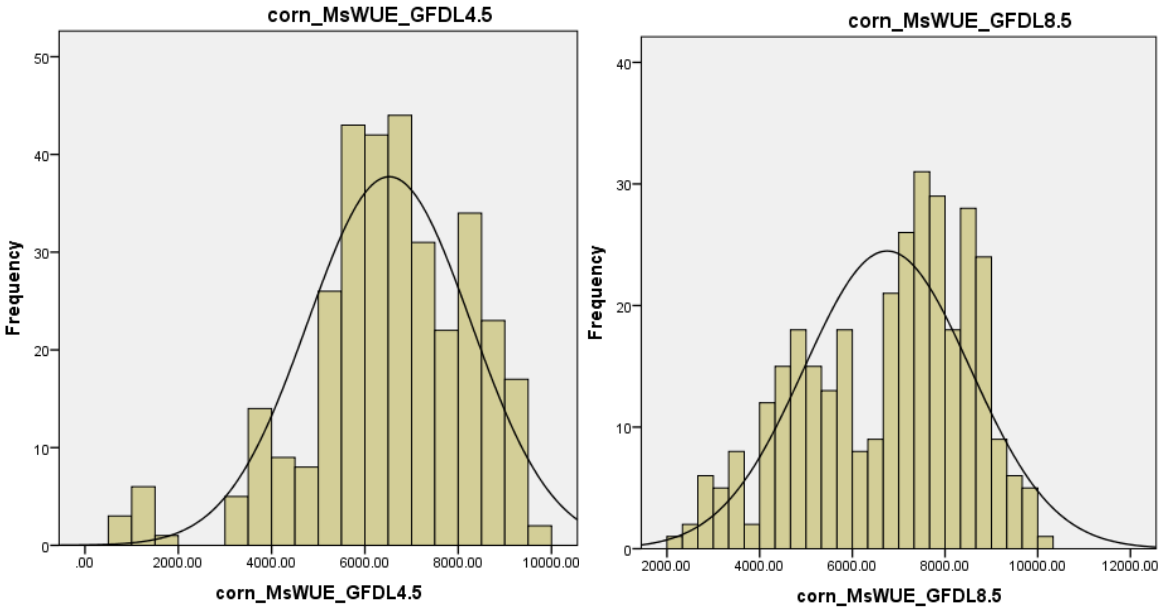


Figure A.4.1-1: GFDL 4.5 and 8.5 Corn Modified sWUE histograms

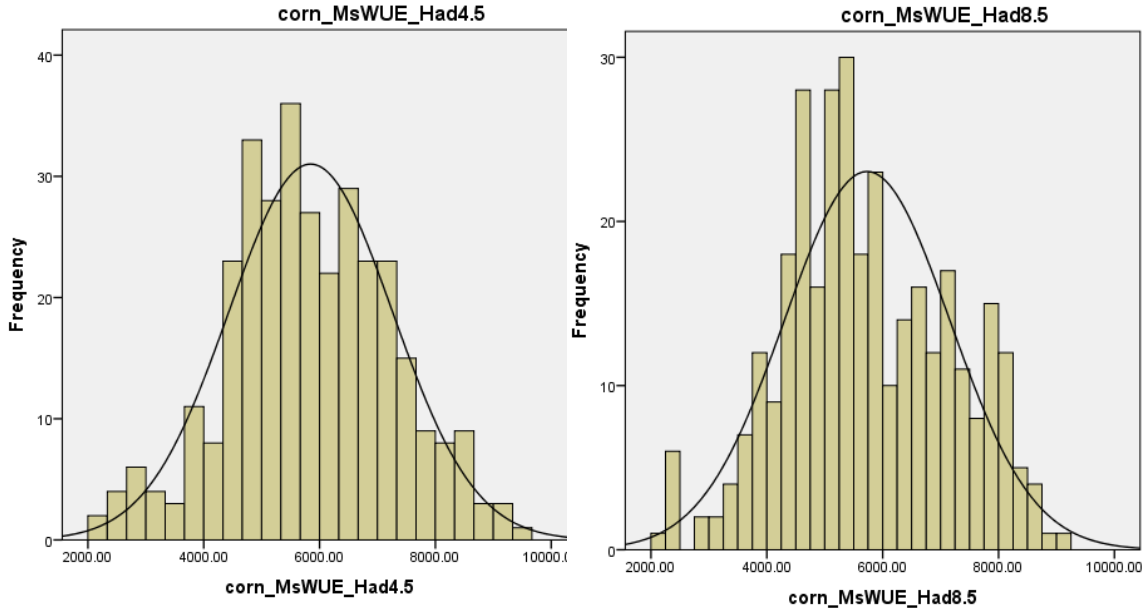


Figure A.4.1-2: Had 4.5 and 8.5 Corn Modified sWUE histograms

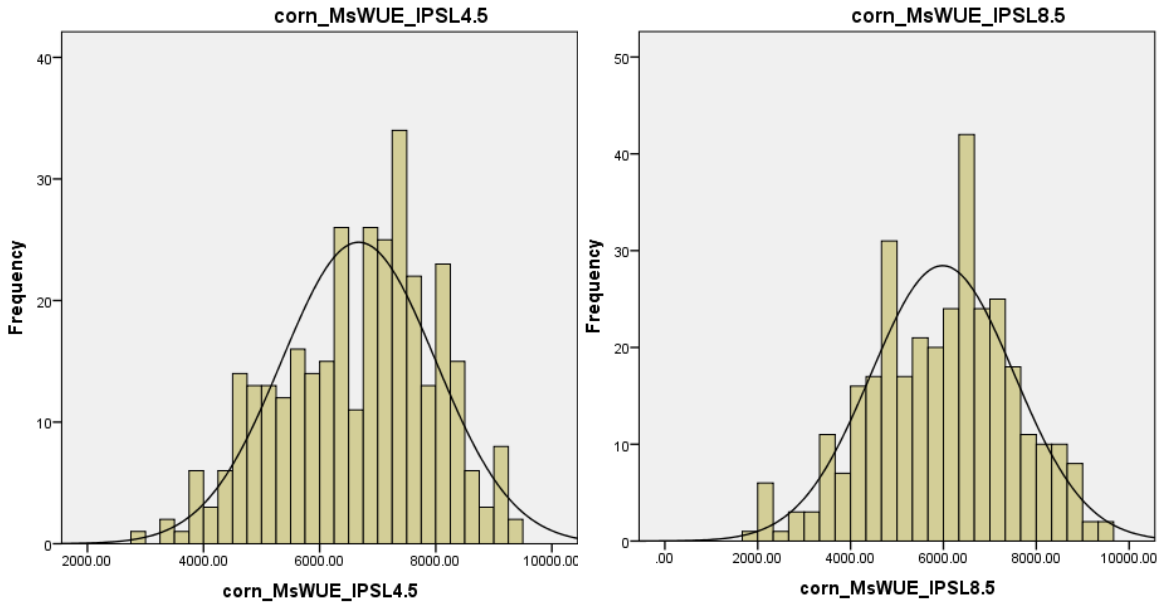


Figure A.4.1-3: IPSL 4.5 and 8.5 Corn Modified sWUE histograms

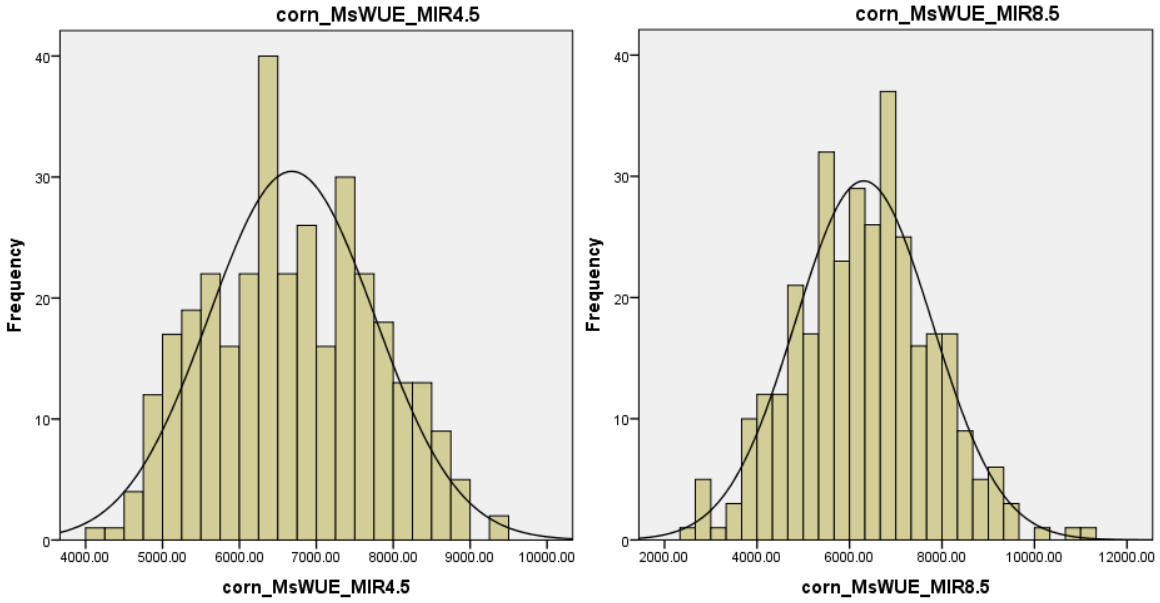


Figure A.4.1-4: MIR 4.5 and 8.5 Corn Modified sWUE histograms

A.4.2 Soy

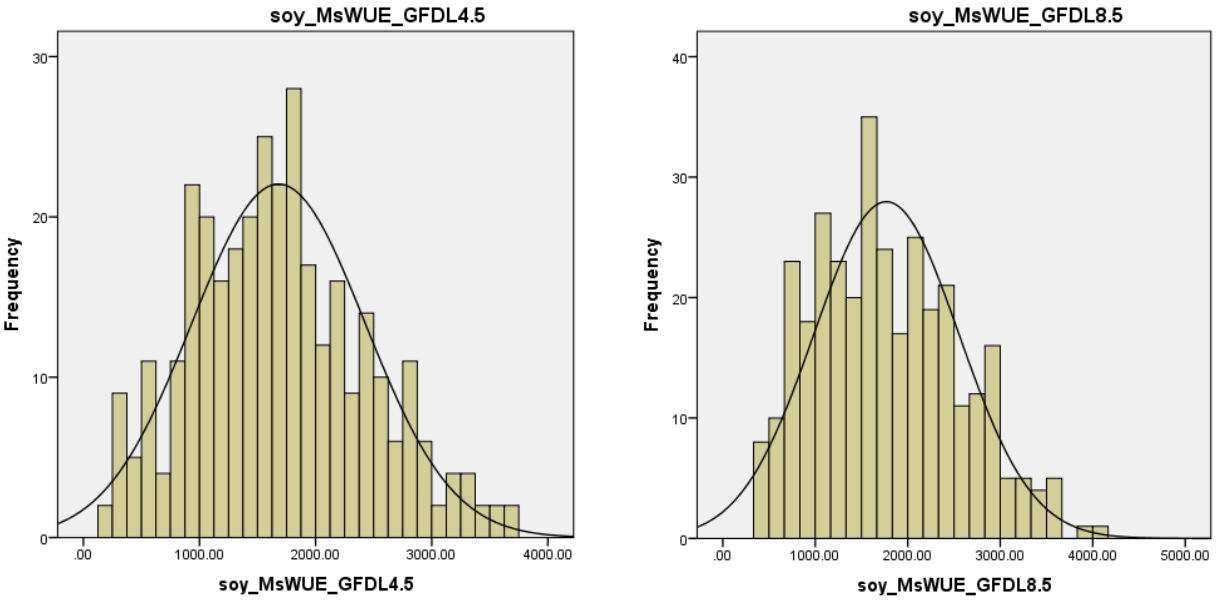


Figure A.4.2-1: GFDL 4.5 and 8.5 Soy Modified sWUE histograms

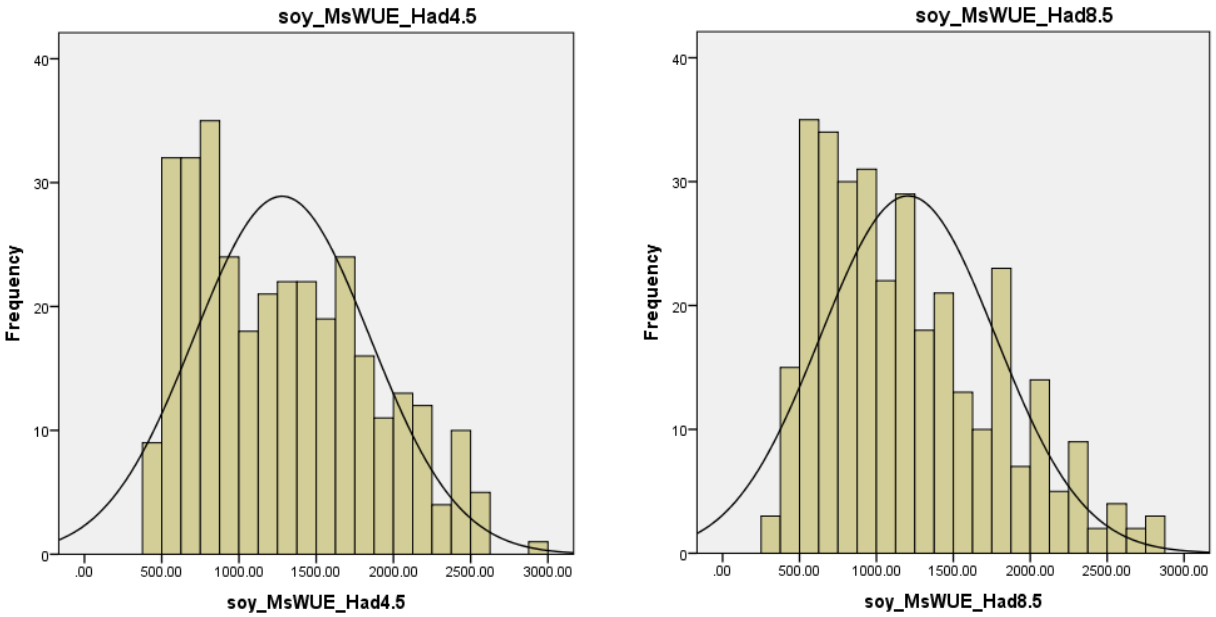


Figure A.4.2-2: Had 4.5 and 8.5 Soy Modified sWUE histograms

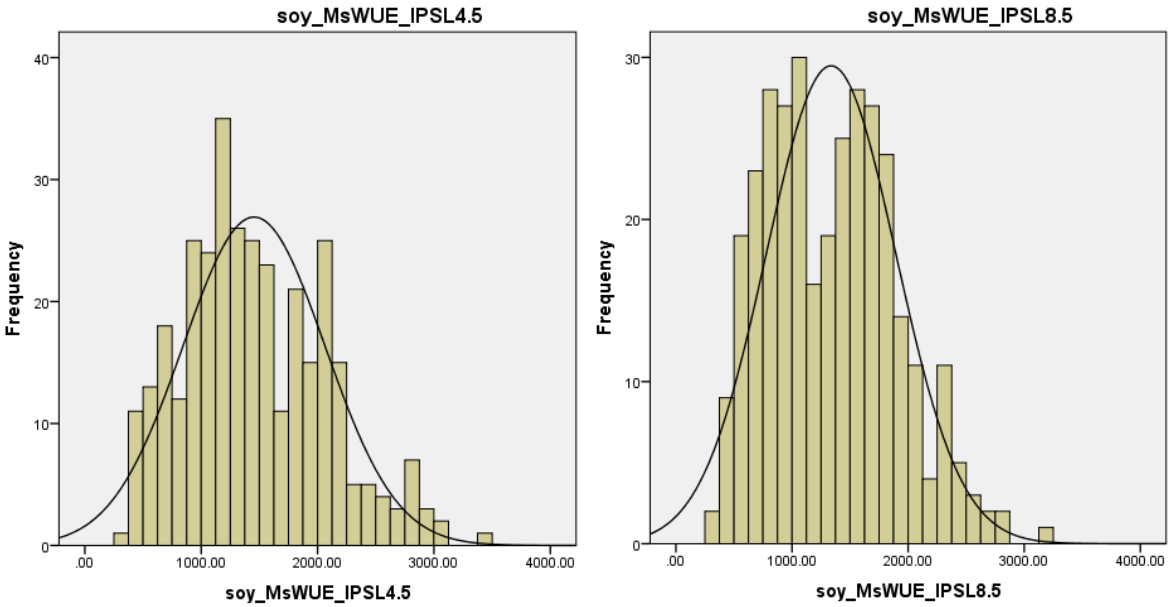


Figure A.4.2-3: IPSL 4.5 and 8.5 Soy Modified sWUE histograms

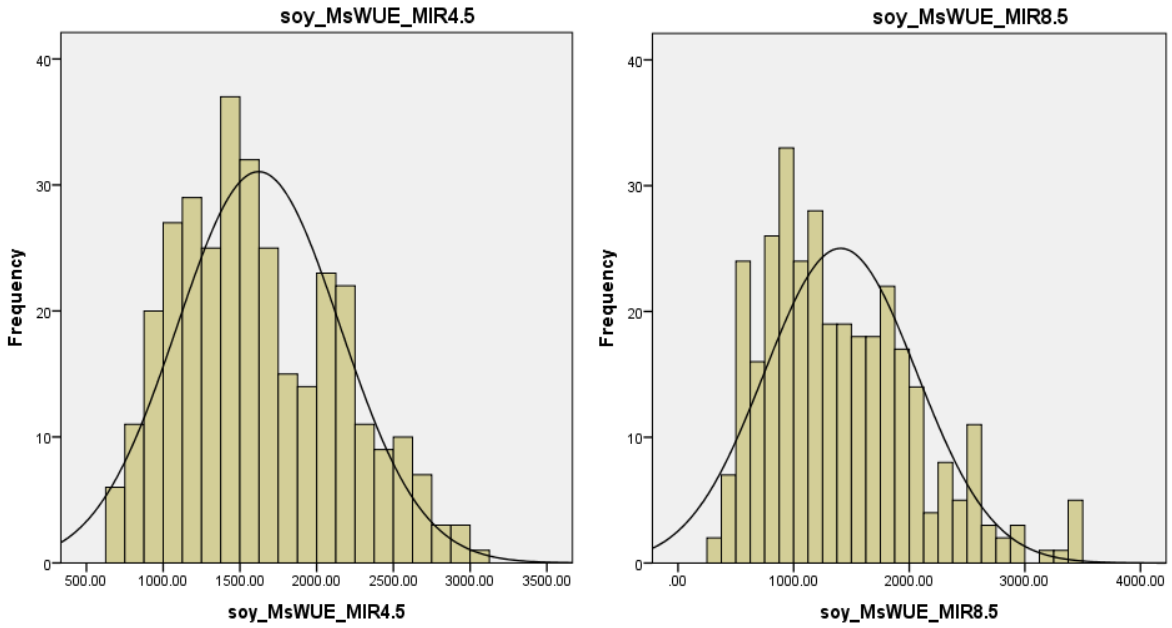


Figure A.4.2-4: MIR 4.5 and 8.5 Soy Modified sWUE histograms

A.4.3 Cotton

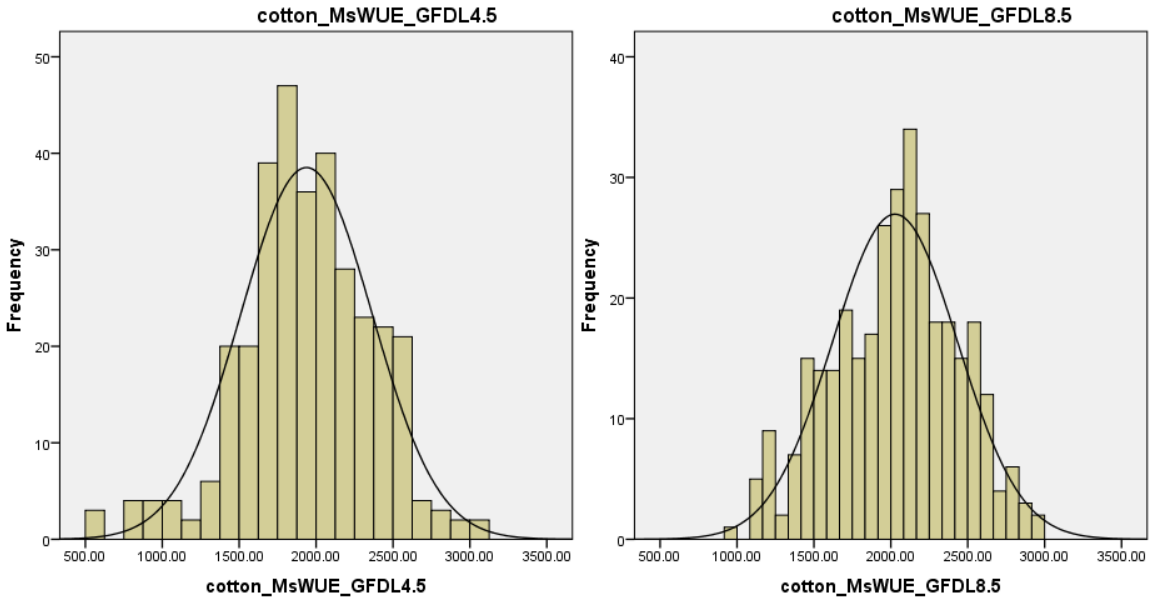


Figure A.4.3-1: GFDL 4.5 and 8.5 Cotton Modified sWUE histograms

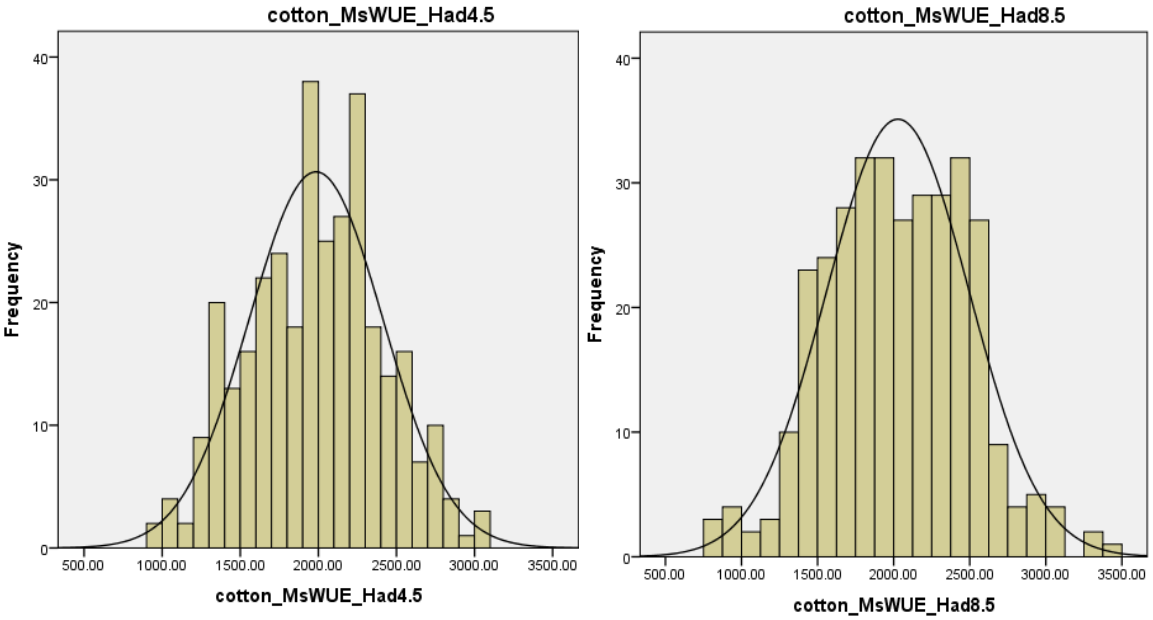


Figure A.4.3-2: Had 4.5 and 8.5 Cotton Modified sWUE histograms

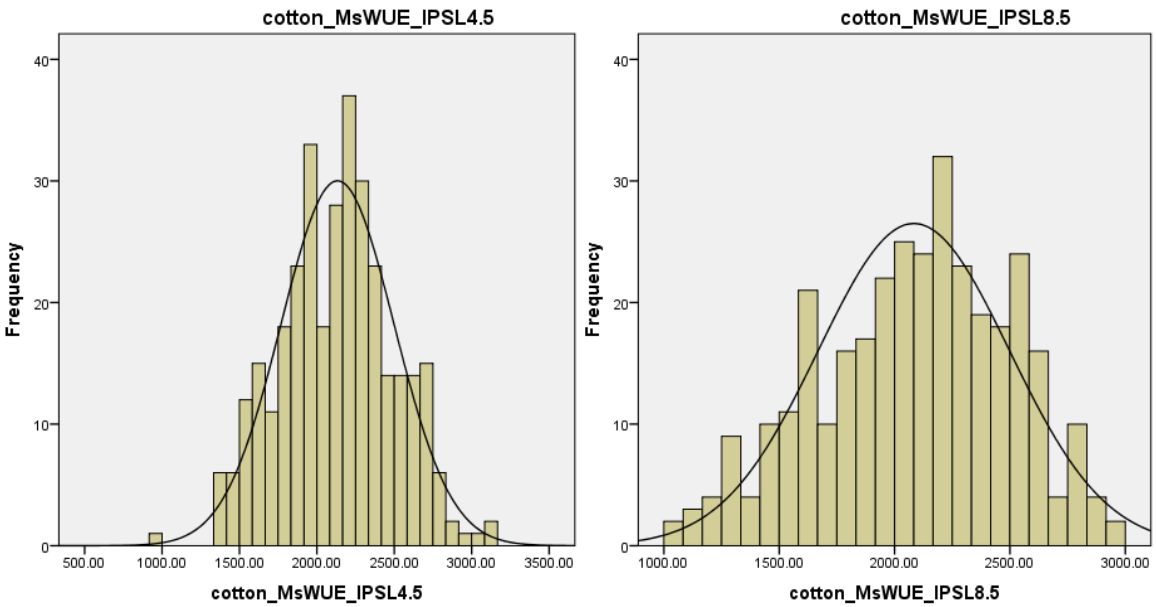


Figure A.4.3-3: IPSL 4.5 and 8.5 Cotton Modified sWUE histograms

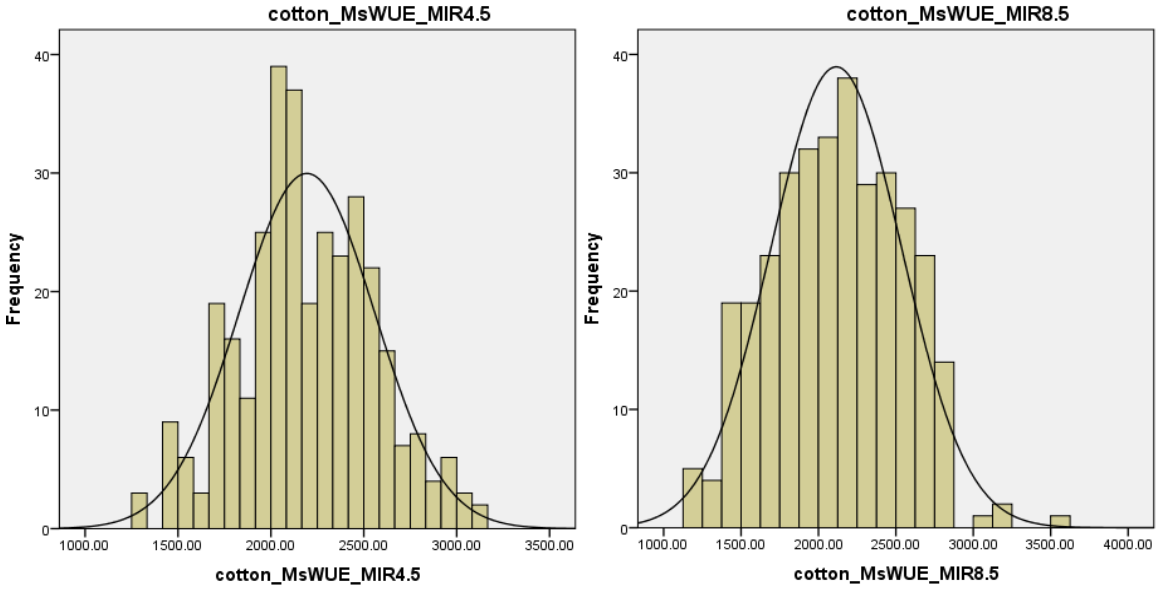


Figure A.4.3-4: MIR 4.5 and 8.5 Cotton Modified sWUE histograms

VITA

Violet Freudenberg was born in the suburbs of Chicago, IL and grew up in Louisville, KY and Boca Raton, FL. She subsequently pursued an undergraduate degree in Civil Engineering at the University of Florida and continued living and working in Gainesville, FL after graduation. Her husband's work transferred their family to Knoxville, TN where they are currently raising their family. A return to graduate school in 2017 has led her following a path to a Master of Science in Environmental Engineering and future gainful employment.